Coordination Chemistry Reviews 255 (2011) 421–450

Contents lists available at ScienceDirect

Coordination Chemistry Reviews

journal homepage: www.elsevier.com/locate/ccr

Review

The coordination chemistry of cyclohexanepolycarboxylate ligands. Structures, conformation and functions

Zhuojia Lin, Ming-Liang Tong*

Key Laboratory of Bioinorganic and Synthetic Chemistry of Ministry of Education/State Key Laboratory of Optoelectronic Materials and Technologies, School of Chemistry and Chemical Engineering, Sun Yat-Sen University, Guangzhou 510275, PR China

Contents

ARTICLE INFO

Article history:
Received 3 July 2010
Accepted 1 October 2010
Available online 30 October 2010

Keywords:
Cyclohexanepolycarboxylate ligands
Flexible conformation
Coordination polymers
Magnetic materials
Conformational transformation

ABSTRACT

This review gives an overview on the coordination chemistry of eight cyclohexanepolycarboxylic acids, *i.e.* cyclohexanecarboxylic acid, 1,2-, 1,3- and 1,4-cyclohexanedicarboxylic acid, 1,3,5- and 1,2,4-cyclohexanetricarboxylic acid, 1,2,4,5-cyclohexanetetracarboxylic acid and 1,2,3,4,5,6-cyclohexanehexacarboxylic acid, and explores their possible applications in materials science, especially as magnetic materials. The conformational transformation of cyclohexanepolycarboxylic acids in the presence of various metal ions under hydrothermal conditions is included and the α-proton removal mechanism is discussed as well.

Abbreviations: 1-CHA, cyclohexanecarboxylic acid; 12-CDA, 1,2-cyclohexanedicarboxylic acid; 13-CDA, 1,3-cyclohexanedicarboxylic acid; 14-CDA, 1,4-cyclohexanedicarboxylic acid; 135-CTA, 1,3,5-cyclohexanetricarboxylic acid; 124-CTA, 1,2,4-cyclohexantricarboxylic acid; 1245-CHA, 1,2,4,5-cyclohexanetetracarboxylic acid; 123456-CHA, 1,2,3,4,5,6-cyclohexanehexacarboxylic acid; 12-chedc, cyclohex-1-ene-1,2-dicarboxylate; 1,3-BDC, 1,3-benzenedicarboxylate; dma, N,N-dimethyl acetamide; bsd, 2,1,3-benzoselena-diazole; TEA, triethylamine; TED, triethylenediamine; hmt, hexamethylenetetramine; 4,4′-bipy, 4,4′-bipyridine; bpe, 1,2-bis(4-pyridyl)ethylene; DMF, dimethylformamide; EG, ethylene glycol; pymc, 2-pyrimidinecarboxylate; 1,10-phen, 1,10-phenanthroline; H_2ip, isophthalic acid; TMA-H_3, trimesic acid.

* Corresponding author. Tel.: +86 20 84110966; fax: +86 20 84112245.
E-mail address: tongml@mail.sysu.edu.cn (M.-L. Tong).

0010-8545/$ – see front matter © 2010 Published by Elsevier B.V.
doi:10.1016/j.ccr.2010.10.006

1. Introduction

Crystalline microporous solids such as zeolites possess characteristic selective catalytic activity, molecular sieving and ion exchange properties, all of which are of high commercial value [1]. Zeolites have been exceptionally successful in industry, nevertheless, there are still considerable challenges to overcome. The nature of tetrahedral aluminosilicate or aluminophosphate frameworks in principle restricts the network topologies. Accordingly new strategies are required to develop new types of networks with various topologies and properties. The metal–ligand coordinate bonds are directional and can be used as reliable tools to construct coordination frameworks [2]. Since metal ions or clusters offer a vast variety of coordination geometries as well as electronic configurations, the design and preparation of metal coordination frameworks with desirable structures and properties are currently under active investigation.

In the context of metal coordination polymers (MCPs), the endless versatility of molecular chemistry provides a huge variety of polytopic organic ligands with different functionalities [3]. The geometries of organic ligands, including the conformation of the ligand backbone, the relative orientation of the functional groups and the spacing between them, impact greatly on the resulting networks. By choosing appropriate organic linkers, it is possible to obtain coordination frameworks with distinctive connectivity [4] and in turn, to provide various properties and application [5].

In the early development of metal coordination polymers, rigid, planar and divergent multi-carboxylate linkers were pursued in the synthesis strategy and have achieved great success. A highly porous yet stable coordination polymer from copper and trimesic acid $[Cu_3\{1,3,5\text{-}C_6H_3\text{-}(COO)_3\}_2(H_2O)_x]_n$ (HKUST-1) [6] offers an excellent model for the preparation of zeolite analogues with diverse functionalities using aromatic ligands with multi-carboxylate groups. Significant work by Yaghi et al. has established the feasibility of designing porous materials with controlled pore sizes [7]. For example, reactions of the rigid linear organic linkers, 1,4-benzenedicarboxylate groups (BDC) with Zn(II) ions led to a series of isorecticular three-dimensional (3D) porous frameworks with general formulas $Zn_4O(R\text{-}BDC)_3$. The resulting networks are highly porous with void space ranging from 55.8 to 91.1% of the total volume and are promising for applications in gas storage. Ferév and his colleagues combined targeted chemistry and computational design to create a crystal structure for porous chromium terephthalate, MIL-101, with very large pore sizes (~30–34 Å) and surface area (for N_2 of $\sim 5900 \pm 300\ m^2/g$) [8]. Beside the usual properties of porous compounds, this solid has the potential as a nanomold for monodisperse nanomaterials.

One of the significant advantages of ligands with aromatic rings in the construction of metal coordination polymers is that they produce inherently rigid structures. The geometries of the metal ions or clusters (nodes) and the organic linkers are more likely to be retained precisely, which gives rise to the control over the dimensionality and topology of the coordination networks to some extent [9]. Large aliphatic organic ligands were virtually unexplored because the lack of rigidity for ligands usually leads to complexity of connectivity and the arrangement between the nodes and linkers.

Flexible organic ligands, *e.g.* straight chained carboxylic acids and cyclohexane multi-carboxylic acids, have, nonetheless, attracted more and more interest in the past decade. Flexible organic ligands were initially investigated in the fields of materials science and supramolecular chemistry due to their structural similarity to rigid aromatic ligands and the utility in designing molecular recognition host systems [10]. The adjustable skeletons of the organic ligands are usually subject to reaction media as well as the surrounding coordination circumstances and adapt various geometries. For instance, a divergent organic ligand with two functional groups may act as a linear or L-shape linker according to different structural conformations [11]. Recent studies show that the flexible and versatile backbones of organic ligands have a delicate effect on the arrangements of the resultant host frameworks, occasionally leading to formation of the third generation of porous metal coordination polymers [12]. In this article we aim to review coordination compounds constructed from one specific type of flexible organic ligands, *i.e.* cyclohexanepolycarboxylic acids.

In principle the amount of the structural isomers for cyclohexanepolycarboxylic acids is much greater than their benzene analogues because each of the carbon atoms on the cyclohexane ring can attach one or two carboxylic groups. Yet only eight of the acids have generally been investigated in the area of coordination and supramolecular solid state chemistry so far, that is, cyclohexanecarboxylic acid (1-CHA), 1,2-, 1,3- and 1,4-cyclohexanedicarboxylic acid (12-CDA, 13-CDA and 14-CDA), 1,3,5- and 1,2,4-cyclohexanetricarboxylic acid (135-CTA and 124-CTA), 1,2,4,5-cyclohexanetetracarboxylic acid (1245-CHA) and 1,2,3,4,5,6-cyclohexanehexacarboxylic acid (123456-CHA) (Scheme 1).

Compared to the planar hexagonal arrangement of benzene, cyclohexane exists in several conformations including envelope, boat, twist or twist-boat and the most stable chair forms [13]. The boat and envelope forms are transition states between the twist forms and the twist and chair forms respectively, and the twist-boat conformation is only 23 kJ/mol less stable than the chair conformation in solution [14]. In the current study, we found that most of the cyclohexanepolycarboxylate ligands adopt the chair forms in the organic adducts or coordination compounds in solid state. However, disorder may make the molecules look as if the cyclohexane rings were in the twist conformation [15].

For the lowest-energy chair conformation of cyclohexanepolycaboxylic acids, the acid groups can be on axial (*a*-) or equatorial (*e*-) positions. In general substituents are more stable on the *e*-positions to minimize the *gauche*-conformation interaction and the axial bonds are hindered because of the 1,3-diaxial interactions [13]. Consequently 1-CHA in most of the coordination and organic compounds, with only one exception [16], adopts the chair conformation with the carboxylic acid on the *e*-position.

For multi-substituted cyclohexane ring, *i.e.* several acid groups on the ring, the relative orientations of the substituents will also have a complicated influence on the free energy of the possible conformations. For 12-CDA and 14-CDA, a *cis*-configuration leads to one axial and one equatorial group and a *trans*-configuration leads to both groups either axial or equatorial while for 13-CDA, the *cis*-form is di-equatorial and the *trans*-one is similar to the *cis*-12- and *cis*-1,4-CDA. Furthermore, the *cis*- and *trans*-conformations of the carboxylic groups on the cyclohexane ring cannot be simply switched by single σ-bond rotation as in cyclohexanecarboxylic acid (1-CHA) and in linear molecules. Switching from *cis*- to *trans*-forms or *vice versa* would require breaking a single bond because of the ring strain. Conformational transformations of cyclohexanepolycarboxylic acids have been widely observed in transition metal coordination compounds (Scheme 2).

The ring structure of cyclohexane brings about chiral center into the ligands, *i.e.* (1*R*,2*R*)- and (1*S*,2*S*)-*trans*-CDA and (1*R*,3*R*)- and (1*S*,3*S*)-*trans*-CDA (Scheme 3) whereas phthalic acid (1,2-benzenedicarboxylic acid) and isophthalic acid (1,3-benzenedicarboxylic acid) are non-chiral. Interestingly the free rotation and disposition of the carboxylic groups can be fixed in the solid state to induce chirality. For example, non-chiral all-*cis*-123456-CHA can crystallize in the space group of $P2_12_12_1$, chirality of which comes from the tiny difference in the rotation angles of the *a*-carboxylic acid groups [17].

In the review we will mainly discuss the coordination chemistry of eight cyclohexanepolycarboxylic acids (CHAs) and explore their

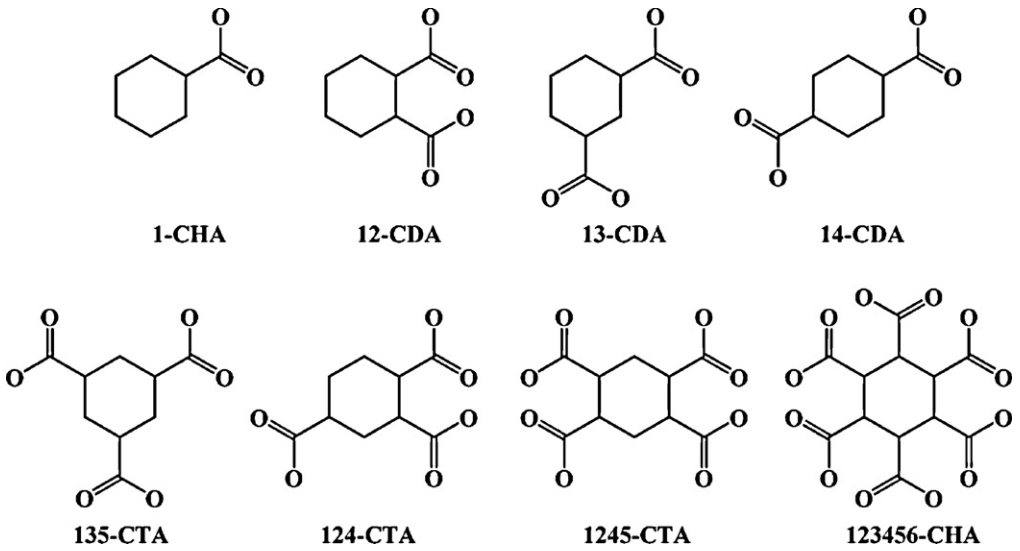

Scheme 1. Eight generally investigated cyclohexanepolycarboxylic acids.

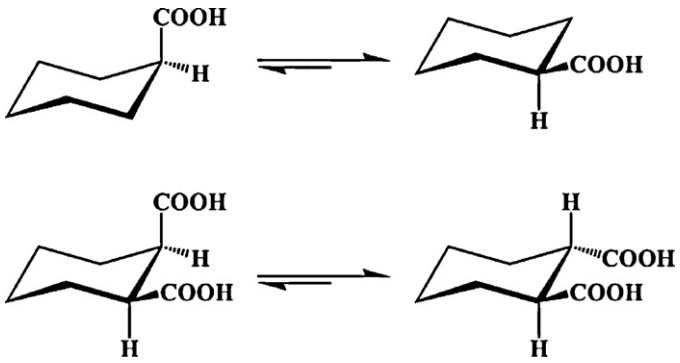

Scheme 2. Comparison of conformational transformations via simply switching σ-bond rotation for 1-CHA and via breaking a single bond for 12-CDA.

possible applications in materials science, especially as magnetic materials. The conformational transformation of CHAs in the presence of various metal ions under hydrothermal conditions will be included, hoping to achieve better understanding on the mechanisms of transformation and to build a bridge between organic and coordination chemistry.

2. The coordination chemistry of cyclohexanemonocarboxylate

Cyclohexanecarboxylic acid (1-CHA) adapts a chair conformation in the *e*-position in most cases in the solid state. The only exception is in a trinuclear oxo-bridged iron(III) complex $[Fe_3OF_3(1\text{-}CHA)_6]^{2-}$ [16], where one of the six crystallographically distinct $1\text{-}CHA^-$ is situated on the *a*-position and the remaining ones are on the common *e*-bonds (Fig. 1).

Low dimensional coordination compounds were obtained from 1-CHA since it has only one carboxylic group. When 1-CHA coordinates to a transition metal ion, it usually links the metal ion(s) in a monodentate, chelation or *syn-syn* mode as a terminal ligand. Thus only mononuclear or multinuclear metal clusters are found for 1-CHA coordination complexes. Typical examples can be found for the drum-shaped and ladder organo-oxotin carboxylate groups, in which the 1-CHAs bridge the tin ions in a *syn-syn* fashion [18]. Due to the oxophilicity of rare earth metals, the carboxylic group on 1-CHA can use the μ_2-η^1:η^2 binding mode as a bridging ligand and links the lanthanide ions into a one-dimensional chain [15a,19].

Tong et al. reported a mixed-valence manganese cluster with a new disk-like Mn_{15} core $[Mn^{III}{}_9Mn^{IV}{}_6(\mu\text{-}1\text{-}CHA)_{12}(\mu_3\text{-}O)_{13}(\mu\text{-}O)_4(\mu\text{-}OMe)_5(MeOH)_3(H_2O)_6]$ solvate [20], in which the cyclohexanecarboxylate could be substituted with benzoate

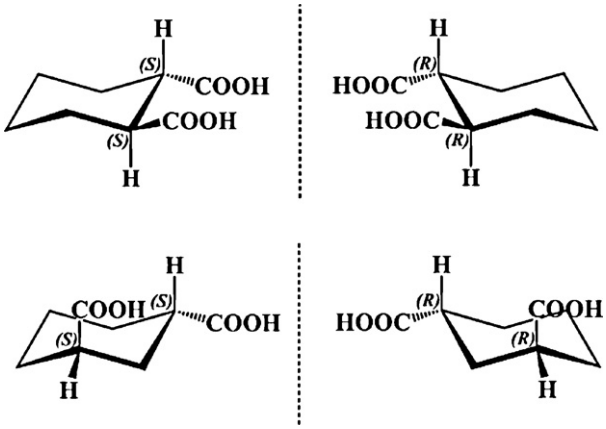

Scheme 3. Chirality in 12-CDA and 13-CDA.

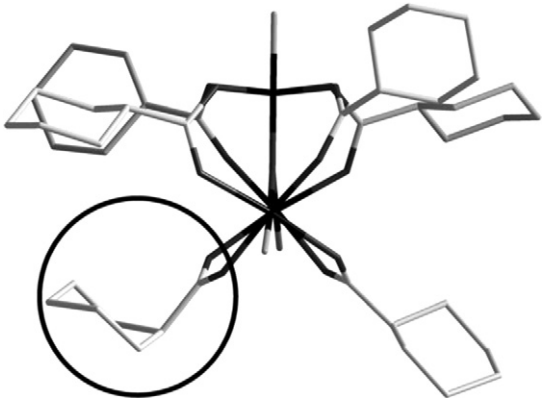

Fig. 1. Crystal structure of $[Fe_3OF_3(1\text{-}CHA)_6]^{2-}$. The black circle highlights the 1-CHA with *a*-carboxylate. The figure is adapted from [16].

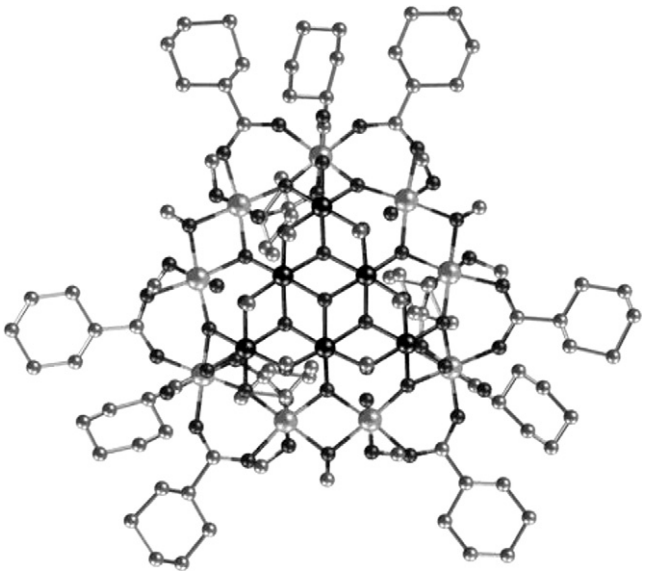

Fig. 2. The disk-like Mn_{15} core of $[Mn^{III}_9Mn^{IV}_6(\mu\text{-}1\text{-CHA})_{12}(\mu_3\text{-}O)_{13}(\mu\text{-}O)_4(\mu\text{-}OMe)_5(MeOH)_3(H_2O)_6]$. The figure is adapted from [17].

(Fig. 2). Though 1-CHA and benzoate are structurally similar, the aliphatic and aromatic rings have delicate and significant effects on both coordination and supramolecular interactions. The replacement resulted in the decrease in the symmetry of the Mn_{15} clusters from C_3 to C_1 and the enhancement of intermolecular interaction from pure van der Waals force to the combination of π–π stacking, leading to a dramatic reduction of the energy barrier for spin reversal. Compared to the silence of the out-of-phase ac susceptibility of the benzoate compound, the 1-CHA one showed slow magnetic relaxation behavior above 1.8 K.

3. The coordination chemistry of cyclohexanedicarboxylates

Addition of one extra carboxylic group on cyclohexane brings about more versatile coordination modes and in particular, the difference in orientation of the substituents towards the ring due to steric strain. The conformations with both of the acid groups on di-equatorial positions are generally the most stable for cyclohexanedicarboxylic acids (12-, 13- and 14-CDAs) in organic crystals or co-crystals. Nonetheless, the linkage upon metal ions helps stabilization of the *a*-carboxylate. The *a*,*e*-form is reasonably stable and the *a*,*a*-form can even be trapped in the coordination compounds. C. N. R. Rao carried out a systematic study on 12-, 13- and 14-CDAs in the construction of cadmium and manganese coordination compounds under hydrothermal conditions and found that the *e*,*e*-conformation is the most favored in all the three isomeric CDAs, although the 1,4-CDA often contains rings formed by both *e*,*e*- and *a*,*e*-conformations [15b].

3.1. Coordination compounds based on 1,2-cyclohexanedicarboxylate

One additional carboxylic group on the cyclohexane ring gives rise to more versatile coordination modes of 12-CDA compared with 1-CHA. Besides the typical μ_2-bridging, 12-CDA is a versatile multidentate ligand (μ_3, μ_4, and μ_5). Most 12-CDAs link metal ions on di-equatorial positions in the *trans*-*e*,*e*-conformation and only four out of thirteen 12-CDA coordination compounds adopt the *cis*-forms (CSD version 5.31, Feb. 2010). The *trans*-*a*,*a*-form is rather rare for 12-CDA due to steric hindrance of two neighboring bulky carboxylic groups. Only few cases have been reported so far, such as in cadmium bipyridiyl coordination compound $[Cd_2(\mu_2\text{-}trans\text{-}a,a\text{-}12\text{-CDA})(\mu_2\text{-}trans\text{-}e,e\text{-}12\text{-CDA-H})_2(4,4'\text{-bipy})_2]\cdot 8H_2O$ [21], where the two conformational distinct species play dramatically different roles in the molecular assembly: the *e*,*e*-12-CDA participates in the formation of the cadmium dinuclear unit in the μ_2-η^1:η^2 mode while the chelating *a*,*a*-12-CDA linker is responsible for the generation of an infinite coordination chain (Fig. 3).

Two *e*,*e*-carboxylate groups have two COOH in the *gauche* relationship, which are more or less aligned in the same direction. Adjacent acid groups facilitate the formation of metal-carboxylate chains or layers while hydrophobic cyclohexane ring tends to approach with one another, leading to distinct organic–inorganic hybrid domains with the organic components situated in between the coordination chains or layers [15b]. Furthermore, since *trans*-*e*,*e*-12-CDA is a chiral molecule, the chirality of the ligand has a certain delicate influence on molecular assembly via imposing steric constraints by having racemic or only one enantiomer in building the frameworks.

Cheetham and his co-workers explored the racemic and homochiral forms of zinc cyclohexane-*trans*-1,2-dicarboxylate, [Zn(*trans*-12-CDA)] using *R*,*R*/*S*,*S*-12-CDA and its enantiomeric *R*,*R*-analogue [22]. Both compounds are layered 2-D coordination polymers, comprising double rows of ZnO_4 tetrahedra with pendant cyclohexane rings decorating both sides of the layers, giving rise to non-covalent interlayer interactions (Fig. 4). In racemic *R*,*R*/*S*,*S*-12-CDA compound, the cyclohexane rings are arranged in a parallel fashion while those in the *R*,*R*-12-CDA compound adopt a fundamentally different herringbone geometry. Forcefield calculations indicated that the less dense racemic structure is indeed more stable than the chiral phase by 21.9 kJ mol^{-1}, in agreement with the experimental observation that the racemic *R*,*R*/*S*,*S*-phase forms in preference to a 50:50 mixture of the *R*,*R*- and *S*,*S*-chiral phases.

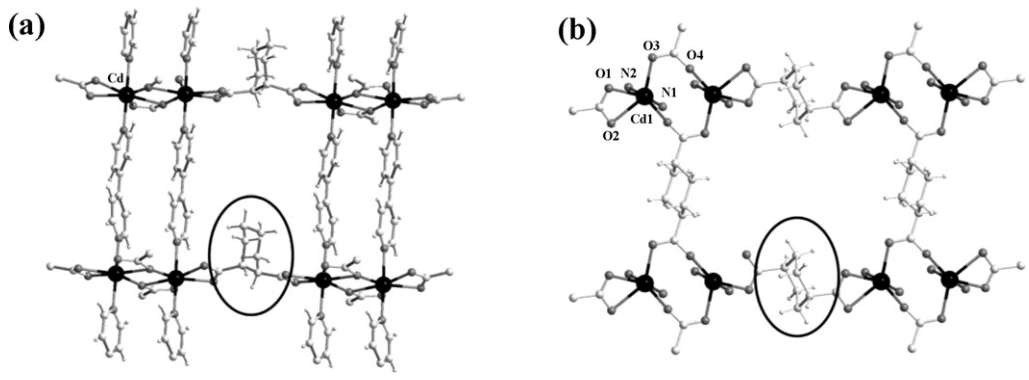

Fig. 3. Crystal structures of $[Cd_2(\mu_2\text{-}trans\text{-}a,a\text{-}12\text{-CDA})(\mu_2\text{-}trans\text{-}e,e\text{-}12\text{-CDA-H})_2(4,4'\text{-bipy})_2]\cdot 8H_2O$ (a) and $[Cd_2(\mu_2\text{-}trans\text{-}a,a\text{-}14\text{-CDA})(\mu_4\text{-}trans\text{-}e,e\text{-}14\text{-CDA})(bpe)_2]$ (b). The *a*,*a*-CDAs are emphasized by the black circles. The figures are adapted from [21].

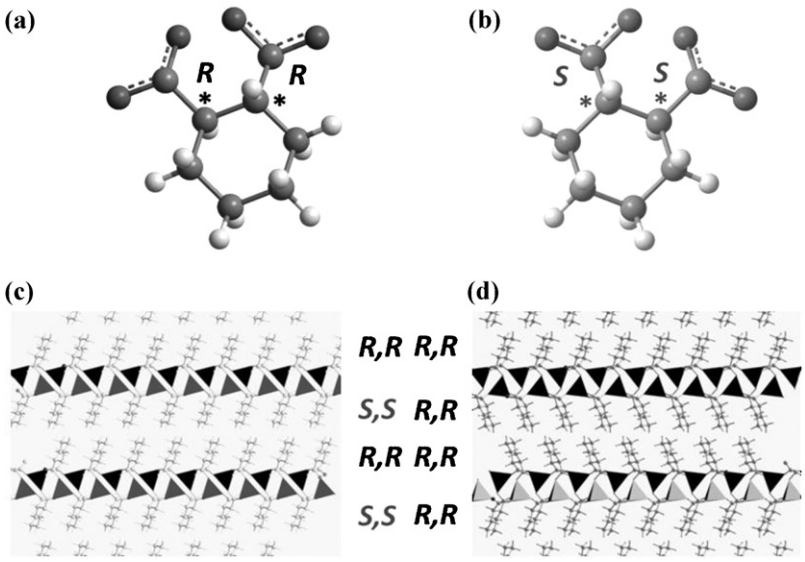

Fig. 4. The *trans*-*R*,*R*-12-CDA (a), *trans*-*S*,*S*-12-CDA (b) and the racemic (c) and homochiral (d) hybrid Zn-dicarboxylate structures. The figures are adapted from [22].

Intensive study on magnetic materials with controllable and/or switchable properties led to the discovery of hybrid organic–inorganic multilayer magnets. In this context, 12-CDA was taken into account in the field of magnetic materials due to the following structural features: 1) multidentate to link metal ions into chains or layers covalently; 2) weak mediator of the spin carriers, *i.e.* magnetically "inertness" to efficiently prevent magnetic interactions between the chains.

Inspired by this strategy, several organo-inorganic lamellar coordination polymers with various magnetic properties were obtained from hydrothermal synthesis subject to different reaction conditions. [$Co_3^{II}(OH)_2$(*trans*-1,2-CDA)$_2$], which is alike to the Kagomé lattice (Fig. 5), shows the coexistence of spin frustration and long range magnetic ordering [23] while [Co^{II}(*trans*-1,2-CDA)] consists of paddle-wheel $Co_2(COO)_4$ chains in parallel arrangement (Fig. 6) and exhibits an interesting single-chain magnet (SCM) behavior [24]. [Fe^{II}(*trans*-1,2-CDA)] has the isostructural coordination network to the cobalt analogue with similar $Fe_2^{II}(COO)_4$ chains; however, it simply behaves as an alternating ferro-antiferro magnetic interaction [25]. Notably in the nickel compound [$Ni^{II}(\mu_2$-$H_2O)$(*cis*-1,2-CDA)], the ligand adopts the *cis*-*a*,*e*-conformation to assemble metal ions into a uniform $Ni^{II}(\mu_2$-$H_2O)(COO)_2$ chain (Fig. 7), which exhibits strong antiferromagnetic interaction and diamagnetic ground state [25].

Moreover, through controlling the conformations of 1,2-CDA and using an analogous ligand, cyclohex-1-ene-1,2-dicarboxylate (12-chedc), three manganese organo-inorganic hybrid compounds with different 2D Mn-COO layers, [Mn^{II}_4(*trans*-1,2-CDA)$_4(H_2O)$], [Mn^{II}_2(*cis*-1,2-CDA)$_2$] and [$Mn^{II}_3(\mu_3$-OH)$_2$(1,2-chedc)$_2$], were obtained [26], which demonstrate the interesting effect of in-plane magnetic correlation on the Néel temperature. The similar interlayer distances for the three above compounds are 12.94 Å, 12.44 Å and 11.11 Å, respectively, corresponding to the increasing Néel temperatures from 5 and 7 K to 42 K (Fig. 8).

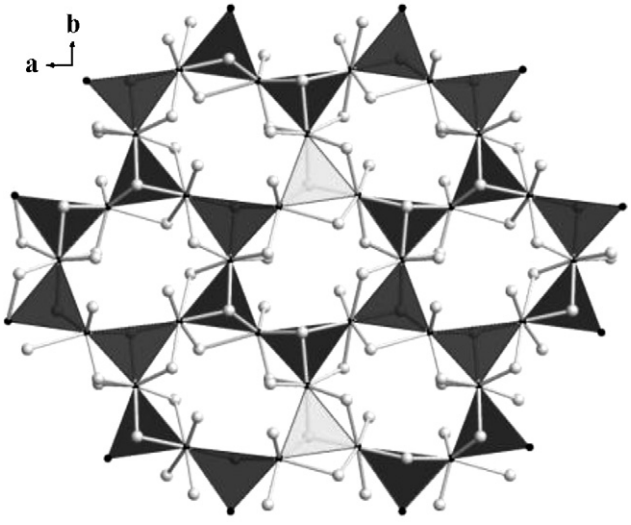

Fig. 5. Crystal structure of the 2D Kagomé-like lattice in [$Co^{II}_3(OH)_2$(*trans*-1,2-CDA)$_2$]. The figure is adapted from [23].

3.2. Coordination compounds based on 1,3-cyclohexanedicarboxylate

1,3-cyclohexanedicarboxylic acid (13-CDA) has two of three possible structural isomers found so far, *i.e.* the *cis*-*e*,*e*- and *trans*-*a*,*e*-forms. The *trans*-*a*,*e*-conformation is potentially chiral but only a racemic crystal has been reported which crystallizes in centrosymmetric space group *P*-1 with both enantiomers in one unit cell [27].

Most 13-CDAs adopt the chair-conformation in coordination compounds though disorder sometimes makes the molecules look as if in the twisted planar (or flattened chair) conformations [15b,c]. The *e*,*e*-form is stable upon coordination, which bridges metal ions into multinuclear species and connects the metal cores into infinite chains or layers as a V-shaped linker [28]. The *a*,*e*-form also occurs in coordination compounds where the ligand connects the metal centers as a T-shaped linker [29].

[$Eu_2(H_2O)_4$(13-CDA)$_3$]·$2H_2O$ (MIL-94) is one of some typical examples [15c], in which the layered structure is built up from europium(III) dimers linked through the 13-CDA moieties. Similar to the 12-CDA coordination compounds, when the layered structure is formed, the hydrophobic cyclohexane ring of 13-CDA is situated between the layers. A comparative study of MIL-94

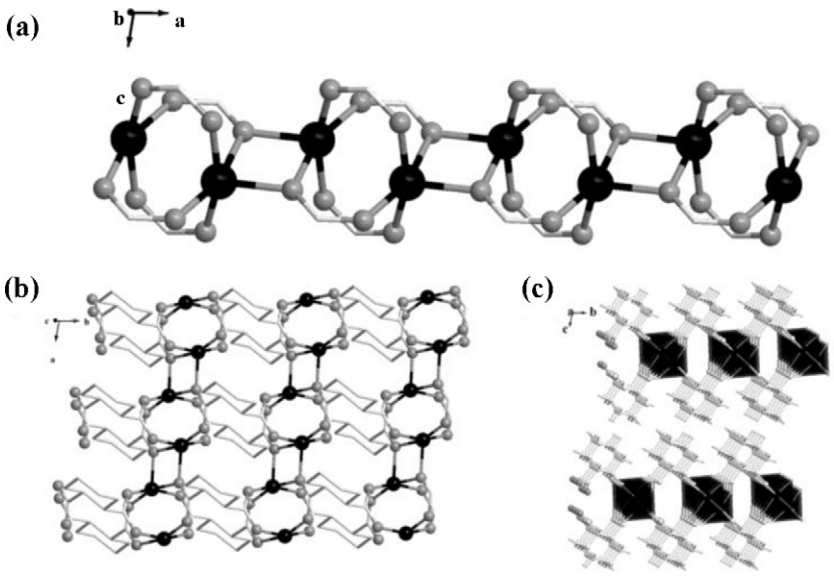

Fig. 6. Perspective views of the paddle-wheel chain (a), layer (b), and crystal packing with the Co^{II} atoms highlighted in polyhedra (c) in [Co^{II}(*trans*-1,2-CDA)]. The figures are adapted from [24].

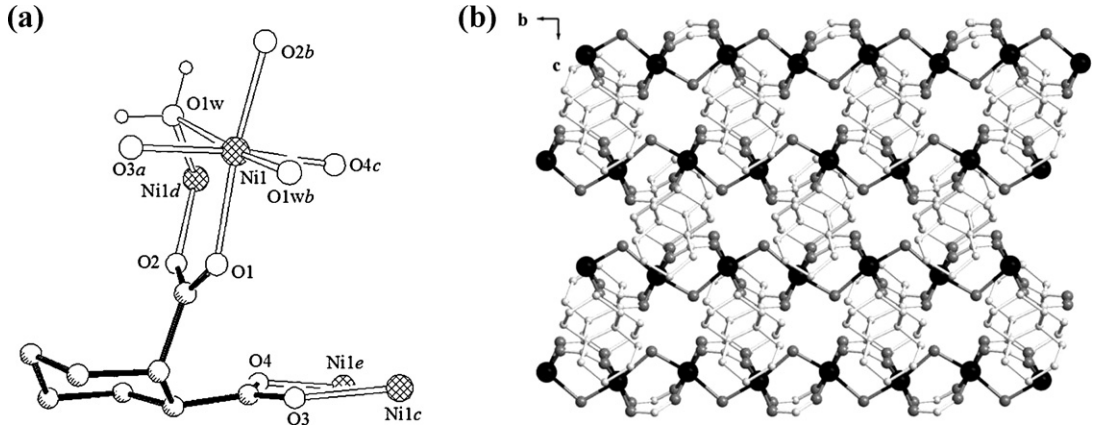

Fig. 7. Crystal structure of [Ni^{II}(μ_2-H_2O)(*cis*-1,2-CDA)]: coordination of *cis*-12-CDA (a) and the layered structure (b). The figures are adapted from [25].

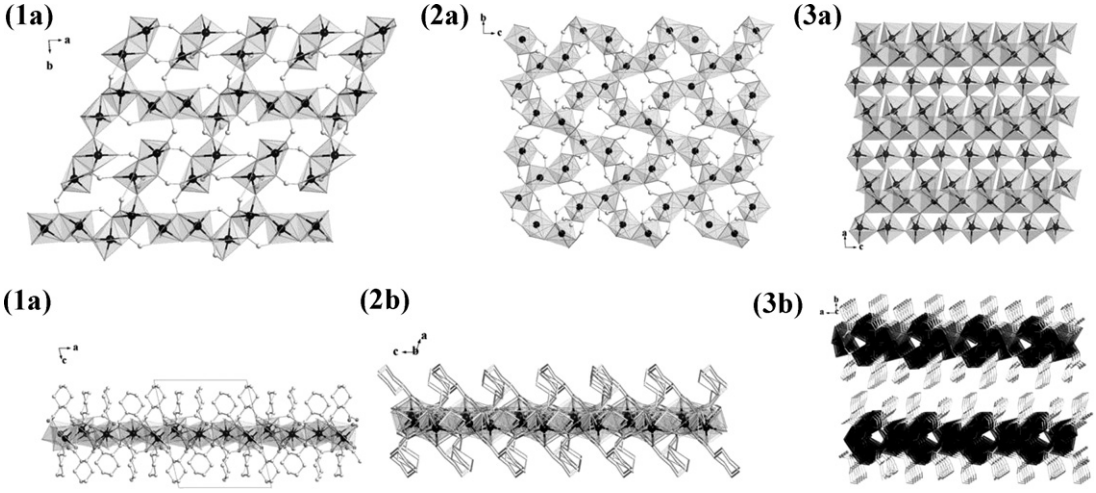

Fig. 8. Crystal structures of three manganese compounds [Mn_4^{II}(*trans*-1,2-CDA)$_4$(H_2O)] (1), [Mn_2^{II}(*cis*-1,2-CDA)$_2$] (2) and [Mn_3^{II}(μ_3-OH)$_2$(1,2-chedc)$_2$] (3): the carboxylate-bridged Mn–O layers (a) and their side views (b). The Mn^{II} ions are all highlighted with polyhedra. The figures are adapted from [26].

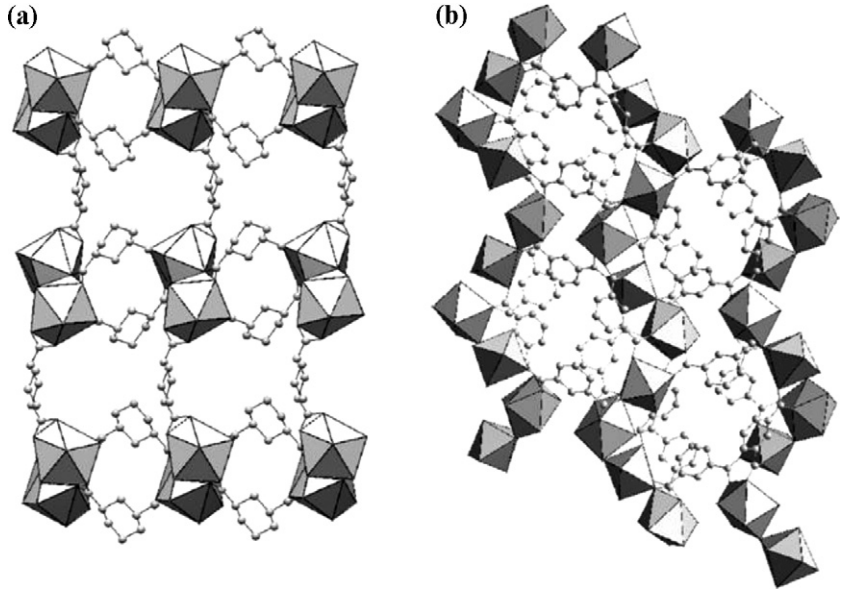

Fig. 9. Crystal structures of MIL-94 and $[Eu_2(H_2O)_2(13\text{-}BDC)_3]$. The figures are adapted from [15c].

and the layered $[Eu_2(H_2O)_2(13\text{-}BDC)_3]$, which is built up from Eu dimers and 1,3-benzenedicarboxylate (1,3-BDC), showed that a slight change in the flexibility in two isotopological ligands is sufficient to induce drastic changes in the topology of the resulting structures and proved that isoreticularity applies only when isorigidity of the different ligands is satisfied (Fig. 9).

13-CDA has more versatile coordination modes varying from monodentate and bridging as a *cis*-μ_3-ligand to μ_3-η^1:η^2 and μ_4-η^2:η^2 as a *trans*-μ_7-linker when binding to main group metal ions with large atomic radii such as Pb^{2+}, leading to high dimensional organo-inorganic frameworks [30]. C.N.R. Rao reported five lead 13-CDA compounds $[Pb(13\text{-}CDA)(H_2O)]$, $[(OPb_4)_2(OH)_2(C_2O_4)(13\text{-}CDA)_4]\cdot H_2O$, $[Pb_2(13\text{-}CDA)_2(H_2O)]$, $[(OPb_3)(13\text{-}CDA)_2]$ [30b] and $[Pb_3O(1,3\text{-}CDA)(1,4\text{-}CDA)]\cdot 0.5H_2O$ [30a] prepared from hydrothermal conditions. The conformation of the 13-CDA anions in above compounds, except the fourth one, is *cis*-*e*,*e*, resulting in hybrid structures possessing extended inorganic connectivity in one or two-dimensions involving infinite Pb–O–Pb linkages along with zero or one-dimensional organic connectivity. In the fourth lead compound $[(OPb_3)(13\text{-}CDA)_2]$, 13CDA adapts the *trans*-*a*,*e*-form to connect the lead ions into a 3-D coordination network without inorganic connectivity (Fig. 10).

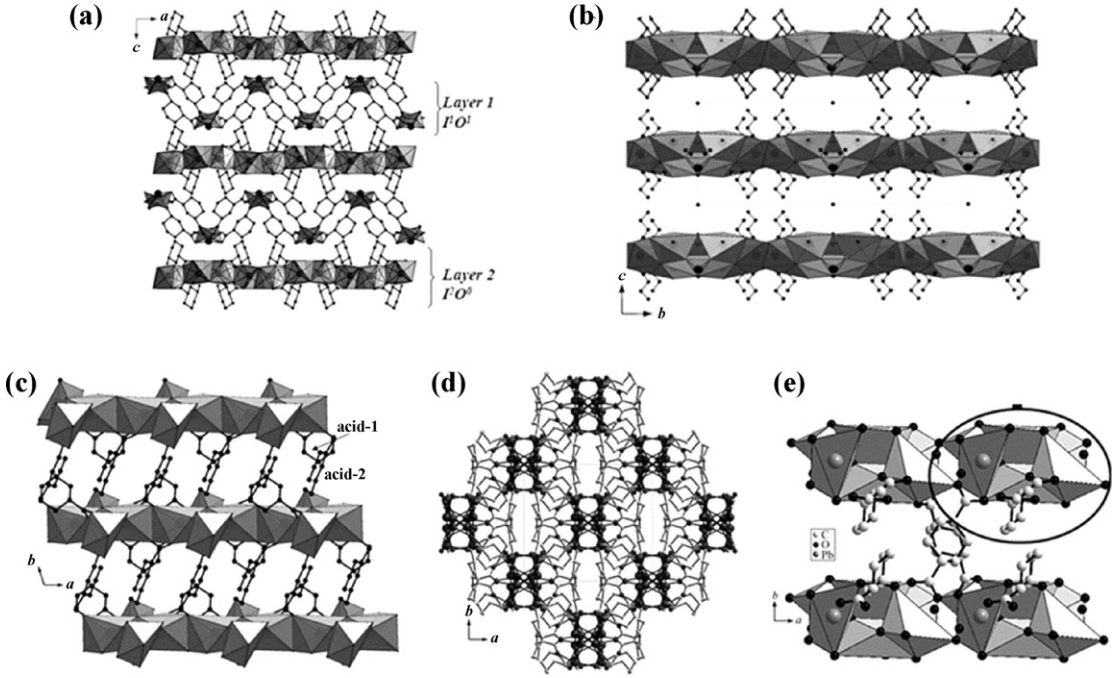

Fig. 10. Crystal structures of five lead 13-CDA compounds: layered $[Pb(13\text{-}CDA)(H_2O)]$ (a), layered $[(OPb_4)_2(OH)_2(C_2O_4)(13\text{-}CDA)_4]\cdot H_2O$ (b), truly 3D hybrid $[Pb_2(13\text{-}CDA)_2(H_2O)]$ (c), 3D organic connected $[(OPb_3)(13\text{-}CDA)_2]$ [30b] and mixed-carboxylate groups $[Pb_3O(1,3\text{-}CDA)(1,4\text{-}CDA)]\cdot 0.5H_2O$ [30a]. The figures are adapted from [30].

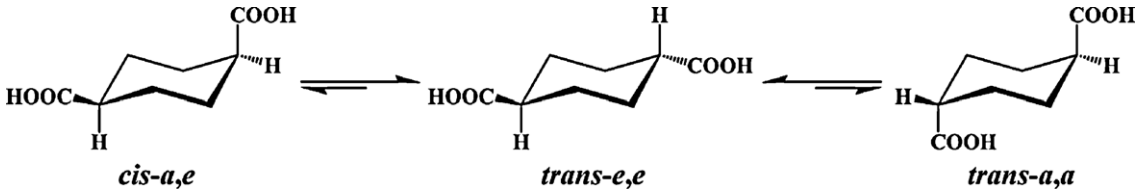

Scheme 4. Conformational transformations of 14-CDA.

3.3. Coordination compounds based on 1,4-cyclohexanedicarboxylate

1,4-cyclohexanedicarboxylic acid (14-CDA) is an extensively used ligand in building metal coordination polymers with high dimensionality. Three conformations, namely *trans*-*e*,*e*, *trans*-*a*,*a* and *cis*-*a*,*e*, have been observed in previously reported coordination compounds. The *trans*-*e*,*e*-form is usually thermodynamically more stable than the *cis*-*e*,*a*-one because of the presence of two equatorial substituents, and the *trans*-*a*,*a*-form is the least stable. Interestingly the number of coordination compounds with the less stable *cis*-*a*,*e* and *trans*-*a*,*a* forms increase dramatically compared with predominant *trans*-*e*,*e*-12-CDA and *cis*-*e*,*e*-13-CDA compounds, suggesting that the energy difference of carboxylate groups between the *a*- and *e*-positions becomes much less than 5 kJ/mol. Indeed according to theoretical calculation, the free energy change is $-1.4\,kcal\,mol^{-1}$ from *cis*-*a*,*e* to *trans*-*e*,*e*-conformation and $-2.8\,kcal\,mol^{-1}$ from *trans*-*a*,*a* to *trans*-*e*,*e*, respectively [31]. Such low energy difference indicates the possibility of conformational inversion (Scheme 4). Two acid groups separated in the opposite directions of the cyclohexane ring reduce the 1,3-diaxial hindrance while the packing and lattice energy upon coordination or other supramolecular interactions may compensate steric disfavor. Coordination polymers based on different coordination motifs constructed by 1,4-cyclohexanedicarboxylic acid has been newly reviewed by Cao and co-workers [11].

Since the most abundant and commercial source of 14-CDA is a mixture of *cis*- and *trans*-geometric forms in a molar ratio of 3:2, most of the reported syntheses used the mixture, rather than one of the isomers, as starting materials and consequently, this introduces segregation and mixing of these isomers in the resulting compounds. Though the former appears to be dominant, two forms mixing in one compound has also been observed in some cadmium, manganese [15b] and lanthanide [30a,32] coordination layered structures. In general, low temperatures and pH values help the formation of *cis*-*a*,*e*-14-CDA complexes whereas high temperatures and pH values result in *trans*-*e*,*e*-14-CDA compounds [32b,33]. Many other studies reveal that other synthesis conditions including the nature of metal ions, addition of ancillary ligands and reaction solvents also have some delicate influence on the tendency of which form of 14-CDA being isolated in the complexes [34].

Two carboxylic groups on the opposite disposition and the flexible ring for 14-CDA have more dramatic influence upon the topology of extended M-COO-M connectivity than those for 12- and 13-CDAs since it can serve as a L-shaped or linear linker respectively according to different conformations while 12- and 13-CDAs usually lead to layered structures possessing multinuclear metal cores. *Cis*-*a*,*e*-14-CDA usually acts as a L-shaped (bent) linker and binds the metal ions into infinite double-threaded or double-lamellar arrays with the hydrocarbon part riding between the chains or layers. The *trans*-*e*,*e*-form, on the contrary, plays a similar role to terephthalic acid connecting metal ions as a linear linker largely in chelating, *syn*-*syn*, *syn*-*anti*, μ_2-η^1:η^2 and μ_3-η^1:η^2 manners. It is notable that inversion operation is sometimes observed at the center of cyclohexane in the metal 14-CDA complexes, whereas very few 12-CDA and 13-CDA compounds [15b,c] have symmetry operation running along or through the ring. Furthermore, the *trans*-*a*,*a*-conformation has also been trapped to bridge metal atoms in a Z shape (Scheme 5) in coordination complexes [21,30a,35].

The influence of geometry and conformation of 14-CDA on framework construction can be highlighted by two lead coordination polymers, 2D [Pb(*trans*-*e*,*e*-14-CDA)(H_2O)] and 3D [Pb_2(*cis*-*a*,*e*-14-CDA)$_2$]·NH(CH_3)$_2$, which were prepared from aqueous solution and N,N-dimethylacetamide (dma), respectively [34e]. Two unique 14-CDAs are present in the former compound, both of which have an inversion center sitting in the middle of cyclohexane. One *trans*-14-CDA bridges four Pb^{2+} ions using a μ_2-η^1:η^2 fashion to form an infinite ladder. The other ligand links two Pb^{2+} ions in a monodentate mode and connects the neighboring ladders into a layer. In the latter compound two distinct *cis*-14-CDAs adapt chelating, *syn*-*anti* and μ_2-η^1:η^2 manners as μ_3 and μ_4 linkers. The Pb^{2+} ions are linked by L-shaped *cis*-14-CDAs to give an unprecedented nanosized [Pb_8(*cis*-14-CDA)$_8$] neutral wheel cluster, which is further linked to each other to generate a rare 3D bcc-type net (Fig. 11).

14-CDA has been widely employed in the construction of functional materials with fascinating magnetic or absorption properties similar to its structural analogue terephthalic acid. Kurmoo and his colleagues have successfully used 14-CDA to develop a series of organo-inorganic hybrid frameworks with infinite metal hydroxide chains or layers, many of which exhibit a coexistence of porosity and magnetic ordering. The compound [$Co_5(OH)_8$(μ_2-*trans*-*e*,*e*-14-CDA)]·4H_2O [36] contains $Co_3^{(oct)}Co_2^{(tet)}(OH)_8$ layers that are linked together by bis(monodentate) 14-CDA pillars (Fig. 12). The material remains monocrystalline during dehydration of lattice aqua molecules in the 1-D channels to become [$Co_5(OH)_8$(14-CDA)] via an intermediate [$Co_5(OH)_8$(14-CDA)]·2H_2O upon heating or evacuation. The anhydrous phase has no void volume and 9% decrease of the interlayer spacing due to a tilting of 14-CDA and will rehydrate rapidly when exposing to air. The material orders as a ferrimagnet at 60.5 K, a temperature that is among the highest seen for spontaneous magnetization in an ordered crystalline inorganic–organic hybrid material. The transi-

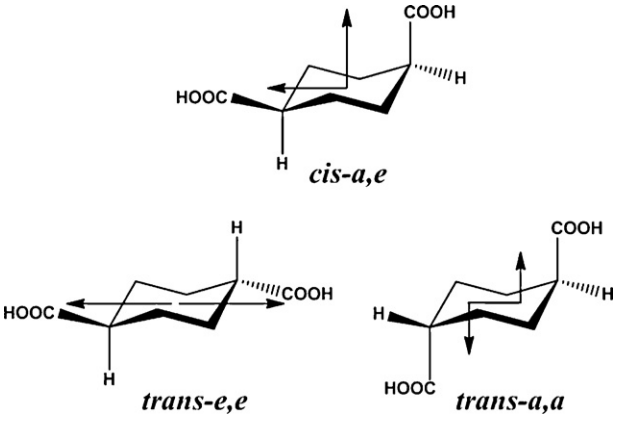

Scheme 5. Coordination geometries of three 14-CDA isomers.

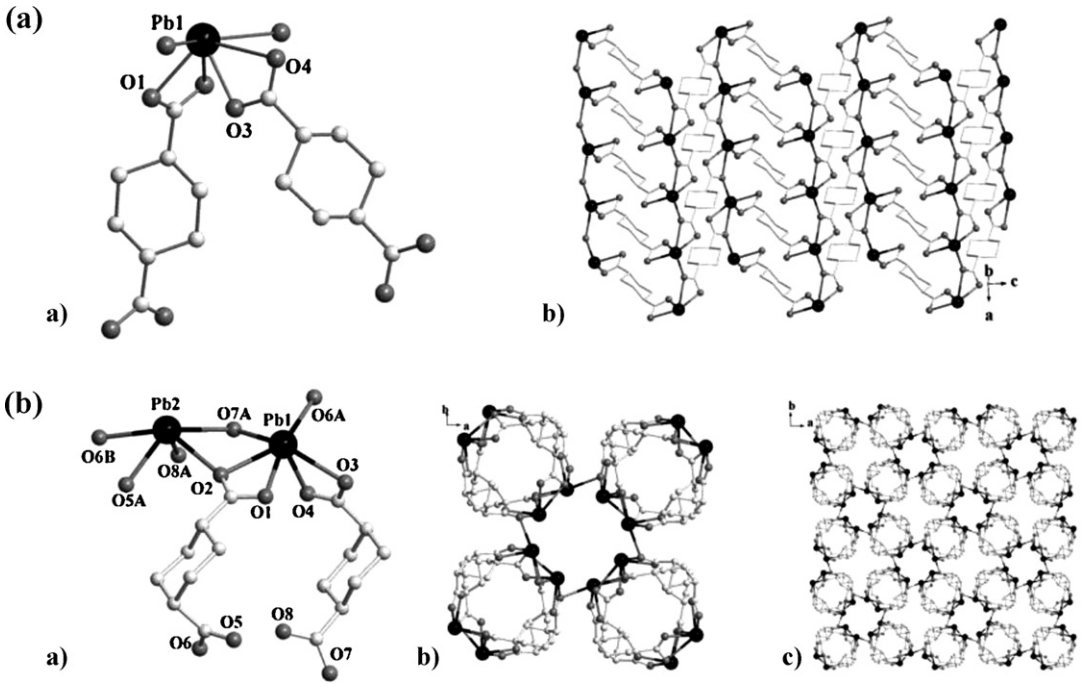

Fig. 11. Crystal structures of [Pb(*trans*-*e*,*e*-14-CDA)(H_2O)] (a) and [Pb_2(*cis*-*a*,*e*-14-CDA)$_2$]·$NH(CH_3)_2$ (b). The figures are adapted from [34e].

tion from paramagnetic to ferrimagnetic state at 60.5 K remains unaltered upon dehydration and rehydration, suggesting that the magnetic properties are highly insensitive to the considerable structural perturbation that arises with dehydration for this material.

The nickel hybrid compounds [$Ni_3(\mu_3$-OH)$_2(\mu_4$-*cis*-*a*,*e*-14-CDA)$_2(H_2O)_4$]·$2H_2O$ and [$Ni_3(\mu_3$-OH)$_2(\mu_4$-*trans*-*e*,*e*-14-CDA)$_2$($H_2O)_4$]·$4H_2O$ [37] are based on $Ni_3(OH)_2$ linear chains connected by either bis(*syn*-*syn*) *cis*- or *trans*-14-CDA, respectively (Fig. 13). The frameworks sustain pores that hold two or four water molecules according to the size and shape of the channels depending on the particular isomer. The former nickel material indicates long-range ordering (LRO) to a ferrimagnetic ground state at 2.1 K that is reversibly transformed into a ferromagnet below 4.4 K upon partial dehydration and rehydration while the latter one tends toward a LRO state to possibly a ferrimagnet below 2 K. Comparatively, 1D coordination chain compound [$Ni(H_2O)_4(\mu_2$-*trans*-*e*,*e*-14-CDA)] consisting of square-planar $Ni(H_2O)_4$ bridged by bis(monodentate) 14-CDA demonstrates uniform antiferromagnetic interaction.

Sodium hydroxide was needed to neutralize the acids for above cobalt and nickel materials while the selectivity of the geometric *cis*- and *trans*-isomers is consistent with different temperatures of the reactions. However for copper coordination complexes, two phases with *cis*- and *trans*-14-CDA were formed for all working temperatures though the proportion of *trans*-isomer increased with rising temperature and neutralization of the acids with NaOH could easily result in forming copper oxides [38]. Accordingly the *cis*-complex [$Cu_2(\mu_4$-*cis*-*a*,*e*-14-CDA$)_2(H_2O)_2$] was prepared from a *cis*- and *trans*-mixture at low temperature and the *trans*-complex [Cu_2(*trans*-*e*,*e*-14-CDA$)_2$] used pure *trans*-acid as starting material. Some common structural features, such as inorganic $M_3(OH)_2$ chains, for nickel and cobalt in their complexes are not the case for the copper compounds. The *cis*-complex consists of two-legged ladders where paddle wheel $Cu_2(COO)_4$ nodes are bridged by pairs of *cis*-14-CDAs in a *syn*-*syn* mode and capped by two water molecules on the ends (Fig. 14). The *trans*-complex is composed of 4×4 Cu_8(*trans*-14-CDA$)_4$ grids with similar dimeric nodes, which are connected to each other resulting in a porous network. Two crystallographically unique 14-CDAs have distinct coordination manners, *i.e.* one μ_4-14-CDA links four copper atoms in a *syn*-*syn* mode and the other μ_6-14-CDA bridges six metal ions in a μ_3-η^1:η^2 pattern. The cyclohexane provides a hydrophobic character to the surface of the cavities and thus repels the water molecules. IR and DT-TGA confirm the absence of water in the empty channels. The magnetic properties of both compounds are dominated by the strong Cu–Cu

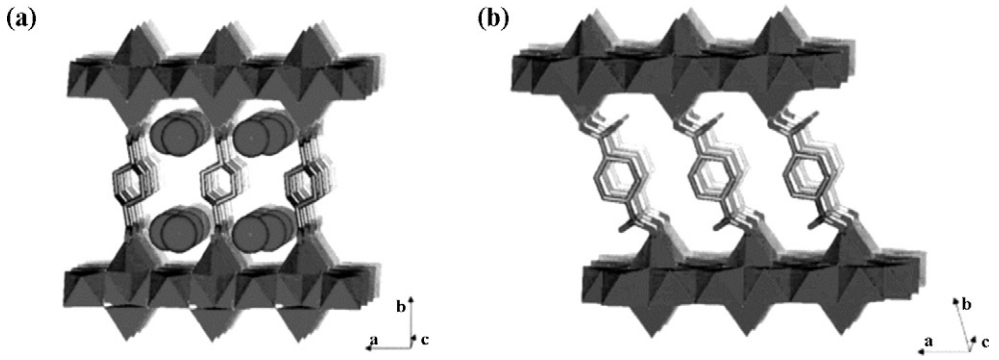

Fig. 12. Crystal structures of [$Co_5(OH)_8(\mu_2$-*trans*-*e*,*e*-14-CDA)]·$4H_2O$ (a) and [$Co_5(OH)_8$(14-CDA)] (b). The figures are adapted from [36].

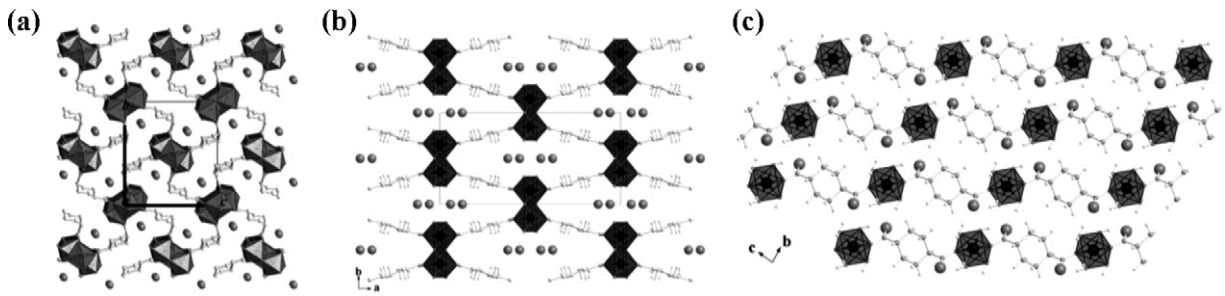

Fig. 13. Crystal structures of three nickel 14-CDA hybrid compounds: $[Ni_3(\mu_3\text{-}OH)_2(\mu_4\text{-}cis\text{-}a,e\text{-}14\text{-}CDA)_2(H_2O)_4]\cdot 2H_2O$ (a), $[Ni_3(\mu_3\text{-}OH)_2(\mu_4\text{-}trans\text{-}e,e\text{-}14\text{-}CDA)_2(H_2O)_4]\cdot 4H_2O$ (b) and $[Ni(H_2O)_4(\mu_2\text{-}trans\text{-}e,e\text{-}14\text{-}CDA)]$ (c). The figures are adapted from [37].

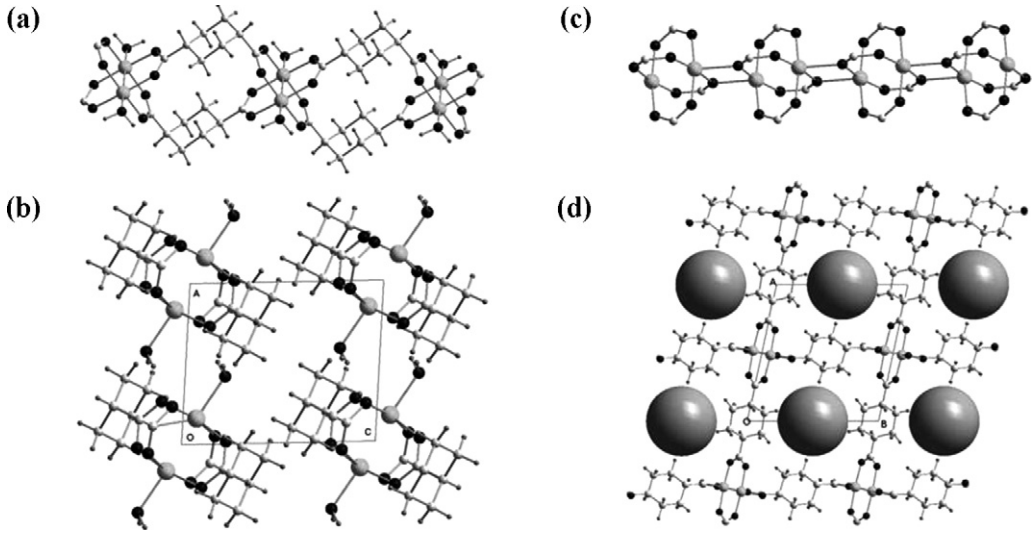

Fig. 14. Structures of $[Cu_2(\mu_4\text{-}cis\text{-}a,e\text{-}14\text{-}CDA)_2(H_2O)_2]$ (a,b) and $[Cu_2(trans\text{-}e,e\text{-}14\text{-}CDA)_2]$ (c,d). The figures are adapted from [38].

antiferromagnetic interaction resulting in singlet–triplet gaps of 493 and 457 K.

Recently Chen and Long combined the strategy of generating triangular frustrated lattices and assembling ferromagnetic chains into two-dimensional network to construct an unprecedented infinite inorganic $[Fe_2^{II}(\mu_4\text{-}O)Fe_2^{III}(\mu_4\text{-}O)]^{6n+}$ mixed-spin and mixed-valence chain in a carboxylate-bridged three-dimensional network [39]. The structure is accomplished by using two bis(μ_3-η^1:η^2) and one bis(*syn-syn*) *trans*-14-CDA ligands to form a $[Fe^{II}Fe^{III}(\mu_4\text{-}O)(\mu_6\text{-}trans\text{-}e,e\text{-}14\text{-}CDA)_{1.5}]$ inorganic–organic hybrid array (Fig. 15). The material exhibits complex magnetic behavior including extensive electronic delocalization between 225 and 310 K, spin frustration in a one-dimensional ferrimagnetic chain above 36 K, interchain exchange interactions that lead to three-dimensional ferrimagnetic ordering below 32 K, and possibly relaxation dynamics of the spins between two different spin-canted magnetic structures or relaxation in a single-chain magnet below 22 K. In addition, as clearly revealed by Mössbauer spectrum study and magnetic susceptibility measurements, this material undergoes a charge order–disorder transition centered at about 275 K

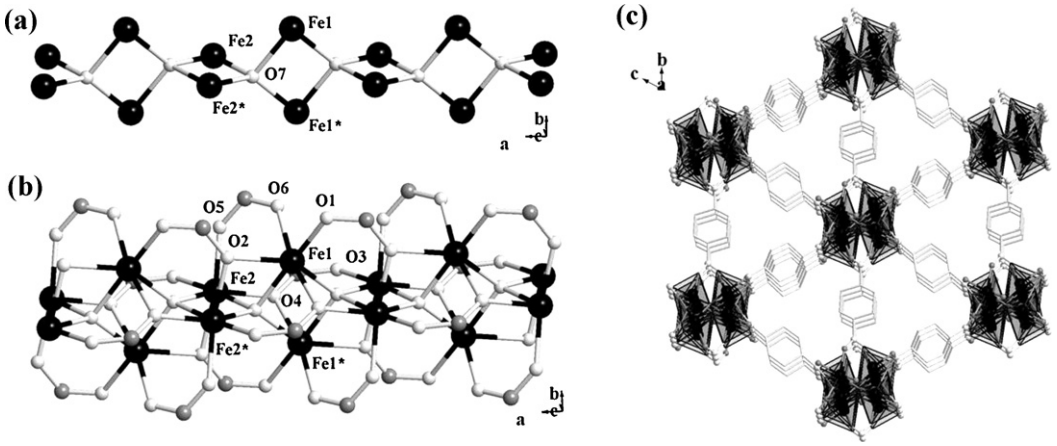

Fig. 15. Structure of $[Fe^{II}Fe^{III}(\mu_4\text{-}O)(\mu_6\text{-}trans\text{-}e,e\text{-}14\text{-}CDA)_{1.5}]$: carboxylate-supported tetrahedral chain (a) and (b), and the framework viewed down the *a*-axis (c). The figures are adapted from [39].

with the charge disorder state occurring through electron tunneling between the two minima in the energy surface or tunneling via vibronic coupling between two iron 3d orbitals.

4. The coordination chemistry of cyclohexanetricarboxylate

Benzenetricarboxylic acid has three isomers, *i.e.* 1,2,3-benzenetricarboxylic acid (hemimellitic acid), 1,2,4-benzenetricarboxylic acid (trimellitic acid) and 1,3,5-benzenetricarboxylic acid (trimesic acid), and cyclohexanetriboxylic acid was supposed to have more structural isomers due to more potentially available substitutable sites on the saturated hydrocarbon ring. However, only 1,3,5-cyclohexanetricarboxylic acid (135-CTA) and 1,2,4-cyclohexanetricarboxylic acid (124-CTA) are commonly commercially available and most research on the coordination chemistry of cyclohexanetriboxylic acid have been focused upon 135-CTA.

4.1. Coordination compounds based on 1,3,5-cyclohexanetricarboxylate

Addition of extra functional groups onto the ring could in principle increase the number of geometrical isomers, as we have discussed in the section of cyclohexanedicarboxylate ligands. Very few conformational transformations for 135-CTA have been reported so far and the ligand exists in the most stable *cis*,*cis*-*e*,*e*,*e*-form in organic adducts and even coordination compounds. The only reported example for *trans*,*trans*-*a*,*e*,*e*-135-CTA in solid state is a supramolecular entity where 135-CTAs are trapped in tripodal amidopyridine receptor [40]. The receptor forms a 1:1 complex with *trans*-135-CTA that is 10 times less stable than the one formed with the corresponding *cis*-isomer due to geometrical features of the ligand (Fig. 16).

1,3,5-Cyclohexanetricarboxylic acid has been extensively used to construct multi-component supramolecular architectures in investigation of hydrogen bonding and self assembly by Nangia [41] and other research groups [42]. The popularity of 135-CTA in crystal engineering may originate from nice solubility in common organic solvents and more importantly, from trimesic acid which is an archetypical organic scaffold for self-assembly of hexagonal (6,3) nets. The supramolecular diversity and complexity of hydrogen bonded networks can be expanded if trimesic acid is replaced by the conformationally flexible and nonplanar 135-CTA. Organic crystals can be very fragile to change in molecular structures because hydrogen bonds are an order of magnitude weaker than metal–ligand coordination bonds (7–15 kcal/mol vs 40–80 kcal/mol) [43], leading to great structural variety in co-crystals.

Similar to the unsaturated trimesic acid, saturated 135-CTA is able to carry three different charges −1, −2 and −3 depending on reaction conditions. In the case of partial deprotonation, 135-CTA acts as an unbonded counterion [44] or links one [45] or two [46] metal ions like 1-CHA and 13-CDA in the monodentate or bis(monodentate) modes whereas it can bridge up to seven metal centers [47] as a multidentate ligand upon full deprotonation. Seemingly the flexible backbone has less influence on the resultant frameworks as it does for the cyclohexanedicarboxylate compounds. Symmetry elements can also be observed on the cyclohexane ring in some 135-CTA coordination complexes, leading to formation of (6,3) honeycomb sheets. For instance, a mirror plane rides perpendicular to the aliphatic ring in $[Zn_3(135\text{-}CTA)_2(4,4'\text{-bipy})]\cdot(DMF)(H_2O)$ [48] and a three-fold rotation axis runs through the center of cyclohexane in $[Ag_3(135\text{-}CTA)(bsd)_3]\cdot 1.5bsd\ 3.5H_2O$ (bsd = 2,1,3-benzoselenadiazole) [49].

Qiu et al. prepared a family of manganese, zinc and cadmium 135-CTA coordination compounds in the presence of different organic bases including triethylamine (TEA), triethylenediamine (TED), hexamethylenetetramine (hmt), 4,4′-bipyridine (4,4′-bipy) and *trans*-bis(4-pyridyl)ethylene (bpe) from different solvents such as water, dimethylformamide (DMF), ethylene glycol (EG) and ethanol [47,48,50]. 135-CTA has versatile coordination manners in these complexes, resulting in 3D non-interpenetrating architectures in various topologies. It is of particular interest that all of them are composed of trinuclear $M_3(135\text{-}CTA)_8$ secondary building units (SBUs) (Fig. 17). The ancillary bridging amines do not play a critical role in the formation of such a SBU and when the amine is replaced with other terminal ligands, the trinuclear $M_3(135\text{-}CTA)_8$ can also be obtained, as shown in $[Mn_3(\mu_7\text{-}135\text{-}CTA)_2(DMF)_2]$, $[Cd_3(\mu_6\text{-}135\text{-}CTA)(\mu_7\text{-}135\text{-}CTA)(H_2O)_3]\cdot H_2O$ [47] and $[Zn_3(\mu_6\text{-}135\text{-}CTA)(C_5H_5N)_2(DMF)_2]$ [51].

In addition, not only metals with half and full occupied *d*-orbitals can form the trinuclear motif with 135-CTA, such SBU has also been observed in the cobalt and nickel compounds $[M_3(\mu_6\text{-}135\text{-}CTA)_2(\mu\text{-}H_2O)_2(H_2O)_2]\cdot 5H_2O$ [52]. In these compounds, eight 135-CTAs link three metal ions in the monodentate, *syn*-*syn* and $\mu_3\text{-}\eta^1\text{:}\eta^2$ fashions to form a trinuclear core. Neighboring $M_3(135\text{-}CTA)_8$ SBUs share one edge of their coordination octahedrons to form a zigzag chain (Fig. 18), which is further connected by 135-CTA into a non-interpenetrated 3D framework. The Co compound demonstrates dominant antiferromagnetic interaction within the SBU with a tendency to ferrimagnetic alignment at low temperatures, and the Ni complex exhibits mostly ferromagnetic interactions.

The reported investigations in coordination chemistry of 135-CTA with lanthanides are mainly focused on heavy rare earth metals, *i.e.* from terbium to ytterbium. Hydrothermal [53] or room temperature solvent diffusion [54] reactions yielded several lan-

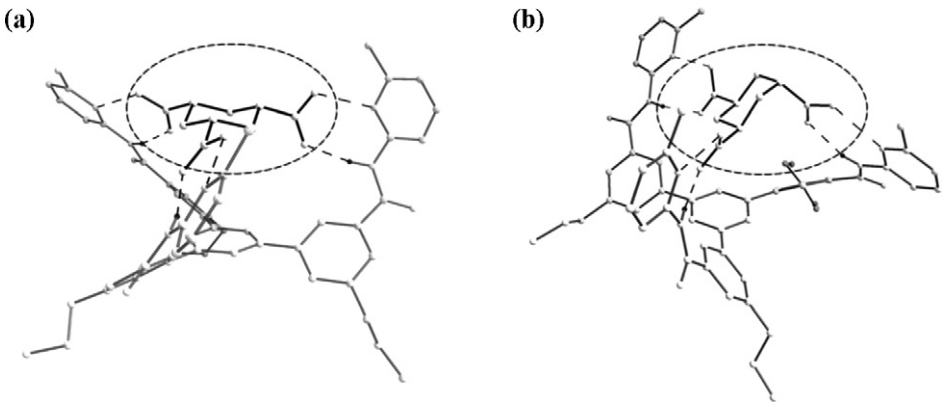

Fig. 16. X-ray structures of the 1:1 complexes composed of tripodal host and *cis*,*cis*-*e*,*e*,*e*-1,3,5-CTA (a) or *trans*,*trans*-*a*,*e*,*e*-135-CTA (b). The figures are adapted from [40].

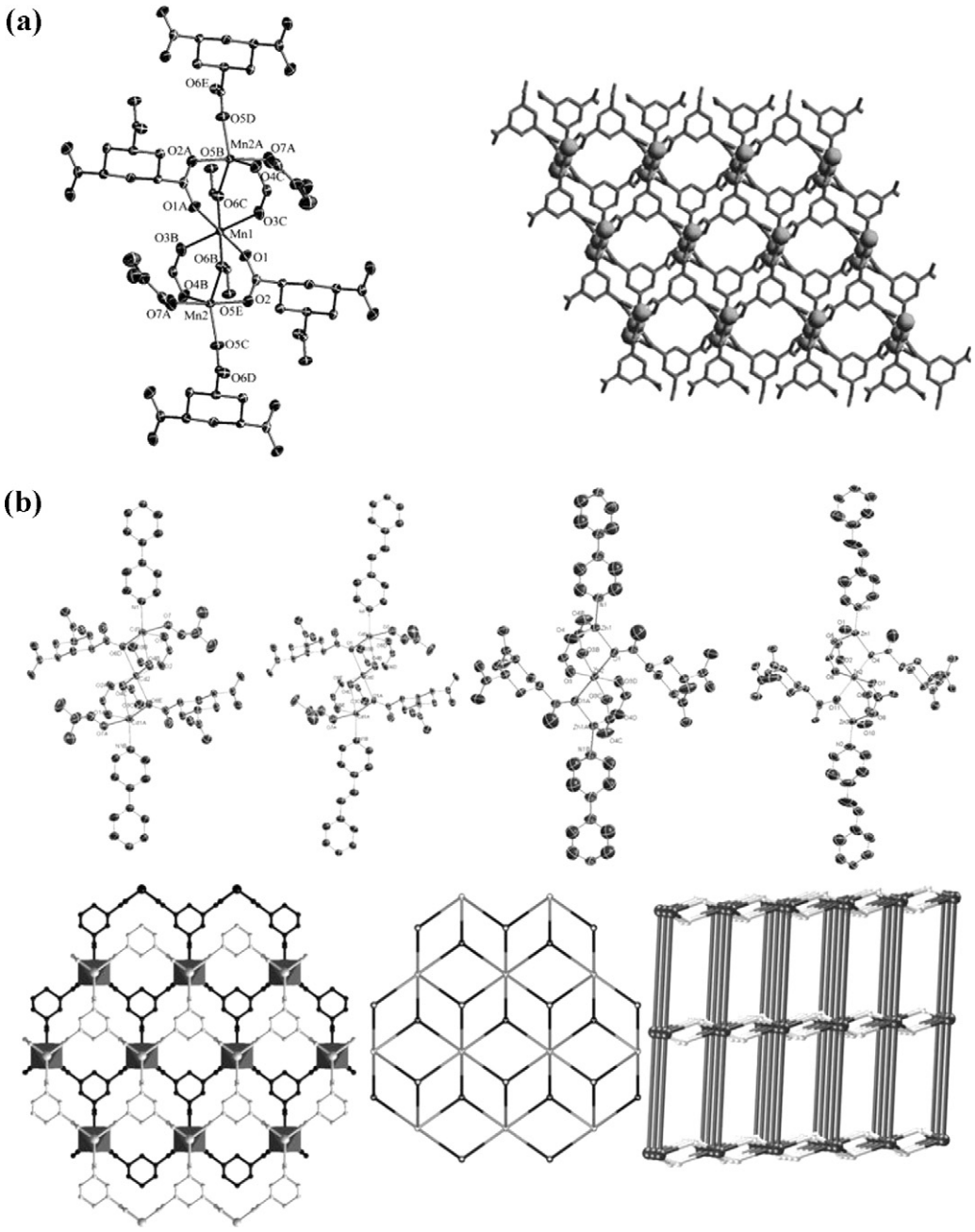

Fig. 17. (a) Typical M_3(135-CTA)$_8$ SBU in [$Mn_3(\mu_7$-135-CTA)$_2$(DMF)$_2$] and its packing diagram [47]; (b) trinuclear M_3(135-CTA)$_8$ SBUs in zinc/cadmium 135-CTA coordination compounds constructed with 4,4′-bipy/bpe (top), their two-fold alternate (6,3) honeycomb net and the topology of 3D networks (bottom) [48]. The figures are adapted from [47,48].

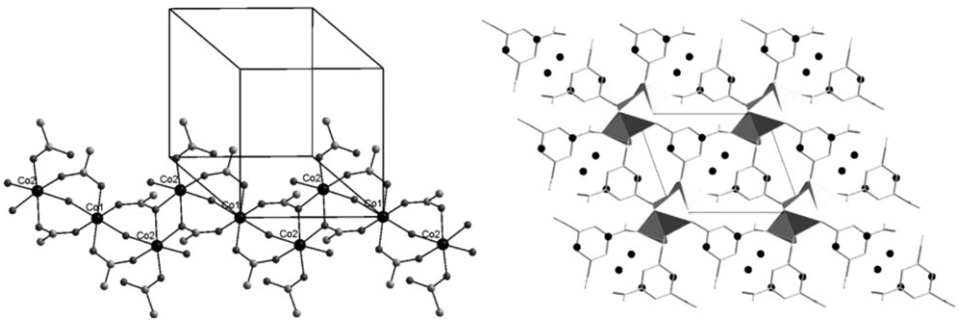

Fig. 18. A zigzag chain composed of M_3(135-CTA)$_8$ SBUs in [$M_3(\mu_6$-135-CTA)$_2(\mu$-$H_2O)_2(H_2O)_2$]·5H_2O (M = Co and Ni) and the packing diagram in which the oxygen atoms of the water molecules are shown as black circles. The figures are adapted from [52].

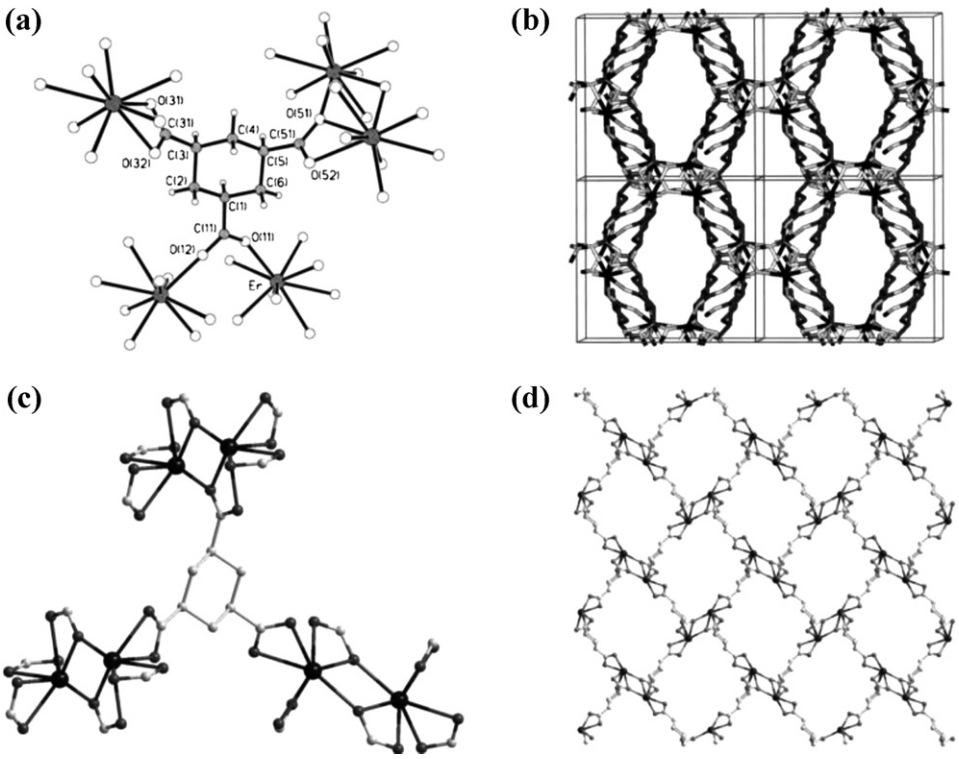

Fig. 19. (a) Coordination environment of 135-CHA in $[Ln(\mu_5\text{-}135\text{-}CTA)(H_2O)_2]\cdot 2.5H_2O$ (Ln = Dy, Ho, Er, Tm and Yb); (b) packing diagram $[Ln(\mu_5\text{-}135\text{-}CTA)(H_2O)_2]\cdot 2.5H_2O$ with 1D tubular channels [53,54]; (c) coordination environment of 135-CHA in $[Ln(\mu_7\text{-}135\text{-}CTC)(DMF)(H_2O)]\cdot(DMF)(H_2O)$ (Ln = Tb, Dy, Ho, Er and Tm); (d) packing diagram of $[Ln(\mu_7\text{-}135\text{-}CTC)(DMF)(H_2O)]\cdot(DMF)(H_2O)$ showing a microporous 3D network in a Rutile topology [55]. The figures are adapted from [53–55].

thanide compounds $[Ln(\mu_5\text{-}135\text{-}CTA)(H_2O)_2]\cdot 2.5H_2O$ (Ln = Dy, Ho, Er, Tm and Yb). The *syn-syn* and $\mu_2\text{-}\eta^1\text{:}\eta^2$ carboxylate groups link the lanthanide ions into an infinite Ln(COO) linear array, which is further connected by 135-CTA via the remaining carboxylate in a chelating mode into a 3D coordination networks with 1D tubular channels (Fig. 19). The materials decomposed at above 250 °C. The integrity of the erbium framework losing 1 equiv of coordinated water remained the same as the original sample and complete dehydration of coordinated aqua molecules irreversibly changed the framework structure [53]. Liquid diffusion in a mixture of DMF and water produced new types of lanthanide compounds $[Ln(\mu_7\text{-}135\text{-}CTC)(DMF)(H_2O)]\cdot(DMF)(H_2O)$ (Ln = Tb, Dy, Ho, Er and Tm) [55]. In these structures, the dinuclear metal center bridging by $\mu_2\text{-}\eta^1\text{:}\eta^2$ carboxylate is connected with six 135-CTA ligands as a six-connected node and each μ_7-135-CTA ligand connects with three dinuclear metal cores using two chelating carboxylate groups as a three-connected node. A microporous 3D network exhibiting a Rutile topology is thus formed with channels along the [1 0 0], [0 1 1] and [0 −1 1] directions. Thermogravimetric analysis indicated the materials decomposed at above 400 °C.

The metal ions in the above two phases are nine-coordinated in the LnO_9 polyhedra, where seven of the oxygen atoms come from the carboxylate groups of 135-CHA and the remaining two oxygen atoms are bound to solvent molecules. de Lill and Cahill used 4,4′-dipyridine as structure-directing agent, hoping to displace the excess water and change the overall channel topology [56]. This serendipitous discovery led to a very interesting, highly symmetric lanthanide-containing material $[Ln(\mu_6\text{-}135\text{-}CTA)]$ (Ln = Er and Tb) without intended guest molecules (Fig. 20). It is quite remarkable that each carboxylate group on 135-CTA exhibits simply *syn-syn* connectivity while the lanthanide ion is in an unusual low coordination of octahedral geometry. The cyclohexane ring of the ligand shows static disorder, indicating that it crystallizes in both the chair and boat conformations. The framework of this material is significantly stable up to 600 °C. According to the authors, the lack of such solvent molecules in the structure and the flexibility of the organic linker may be key factors that contribute to its strikingly high thermal stability. In architectures with more rigid ligands (*e.g.*, aromatics), it is perhaps more difficult to accommodate distortions in the structure caused by heating whereas a less rigid linker adds

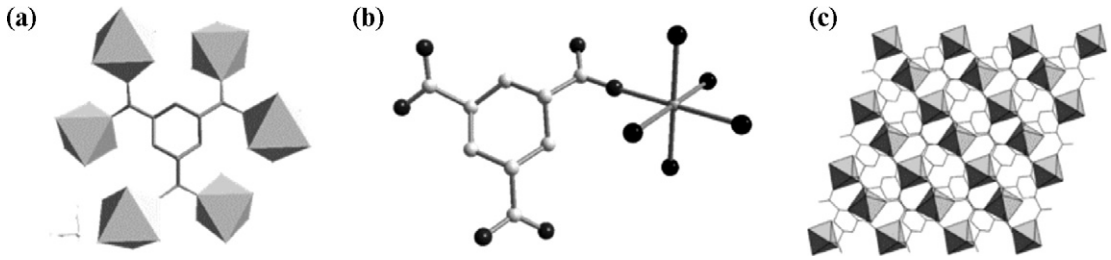

Fig. 20. (a) Coordination environment of 135-CHA in $[Ln(\mu_6\text{-}135\text{-}CTA)]$ (Ln = Er and Tb); (b) coordination environment of Ln^{3+} ion; (c) packing diagram viewed along the *c*-axis. The figures are adapted from [56].

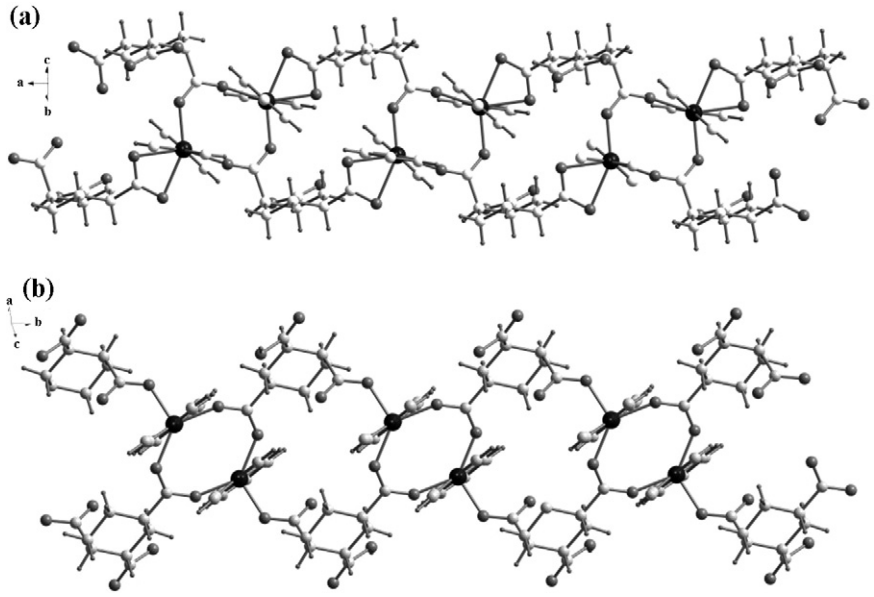

Fig. 21. Layered structures of [Co(μ_3-124-CHA-H)(4,4′-bipy)](H_2O) (a) and [Co(μ_3-124-CHA-H)(bpe)] (b), in which the layers are composed of Co_2(124-CHA-H)$_2$ chains connected via 4,4′-bipy or bpe [57].

a degree of flexibility that allows for small perturbations without breaking the coordination bonds.

4.2. Coordination compounds based on 1,2,4-cyclohexanetricarboxylate

1,2,4-cyclohexanetricarboxylic acid (124-CTA) is an almost undeveloped ligand in the field of coordination chemistry. In the systematic investigation of metal cyclohexanepolycarboxylate ligands, we have obtained two cobalt coordination compounds using 124-CTA, that is, [Co(μ_3-124-CHA-H)(4,4′-bipy)](H_2O) and [Co(μ_3-124-CHA-H)(bpe)] (bpe = *trans*-bis(4-pyridyl)ethylene) [57]. The two compounds have analogous layered structures, which are composed of Co_2(124-CHA-H)$_2$ chains connected via 4,4′-bipy or bpe linkers (Fig. 21). The 124-CTA-Hs in both compounds adopt the (1*a*, 2*e*, 4*e*) conformation with carboxylic group on the 2*e*-position. The small difference lies on the coordination behavior of 124-CHA, where in the 4,4′-bipy compound, the 1*a*-carboxylate links two cobalt atoms in a *syn-syn* mode and the 4*e*-COO^- connects one cobalt atom in a monodentate way while in the bpe compound, the 1*a*-carboxylate is in a monodentate manner and the 4*e*-COO^-, *syn-syn* mode.

5. The coordination chemistry of 1,2,4,5-cyclohexanetetracarboxylate

The only commercial available tetraacid is 1,2,4,5-cyclohexanetetracarboxylic acid (1245-CHA), which exists in the all-*cis*-1*e*,2*a*,4*a*,5*e*-form in solid state [58]. It is a far less explored ligand in coordination chemistry.

5.1. Conformation studies on 1,2,4,5-cyclohexanetetracarboxylate

Conformational transformation has been commonly observed for organic ligands with flexible backbones or adaptable conformations in metal complexes. Apparently, when there are more carboxylic groups on the cyclohexane ring, there will be more possible conformations; consequently, it is more difficult to control their orientations in the final coordination structures. The reaction conditions at which the conformational conversion would occur and the transformation mechanisms are vital to be understood in the field of coordination chemistry.

Theoretical calculation shows that 1245-CHA has four possible stable forms, that is **I**(*e*,*a*,*a*,*e*), **II**(*e*,*a*,*e*,*e*), **III**(*e*,*a*,*e*,*a*), and **IV**(*e*,*e*,*e*,*e*) (Scheme 6), in gas phase or as a solvate in water [59]. Free energy values indicate that **II** is the most stable while **I** is the least stable among the four conformations in both gas and solution phases (Fig. 22). Therefore the conformational change from **I** to **II**, **III**, or **IV** is thermodynamically feasible, which is in agreement with our observations that **II** and **IV** could be converted from **I** and trapped in various metal complexes under hydrothermal conditions. Notably the free energies for the four 1245-CHA isomers upon coordination in solid state may not be the same as those in gas or solution phases. The energy disadvantage can be compensated by coordination and in some cases, hydrogen-bonding interactions and the lattice energy of close packing. Although conformation **III** has similar free energy value to **II**, it has not yet been found. The possible reason that **I** can more easily transform to **II** or **IV** rather than to **III** may lie in the fact that when changing from **I** to **II** or **IV**, one or two *a*-COOH groups are required to turn into the *e*-positions, whereas for the transformation from **I** to **III**, two COOH groups are required

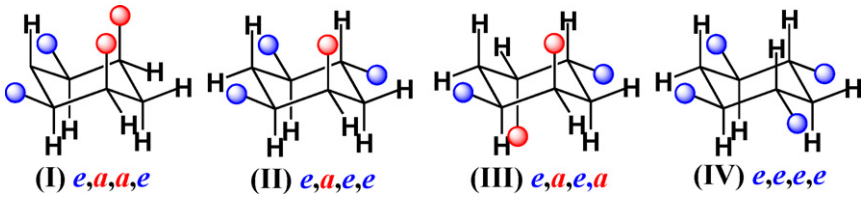

Scheme 6. Four possible stable conformations of 1245-CHA.

(a)

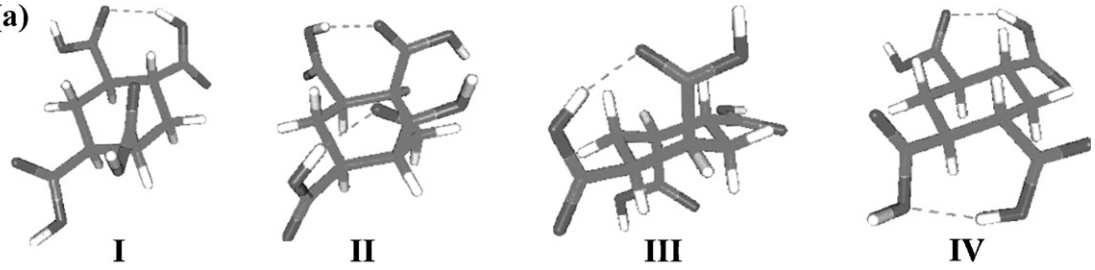

(b)

	gas phase		solvate in water	
	a.u.	kcal mol^{-1}(ΔG)	a.u.	kcal mol^{-1}(ΔG)
I	-989.964446	0	-990.007046	0
II	-989.987394	-14.40	-990.026199	-12.02
III	-989.983688	-12.07	-990.025561	-11.62
IV	-989.976385	-7.49	-990.016613	-6.00

Fig. 22. (a) Structures of conformations **I**(*e*,*a*,*a*,*e*), **II**(*e*,*a*,*e*,*e*), **III**(*e*,*a*,*e*,*a*), and **IV**(*e*,*e*,*e*,*e*) for 1245-CHA in water optimized by the B3LYP method and 6-21G (d,p); (b) free energies of various conformations and ΔG values compared with conformation **I**. The figures are adapted from [59].

to change their positions (4*a* to 4*e* and 5*e* to 5*a*). The conversion of 5-carboxylate from the *e*- to *a*-position is less likely owing to enthalpy and entropy preference as well as the steric hindrance.

The nature of metal ions may play a delicate role in controlling the orientations of carboxylate groups on the cyclohexane ring in the 1245-CHA system. In a previous study, diverse metal ions with different charge and ionic radii including Ag^{+}, Mn^{2+} [59], Co^{2+}, Ni^{2+} [60], Tb^{3+}, Yb^{3+} and Dy^{3+} [61] were employed in building coordination frameworks with 1245-CHA. The coordination bonds help to stabilize the energetically less favorable conformation and it is still the original form **I**(*e*,*a*,*a*,*e*) that exists in the ambient-temperature and low-temperature hydrothermal products.

Conformation **II** was found only in manganese compound [Mn_2(μ_7-1245-CHA$^{\mathbf{II}}$)(H_2O)$_3$], which was prepared at higher temperature (160 °C) for longer time (4 days) (Scheme 7). Such conformational transformation is in agreement with the theoretical calculation result that **II** is thermodynamically more stable. A different manganese compound [Mn_2(μ_8-1245-CHA$^{\mathbf{I}}$)(H_2O)$_2$] with form **I** coexisted in the same reaction. The amount of the phase with 1245-CHA in form **II** would increase with longer reaction duration and by carefully tuning the time, pure phases of two distinct manganese compounds could be obtained. Furthermore, the alkali metal ions used to adjust the pH values of the solution may also have some effect on the yield of different phases of the products. For reactions for the same time at 150 °C, the two manganese compounds with 1245-CHA in forms **I** or **II** were favorable in the presence of NaOH or KOH, respectively [59].

Auxiliary ligands also have some delicate influence on the conformations of flexible 1245-CHA [60]. In a family of cobalt compounds prepared at the same temperature (160 °C) and

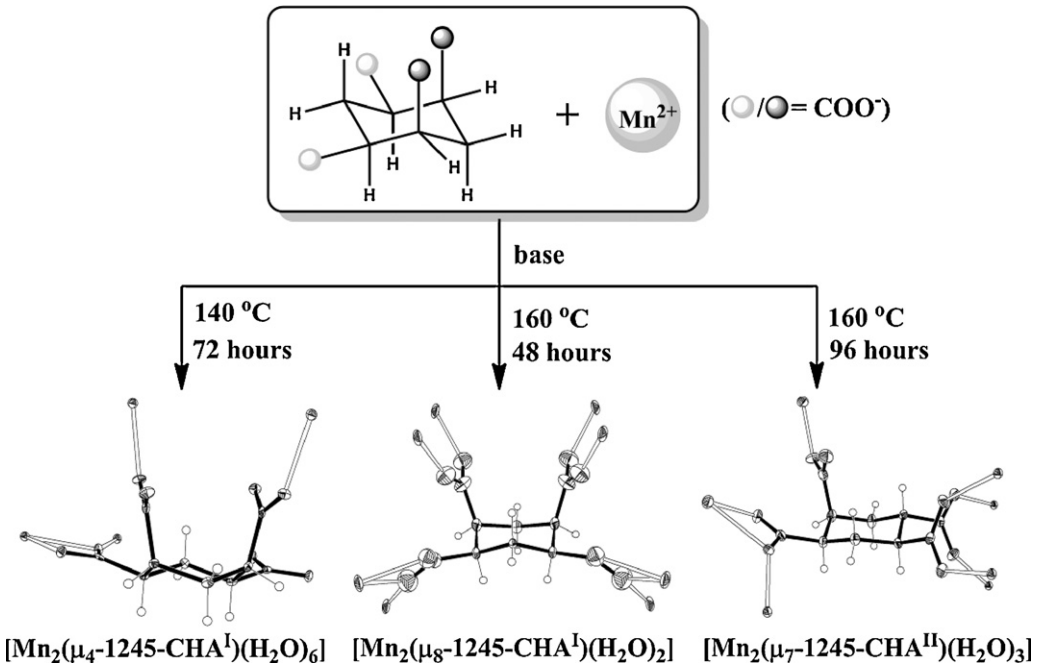

Scheme 7. Temperature- and time-dependent conformational transformation of 1245-CHA in the synthesis of manganese 1245-CHA compounds. The figures are adapted from [59].

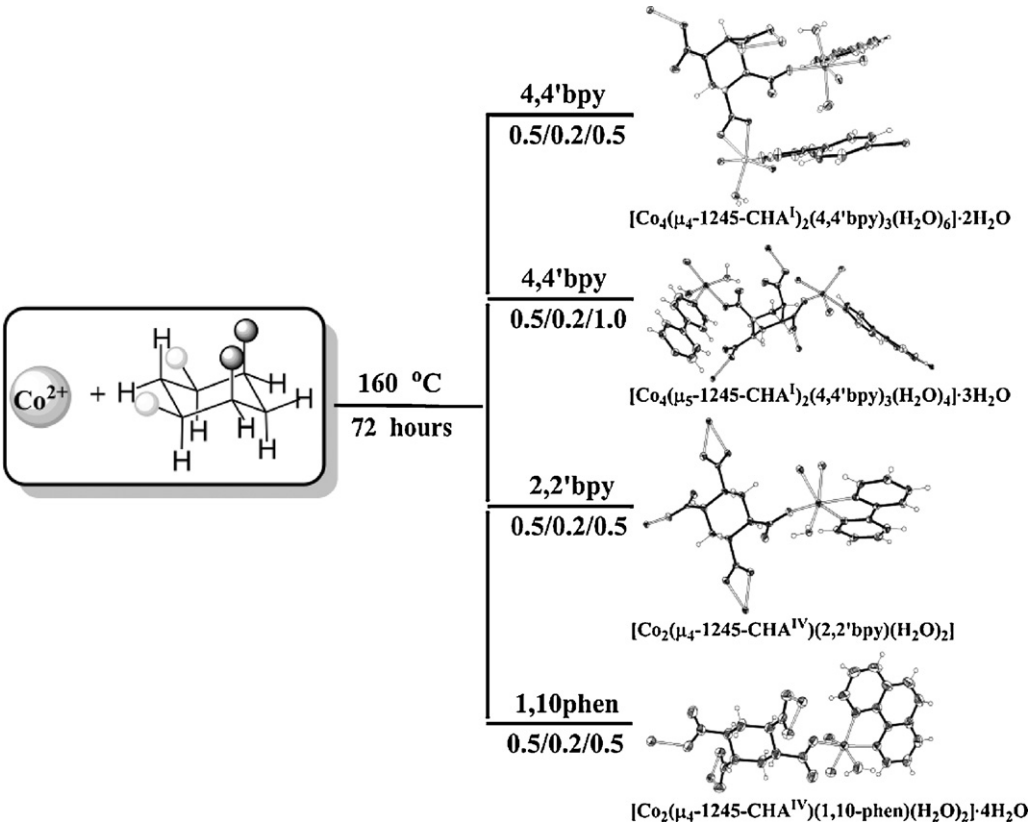

Scheme 8. Conformational transformation of 1245-CHA in the presence of different auxiliary ligands in the synthesis of cobalt 1245-CHA compounds. The figures are adapted from [60].

for the same reaction period (72 h) under hydrothermal conditions, the ligand remained the original conformation **I**(*e*,*a*,*a*,*e*) in compounds $[Co_4(\mu_4\text{-}1245\text{-}CHA^{I})_2(4,4'\text{-}bipy)_3(H_2O)_6]\cdot 2H_2O$ and $[Co_4(\mu_5\text{-}1245\text{-}CHA^{I})_2(4,4'\text{-}bipy)_3(H_2O)_4]\cdot 3H_2O$ when using linear 4,4′-bipy as the ancillary ligand; nevertheless, it converted to the fourth conformation **IV**(*e*,*e*,*e*,*e*) in compounds $[Co_2(\mu_4\text{-}1245\text{-}CHA^{IV})(2,2'\text{-}bipy)_2(H_2O)_2]$ and $[Co_2(\mu_4\text{-}1245\text{-}CHA^{IV})(1,10\text{-}phen)_2(H_2O)_2]\cdot 4H_2O$ when the chelating ligands 2,2′-bipy or 1,10-phenanthroline (1,10-phen) were introduced (Scheme 8). In the case where there existed both linear and chelating ligands, the chelating ligand could still promote the conformational transformation from forms **I** to **IV**, as shown in $[Ni_4(\mu_2\text{-}OH)_2(\mu_6\text{-}1245\text{-}CHA^{IV})_2(pymc)(4,4'\text{-}bipy)(H_2O)_2](OH)\cdot 9H_2O$ (pymc = 2-pyrimidinecarboxylate) [62].

In a previous section, the three conformations of 1,4-cyclohexanedicarboxylic acid (14-CDA) were inter-convertible in a reversible equilibrium. The proposed mechanism is that the *a*-protons attached to the 1,4-carbons of cyclohexane can be easily removed, which accelerates the interconversion equilibrium between the different conformations [63]. However, the details of reaction mechanism and intermediates needed further clarification. One of the most direct and reliable methods is to trap the proposed transformation intermediates of 1245-CHA in order to study and support the mechanism of conformational transformation. Accordingly relatively reactive and catalytically active metal ion Cu^{2+} was chosen to react with 1245-CHA, hoping to trap the intermediates during the reaction. As expected, hydrothermal reaction of copper acetate, 1245-CHA and 4,4′-bipy produced yellow lamellar crystals of $[Cu^{I}(4,4'\text{-}bipy)(H_2O)]_2(ip)\cdot 2H_2O$ (H_2ip = isophthalic acid) [64]. The successful isolation of isophthalate from the reaction system of $Cu(OAc)_2$, 1245-CHA and 4,4′-bipy helped to confirm the α-proton removal conformational transformation mechanism.

During the hydrothermal reaction, the removal and re-assembly of α-protons are in an equilibrium process and even a trivial change in reaction condition would break the equilibrium (Scheme 9). For metal coordination compounds with 1245-CHA in forms **I**, **II** or **IV**, the ligand was inclined to accept α-protons and kept integral in the resulted frameworks. In the copper compound, Cu^{2+} ions were reduced into Cu^{+}, whereas the 1245-CHA ligand became isophthalic acid via removing two carboxylate groups and two α-protons. Here redox reaction might play a vital role in favor of decarboxylation and removal of α-protons.

5.2. Coordination compounds based on 1,2,4,5-cyclohexanetetracarboxylate

It is not surprising that 1245-CHA links different metal ions as a multidentate ligand in versatile manners. For example in the manganese family, the ligand in conformation **I**(*e*,*a*,*a*,*e*) connects Mn^{2+} as μ_4 and μ_8-linkers, leading to formation of a 1D chained structure $[Mn_2(\mu_4\text{-}1245\text{-}CHA^{I})(H_2O)_6]$ with dinuclear manganese units and a 3D coordination network $[Mn_2(\mu_8\text{-}1245\text{-}CHA^{I})(H_2O)_2]$ with infinite Mn-carboxylate chains, respectively [59]. The carboxylate groups on 1245-CHA in the low-dimensional complex adopt the $\mu_2\text{-}\eta^1\text{:}\eta^2$ (*e*-), monodentate (two *a*-) and unbonded modes whereas in the 3D compound, they adjust to the $\mu_2\text{-}\eta^1\text{:}\eta^2$ (two *e*-) and *syn-syn* (two *a*-) fashion, resulting in antiferromagnetic interaction between the manganese ions in both compounds. By careful control of reaction conditions, a third manganese compound $[Mn_2(\mu_7\text{-}1245\text{-}CHA^{II})(H_2O)_3]$ was obtained, where 1245-CHA existed in form **II**. The ligands link the metal centers into a 3D network consisting of typical $Mn_2(COO)_4$ paddle wheels in the $\mu_2\text{-}\eta^1\text{:}\eta^2$ (*e*-), *syn-syn* (two remaining *e*-) and monodentate (*a*-) modes (Fig. 23). The difference in coordination behaviors between the *a*- and *e*-carboxylate groups for conforma-

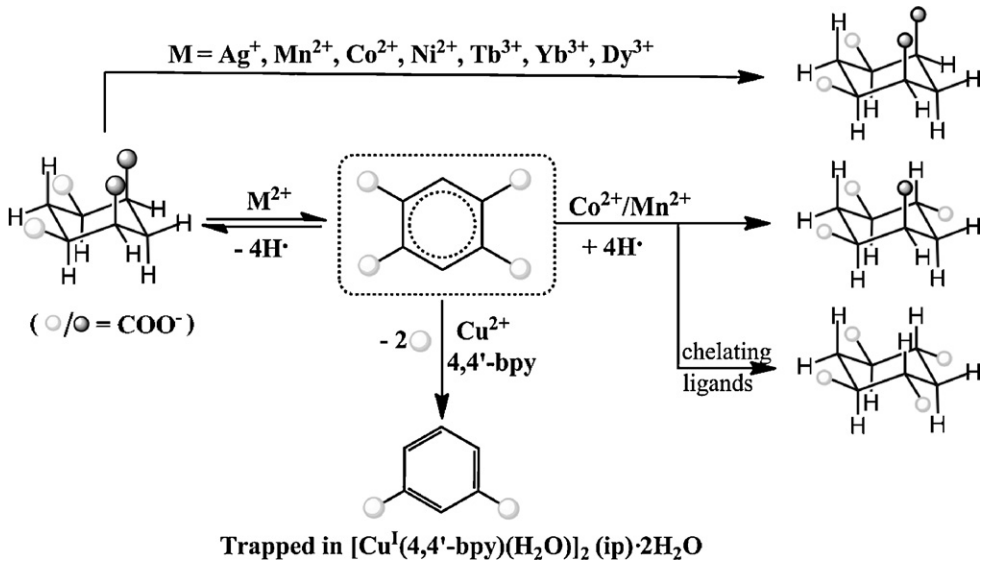

Scheme 9. Possible reaction mechanism of the conformational transformation of 1245-CHA under hydrothermal conditions.

tions **I** and **II** suggest that the conformational transformation of the ligand should occur in solution and phase conversion in different manganese compounds might involve a coordination disassembly and re-assembly process.

The cobalt 1245-CHA series, where conformational transformation from **I** to **IV** was observed, showed similar changes in the coordination of the ligand. 1245-CHAs assemble the cobalt ions into two 3D frameworks $[Co_4(\mu_4\text{-1245-CHA}^{\mathbf{I}})_2(4,4'\text{-bipy})_3(H_2O)_6]\cdot 2H_2O$ via the monodentate (*e*- and *a*-) and chelating (*e*- and *a*-) manners and $[Co_4(\mu_5\text{-1245-CHA}^{\mathbf{I}})_2(4,4'\text{-bipy})_3(H_2O)_4]\cdot 3H_2O$ via the *syn-syn* (*e*-) and monodentate (*e*- and two *a*-) way, respectively [60]. When the ligand is in conformation **IV**, it links Co^{2+} via the monodentate (two *e*-) and chelating (two *e*-) modes and along with 2,2′bipy or 1,10-phen, forms 1D tape structures $[Co_2(\mu_4\text{-1245-CHA}^{\mathbf{IV}})(2,2'\text{-bipy})_2(H_2O)_2]$ and $[Co_2(\mu_4\text{-1245-CHA}^{\mathbf{IV}})(1,10\text{-phen})_2(H_2O)_2]\cdot 4H_2O$ (Fig. 24).

In the case of lanthanide 1245-CHA compounds, the ligand in form **I** bridges the Ln^{3+} via the monodentate (*a*-), *syn-anti* (*a*-) and chelating (two *e*-) styles into a two-fold interpenetrated 3D framework $[Ln_4(\mu_4\text{-1245-CHA}^{\mathbf{I}})_3(H_2O)_{10}]\cdot 9H_2O$ (Ln = Tb, Yb and Dy) [61]. The most interesting structural features for these three compounds is that a unique $(H_2O)_{14}$ water cluster, which is the derivative of theoretically unstable $(H_2O)_{12}$ cluster, and a truncated cubic $(H_2O)_{12}$ cluster originated from coordinated and lattice water molecules were captured within the pores between two interpenetrating networks (Fig. 25). The terbium compound has intense green luminescence characteristic of Tb^{3+} ion in the visible region while the ytterbium complex exhibits near-infrared (NIR) luminescence properties.

Li et al reported three complexes $[Co_5(\mu_3\text{-OH})_2(\mu_5\text{-1245-CHA}^{\mathbf{I}})_2(H_2O)_{10}]\cdot 2H_2O$, $[Zn_2(\mu_7\text{-1245-CHA}^{\mathbf{I}})(H_2O)_3]\cdot H_2O$ and $[Cd_2(\mu_5\text{-1245-CHA}^{\mathbf{I}})(H_2O)_5]\cdot 2H_2O$ prepared from hydrothermal

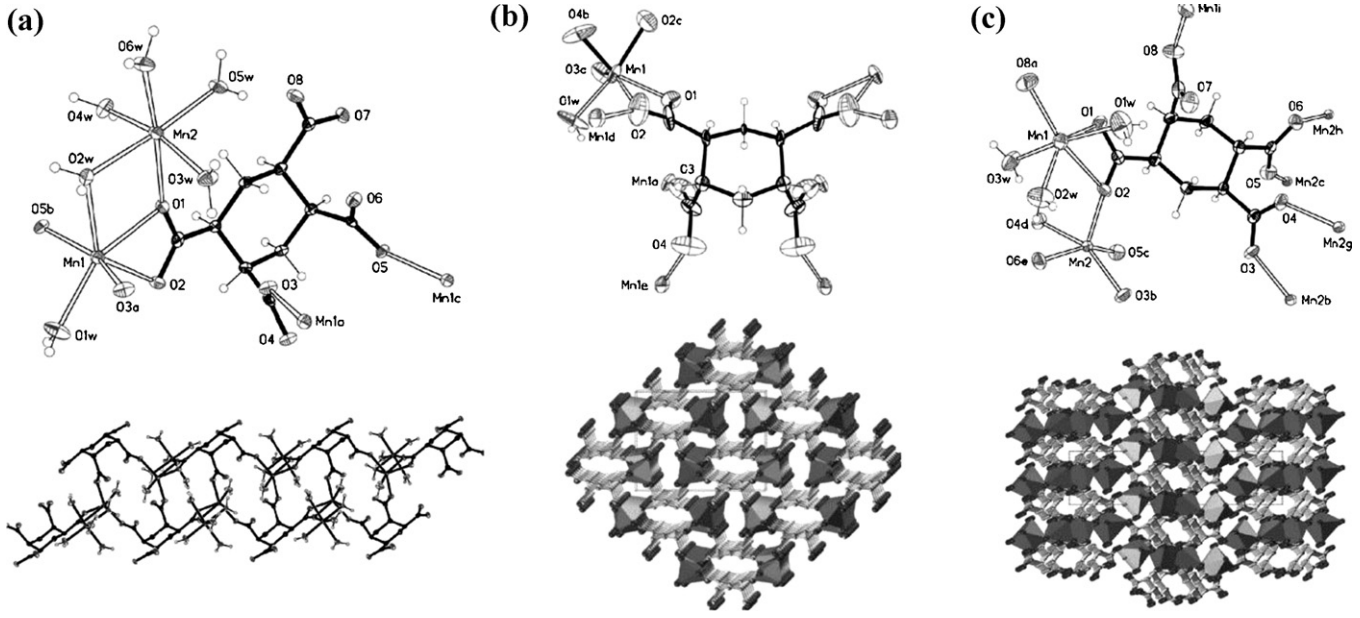

Fig. 23. (a) The bridging mode of 1245-CHA$^{\mathbf{I}}$ and the 1D chain with dinuclear manganese units in $[Mn_2(\mu_4\text{-1245-CHA}^{\mathbf{I}})(H_2O)_6]$; (b) the bridging mode of 1245-CHA$^{\mathbf{I}}$ and the 3D coordination network of $[Mn_2(\mu_8\text{-1245-CHA}^{\mathbf{I}})(H_2O)_2]$ viewed along the *a* axis; (c) the bridging mode of 1245-CHA$^{\mathbf{II}}$ and the 3D network of $[Mn_2(\mu_7\text{-1245-CHA}^{\mathbf{II}})(H_2O)_3]$ along the *c* axis. The figures are adapted from [59].

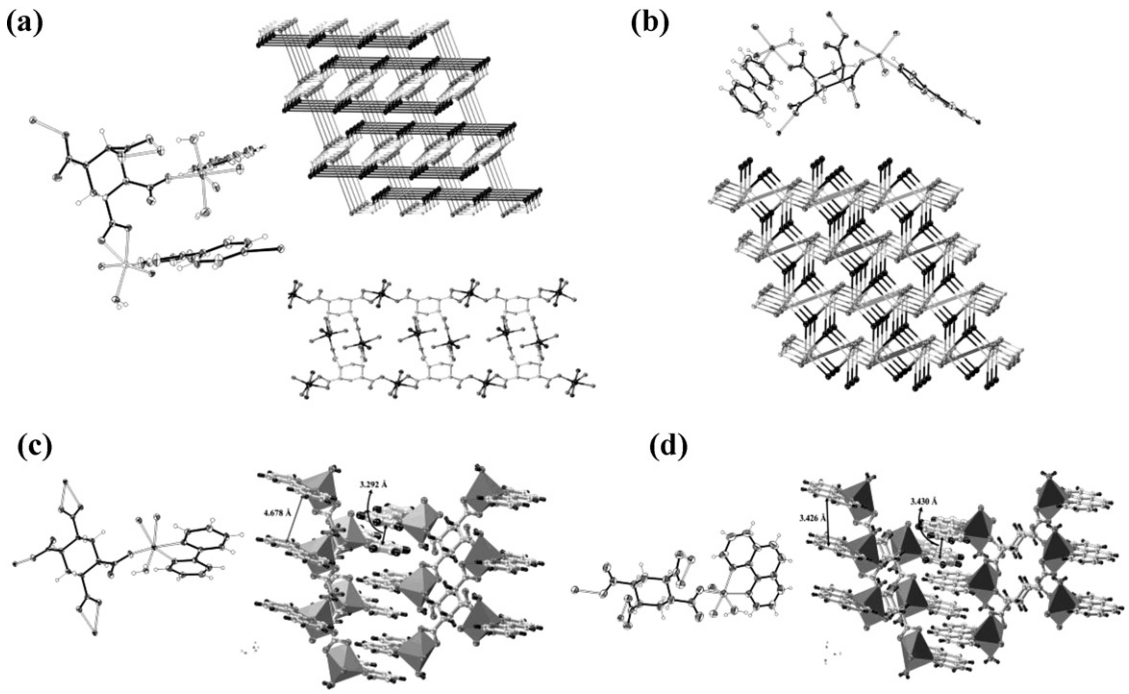

Fig. 24. (a) The bridging mode of 1245-CHA$^{\mathbf{I}}$ and the 3D network in $[Co_4(\mu_4\text{-}1245\text{-}CHA^{\mathbf{I}})_2(4,4'\text{-bipy})_3(H_2O)_6]\cdot 2H_2O$; (b) the bridging mode of 1245-CHA$^{\mathbf{I}}$ and the 3D network of $[Co_4(\mu_5\text{-}1245\text{-}CHA^{\mathbf{I}})_2(4,4'\text{-bipy})_3(H_2O)_4]\cdot 3H_2O$ viewed along the *b* axis; (c) the bridging mode of 1245-CHA$^{\mathbf{IV}}$ and the 3D network of $[Co_2(\mu_4\text{-}1245\text{-}CHA^{\mathbf{IV}})(2,2'\text{-bipy})_2(H_2O)_2]$; (d) the bridging mode of 1245-CHA$^{\mathbf{IV}}$ and the 3D network of $[Co_2(\mu_4\text{-}1245\text{-}CHA^{\mathbf{IV}})(1,10\text{-phen})_2(H_2O)_2]\cdot 4H_2O$. The figures are adapted from [60].

reactions, where 1245-CHA is in conformation **I** as well [65]. In the cobalt compound, the *a*- and *e*-carboxylate groups on the ligand in form **I**(*e*,*a*,*a*,*e*) have distinctive roles in constructing the coordination layer; that is, both *a*-carboxylate groups adopt the *syn-syn* manner to connect three metal ions and form a $Co_3(\mu_3\text{-}OH)_2(a\text{-}COO)_4$ chains while the *e*-carboxylate groups link another two cobalt ions in the monodentate and chelating modes and thus bridge the hydroxide chains into an infinite layer (Fig. 26). The zinc complex possesses a 3D MOF structure that consists of one μ_7-1245-CHA$^{\mathbf{I}}$ and two types of zinc atoms in tetrahedral

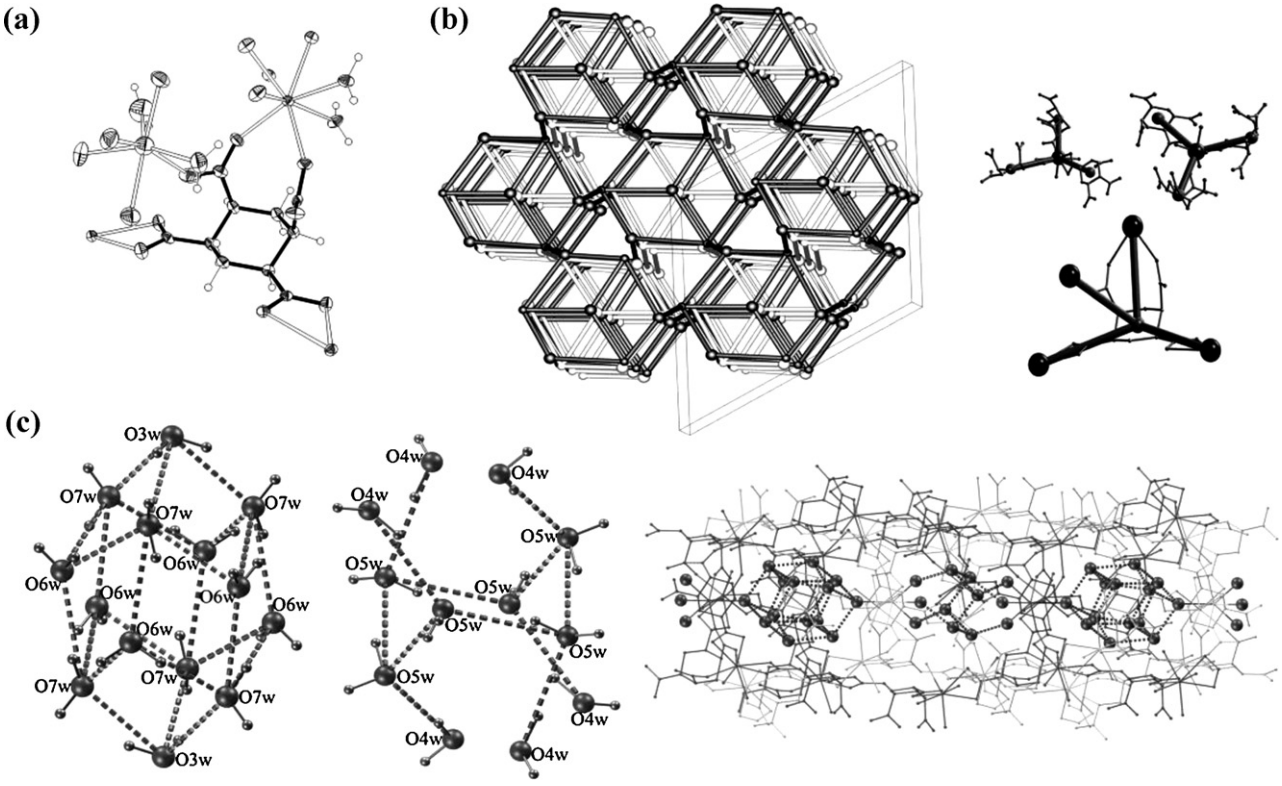

Fig. 25. (a) The bridging mode of 1245-CHA$^{\mathbf{I}}$ in $[Ln_4(\mu_4\text{-}1245\text{-}CHA^{\mathbf{I}})_3(H_2O)_{10}]\cdot 9H_2O$ (Ln = Tb, Yb and Dy); (b) two-fold interpenetrated (3,4)-connected topology network along the *c*-axis and (c) the two-fold interpenetrating host channels with two types of water clusters $(H_2O)_{14}$ and $(H_2O)_{12}$. The figures are adapted from [61].

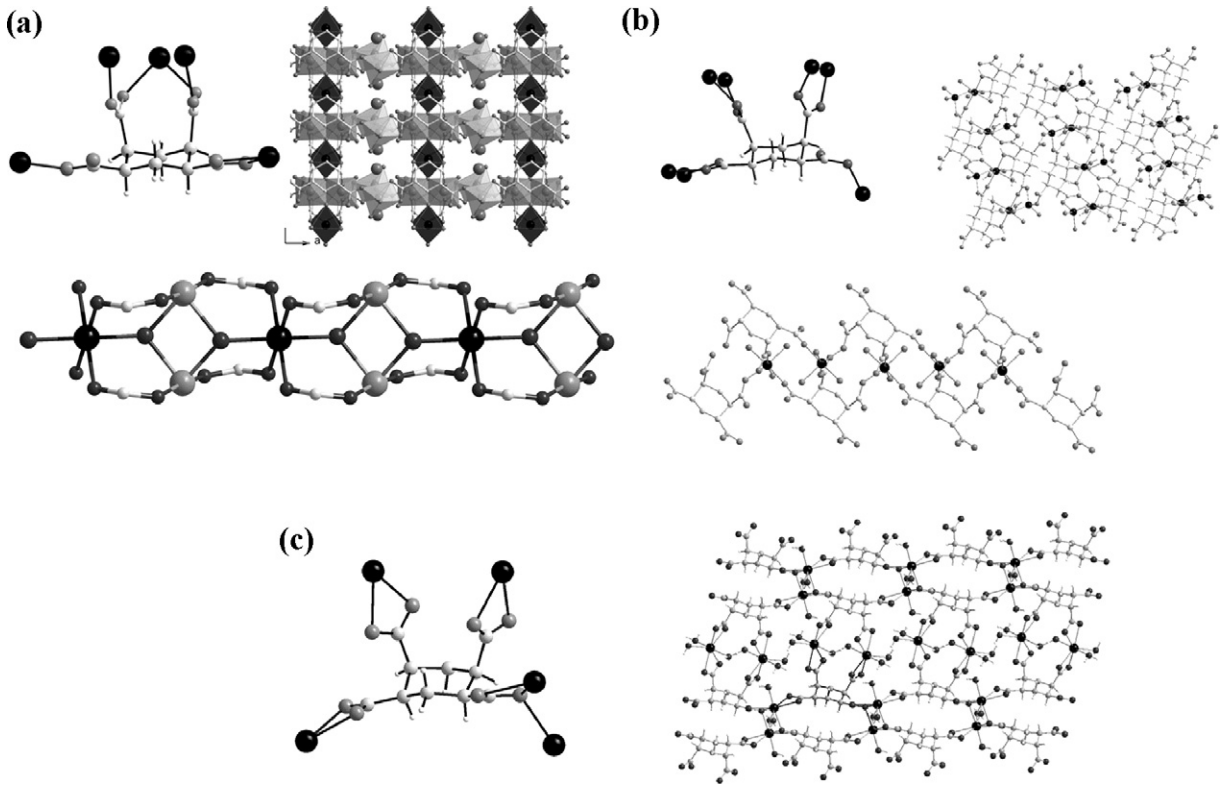

Fig. 26. (a) Structure $[Co_5(\mu_3\text{-}OH)_2(\mu_5\text{-}1245\text{-}CHA^{I})_2(H_2O)_{10}]\cdot 2H_2O$; (b) structure of $[Zn_2(\mu_7\text{-}1245\text{-}CHA^{I})(H_2O)_3]\cdot H_2O$; (c) structure of $[Cd_2(\mu_5\text{-}1245\text{-}CHA^{I})(H_2O)_5]\cdot 2H_2O$ [65].

and octahedral geometries. Each μ_7-1245-CHA^{I} bridges seven Zn^{2+} ions in the monodentate and *syn-syn* (two *a*- and one *e*-) styles. The cadmium compound has again a layered structure. The *e*-carboxylate groups of two parallel 1245-CHA^{I} ligands are connected to cadmium atoms via the chelating and μ_2-η^1:η^2 modes to form 1D chains, which are further linked through *a*-carboxylate groups in a chelating manner to assemble a 2D structure. The zinc and cadmium complexes showed strong fluorescent emissions in the blue region.

Very recently a family of novel organo-inorganic hybrid layered structures built from metal hydroxide chains and 1245-CHA exhibiting very interesting magnetic properties was prepared and systematically characterized in our group [66]. The three complexes are isostructural to each other and to the reported compound [65] with the formula of $[M_5(\mu_3\text{-}OH)_2(\mu_5\text{-}1245\text{-}CHA^{I})_2(H_2O)_{10}]\cdot 2H_2O$ (M_5 = Co_5, Ni_5 and $Ni_{3.9}Mn_{1.1}$). The single crystal structural determination of the Co and Ni-Mn compounds was carried out, while the nickel species was established by powder X-Ray diffraction by comparison with that of cobalt analogue since only a light green microcrystalline powder was obtained. The ratio of nickel to manganese in the Ni–Mn solid solution complex was confirmed by single crystal X-ray diffraction and energy-dispersive X-ray spectroscopy (EDXS). The magnetic properties of the three compounds have been studied employing different experimental protocols and using both ac- and dc-modes. In correlation with the feature of the $M_3(\mu_3\text{-}OH)_2$ chain subunits within the three structures, the onset of χT product could be probably the result of ferrimagnetic ground state. The χ values show the similar cusps, corresponding to the Néel temperature, at 5.8 K (Co_5), 3.2 K (Ni5) and 2.9 K ($Ni_{3.9}Mn_{1.1}$) at low applied fields. Curie–Weiss fits of the dc-susceptibilities data in the high temperature region give $C = 17.28\ cm^3$ K/mol and $\theta = -40.9$ K for the cobalt compound, $C = 7.30\ cm^3$ K/mol and $\theta = -8.70$ K for the nickle species, and $C = 10.40\ cm^3$ K/mol and $\theta = -37.90$ K for the Ni–Mn-mixed species, respectively. The negative values of the Weiss constants suggest antiferromagnetic interaction dominates the high temperature region (Figs. 27 and 28).

The moments are easily reversed in an applied field of 150 Oe (Co5) and 300 Oe (Ni_5 and $Ni_{3.9}Mn_{1.1}$) to a ferrimagnet with one uncompensated moment followed by a non-linear increase to saturation corresponding to a ferrimagnet with three uncompensated moments. Moreover, the cobalt species exhibits single-chain magnet behavior below 3 K, quite different from both nickle and nickle–manganese species.

6. The coordination chemistry of 1,2,3,4,5,6-cyclohexanehexacarboxylate

1,2,3,4,5,6-Cyclohexanehexacarboxylic acid (123456-CHA) is characteristic of multiple binding sites and pH-dependent versatile coordination modes. Similar to 1245-CHA, 123456-CHA has six potentially stable conformations [31], *i.e.* **I**(*a*,*e*,*a*,*e*,*a*,*e*), **II**(*e*,*e*,*e*,*e*,*e*,*e*), **III**(*e*,*e*,*e*,*e*,*a*,*a*), **IV**(*e*,*e*,*e*,*a*,*e*,*a*), **V**(*e*,*e*,*a*,*e*,*e*,*a*) and **VI**(*e*,*e*,*e*,*e*,*e*,*a*) (Scheme 10). Bulky substituents on a cyclohexane ring prefer to reside in the *e*-position to the *a*-position; however, in the case where cyclohexane bears six equivalent groups such as in 123456-CHA, the peripheral ring becomes very crowded when six neighboring carboxylate groups are situated on the all-*trans*-*e*-positions. The large steric hindrance may lead to a compromise of the energy difference between the *e*- and *a*-positions and accordingly the conformation of 123456-CHA becomes rather flexible [67].

The ligand crystallizes in monohydrate (123456-CHA·H_2O) in the all-*cis* conformation of **I** with extensive hydrogen bonds with each other and with the aqua molecules [68]. Comparatively, its hexamethyl ester has two conformations of **I**(*a*,*e*,*a*,*e*,*a*,*e*) [68] and **VI**(*e*,*e*,*e*,*e*,*e*,*a*) [69] prepared from different conditions (Fig. 29). It can be expected that 123456-CHA can adopt more versatile coor-

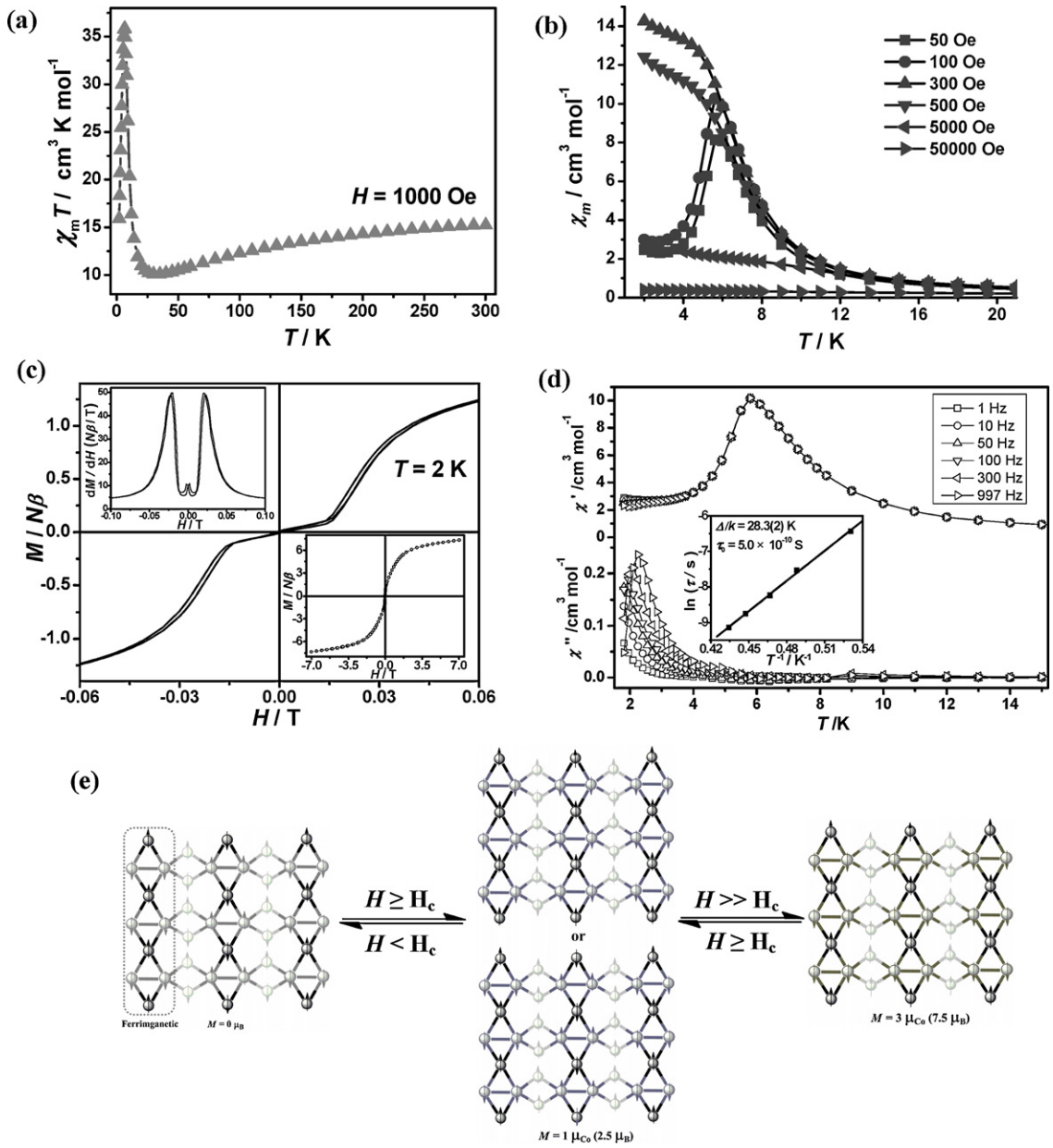

Fig. 27. Magnetic properties for $[Co_5(\mu_3\text{-}OH)_2(\mu_5\text{-}1245\text{-}CHA^{\mathbf{I}})_2(H_2O)_{10}]\cdot 2H_2O$: (a) temperature dependence of $\chi_M T$ (▲); (b) χ value in different dc fields at low temperatures; (c) the field-dependent magnetization in the range of −0.06 to 0.06 T at 2 K; (Inset) upper left, field dependence of dM/dH; lower right, the field-dependant magnetization in the range of −7 to 7 T at 2 K; (d) temperature dependence of the real (top) and imaginary (bottom) components of the ac susceptibility in zero applied static field with an oscillating field of 3 Oe at a frequency of 1–997 Hz; (Inset) linear fitted by Arrhenius law with the energy barrier of 28.3 K; (e) proposed magnetic structures in the three states (left: $H = 0$, middle: $H \geq H_c$, right: $H \gg H_c$) [66].

dination behavior in metal complexes in the presence of various metal ions. In this section, we will review the coordination chemistry of 123456-CHA and discuss its conformational transformation during the formation of metal coordination compounds.

6.1. Coordination compounds based on 1,2,3,4,5,6-cyclohexanehexacarboxylate

In the early investigation of the coordination chemistry of 123456-CHA, two silver coordination polymers, $[Ag_3(\mu_8\text{-}123456\text{-}CHA^{\mathbf{I}}\text{-}H_3)(H_2O)_2]\cdot 2H_2O$ and $[Ag_6(\mu_{13}\text{-}123456\text{-}CHA^{\mathbf{I}})(NH_3)(H_2O)_3]\cdot H_2O$, were reported obtained from room temperature reactions of $[Ag(NH_3)_2](OH)$ solution [70]. The first compound consists of the bis(*syn-syn*) and μ_3-η^1:η^2 carboxylato-supported Ag–Ag dimer chains, which are connected by the ligands via two monodentate carboxylate groups into a 3D coordination framework with 1D rectangular channels (Fig. 30). Notably the ligand is half protonated on three *a*-carboxylic groups in all-*cis* conformation **I**. The second silver complex also has a 3D MOF structure constructed by two types of Ag–Ag chains with Ag_8 cluster units and linear Ag_4 units, respectively. The ligand is fully deprotonated in form **I** as well, connecting thirteen silver atoms in the *syn-syn* (2*e*, 4*e* and 5*a*) and μ_3-η^1:η^2 (1*a*, 3*a* and 6*e*) manners.

In the recently reported lanthanide 123456-CHA compounds, the ligand is also in conformation **I** although the products were prepared either from slow evaporation at ambient temperature or hydrothermally at 180 °C. In the europium compounds $[Eu(123456\text{-}CHA^{\mathbf{I}}\text{-}H_3)(H_2O)_4]\cdot xH_2O$ with $x = 3$ or 6, three carboxylate groups are in the equatorial position and the carboxylic groups are axial [71]. The carboxylate groups are all chelating in the

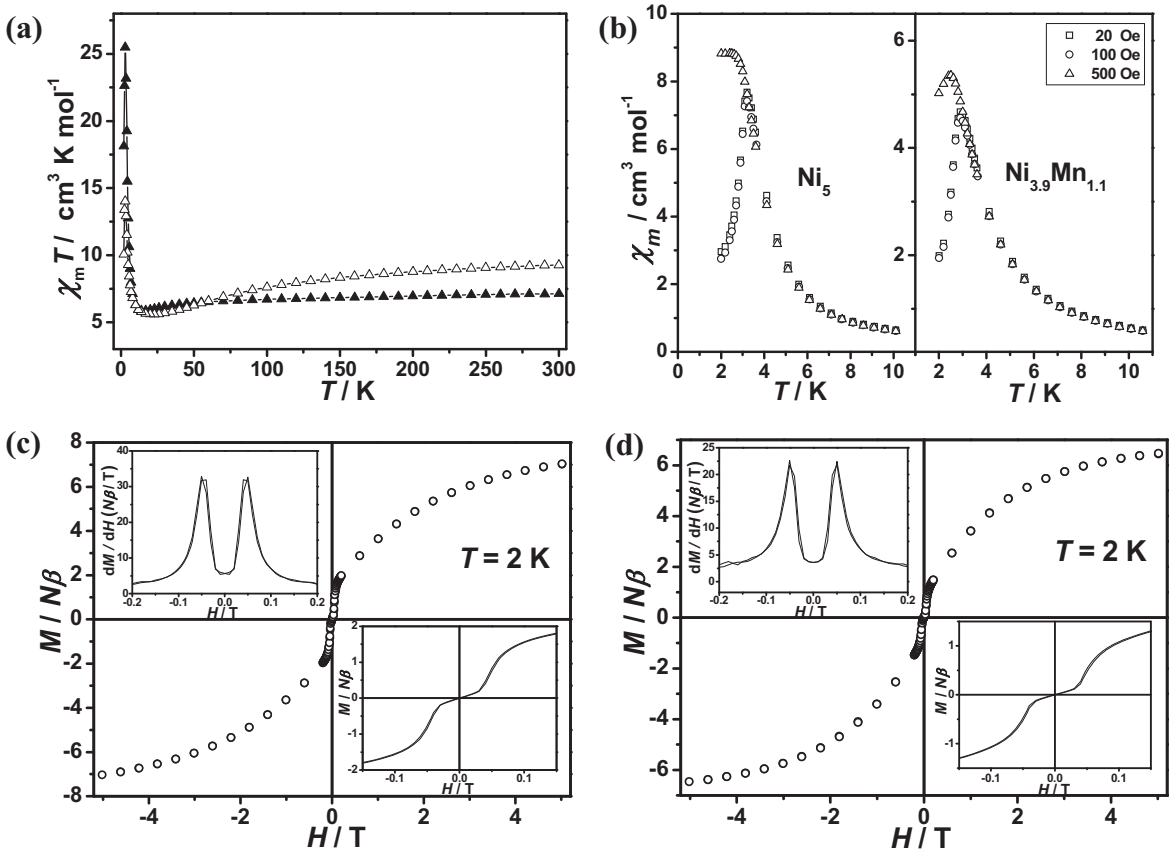

Fig. 28. The field-dependent magnetization in the range of −5 to 5 T at 2 K for $[Ni_5(\mu_3\text{-}OH)_2(\mu_5\text{-}1245\text{-}CHA^I)_2(H_2O)_{10}]\cdot 2H_2O$ (a) and $[Ni_{3.9}Mn_{1.1}(\mu_3\text{-}OH)_2(\mu_5\text{-}1245\text{-}CHA^I)_2(H_2O)_{10}]\cdot 2H_2O$ (b), (inset) upper left, field dependence of dM/dH; lower right, the field-dependant magnetization in the range of −0.15 to 0.15 T at 2 K [66].

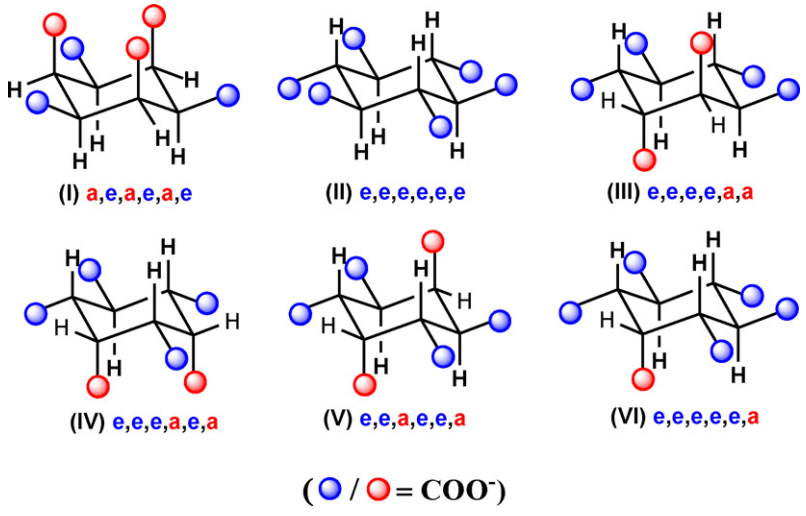

Scheme 10. Six possible stable conformations of 123456-CHA.

Fig. 29. Structure of 123456-CHA·H_2O in conformation **I**(*a,e,a,e,a,e*) (a) and its hexamethyl ester in **I**(*a,e,a,e,a,e*) (b) and **VI**(*e,e,e,e,e,a*) (c) forms. Hydrogen atoms are omitted for clarity. The figures are adapted from [68,69].

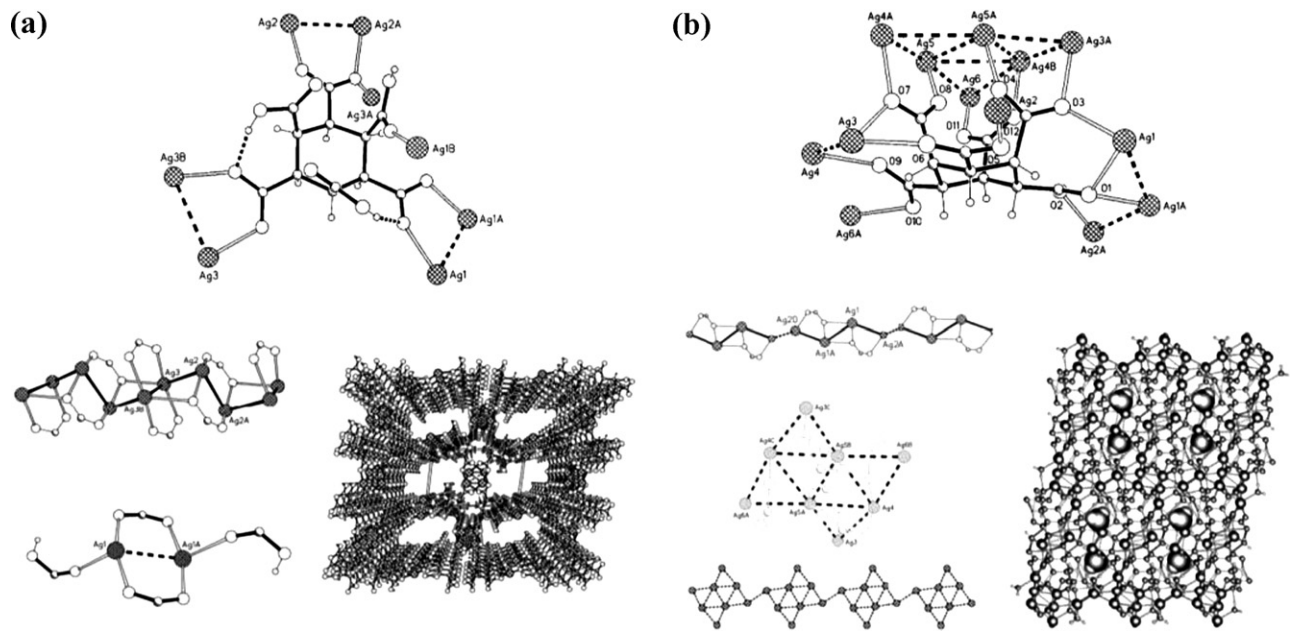

Fig. 30. Structures of $[Ag_3(\mu_8\text{-}123456\text{-}CHA^{I}\text{-}H_3)(H_2O)_2]\cdot 2H_2O$ (a) and $[Ag_6(\mu_{13}\text{-}123456\text{-}CHA^{I})(NH_3)(H_2O)_3]\cdot H_2O$ (b). The figures are adapted from [70].

trihydrate compound, giving a hexagonal 2D layer while in the hexahydrate complex three carboxylate groups are in the monodentate, chelating and *syn-anti* modes, and the resulting 2D assembly displays a tetragonal arrangement (Fig. 31). A serial of isomorphous complexes $[UO_2Ln(\mu_4\text{-}123456\text{-}CHA^{I}\text{-}H)(H_2O)_7]\cdot H_2O$ (Ln = Pr, Eu, Tb and Er) have analogous (6,3) hexagonal layered structures, where the three carboxylate groups of 123456-CHA on *e*-positions on the cyclohexane are bound to uranyl ions in a chelating style and one of the carboxylate groups in an axial position chelates the $[Ln(H_2O)_7]^{3+}$ group, resulting in the sheets decorated by lanthanide ions on both sides [72]. The two remaining *a*-carboxylate groups are hydrogen bonded with one another via the disordered hydrogen atoms (Fig. 31).

Similar coordination modes for 123456-CHA and in turn, similar topological arrangements occur in two gadolinium complexes, $[Gd(\mu_3\text{-}123456\text{-}CHA^{I}\text{-}H_3)(H_2O)_4]\cdot 3H_2O$ and $[Gd(\mu_4\text{-}123456\text{-}CHA^{I}\text{-}H_3)(H_2O)_4]\cdot 6H_2O$ [73], which were prepared using gel technique with different pH values of the gels at ambient tem-

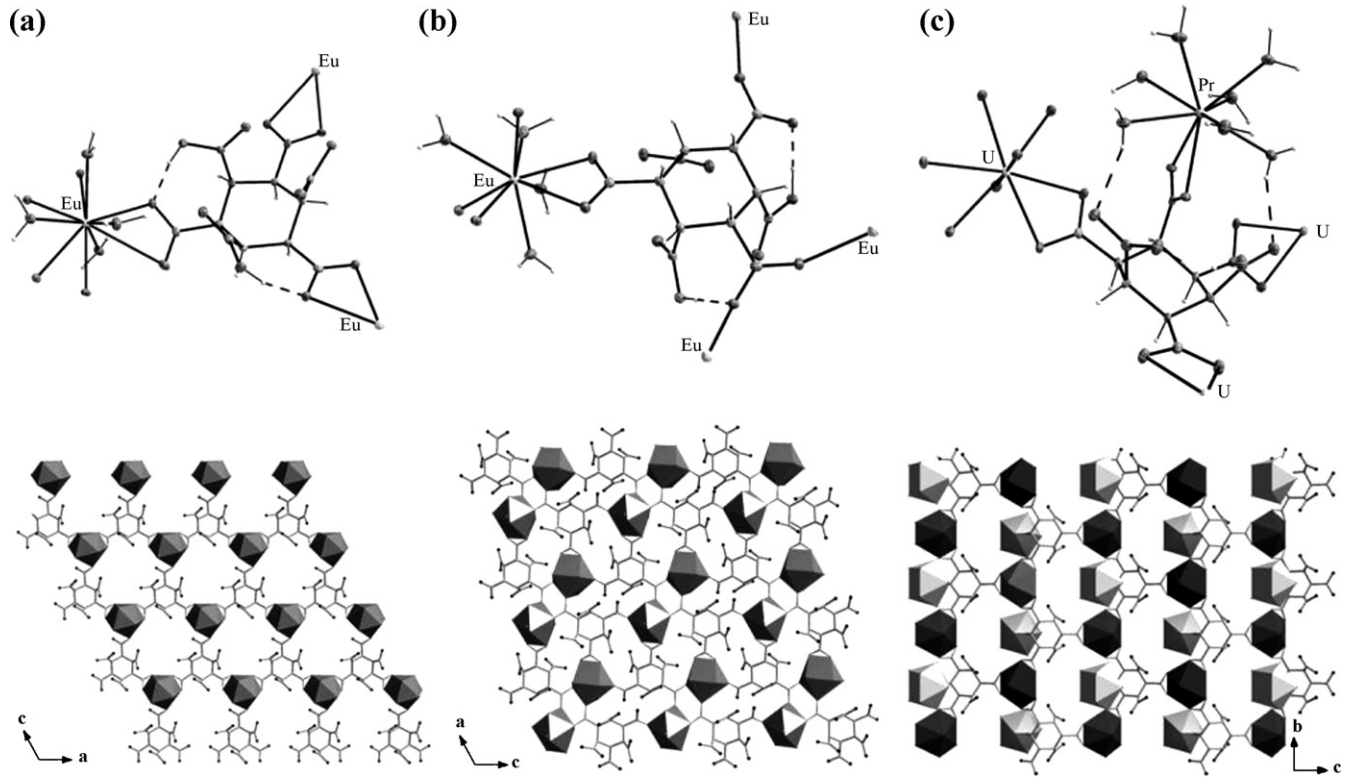

Fig. 31. Structures of $[Eu(123456\text{-}CHA^{I}\text{-}H_3)(H_2O)_4]\cdot xH_2O$ with $x = 3$ (a) or 6 (b) and $[UO_2Ln(\mu_4\text{-}123456\text{-}CHA^{I}\text{-}H)(H_2O)_7]\cdot H_2O$ (Ln = Pr, Eu, Tb and Er) (c). The figures are adapted from [71,72].

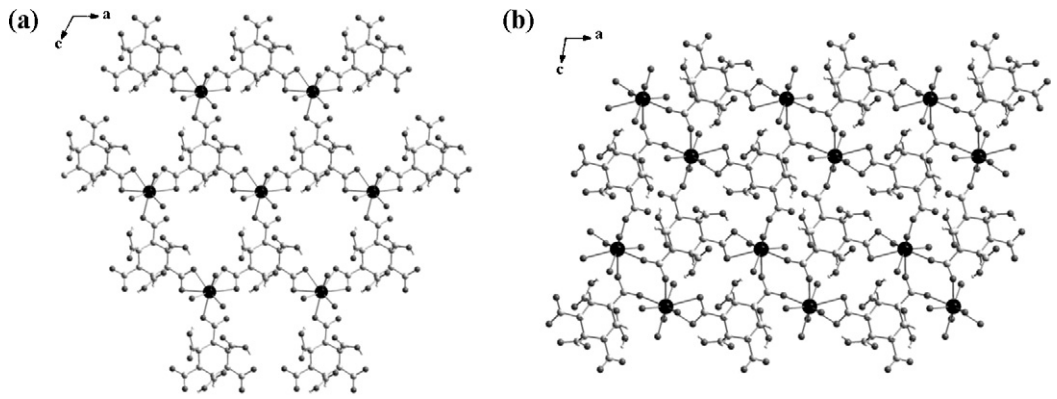

Fig. 32. (a) The (6,3) honeycomb coordination layer of $[Gd(\mu_3\text{-}123456\text{-}CHA^{I}\text{-}H_3)(H_2O)_4]\cdot 3H_2O$ and (b) a [44,62] 2D network in $[Gd(\mu_4\text{-}123456\text{-}CHA^{I}\text{-}H_3)(H_2O)_4]\cdot 6H_2O$. The figures are adapted from [73].

perature. In the first gadolinium compound, 123456-CHA links the metal ions via three *e*-carboxylate groups in the monodentate and bis(chelating) modes to form a (6,3) honeycomb layer while the second gadolinium compound consists of a $[4^4,6^2]$ 2D network in which 123456-CHA acts as a four-fold connector via the monodentate, chelating and *syn-syn e*-carboxylate groups (Fig. 32). The investigation of magnetic properties in the temperature range of 1.9–300 K revealed a Curie law behavior for the two compounds.

The only exception in lanthanide 123456-CHA compounds where the ligand adopts a conformation other than form **I** is found in $[Eu_2(\mu_6\text{-}123456\text{-}CHA^{II})(H_2O)_8]\cdot 4H_2O$ [71], where the products was obtained hydrothermally from reaction of 123456-CHA in very low yield or from in situ hydrolysis, oxidation and isomerization of bicyclo[2.2.2]oct-7-ene-2,3,5,6-tetracarboxylic dianhydride. All six carboxylate groups are in equatorial positions; four of them being chelating give rise to planar ribbon-like subunits, which are assembled into a 3D framework of Rutile-type topology by the other two monodentate carboxylates (1*e* and 4*e*) (Fig. 33).

The all-*trans* form **II**(*e*,*e*,*e*,*e*,*e*,*e*) is primarily observed in a series of 3D metal coordination frameworks $[M_3(\mu_9\text{-}123456\text{-}CHA^{II})(H_2O)_6]$ (M = Mn, Fe, Co and Ni) crystallized in high symmetry of R-3 [74–75]. The 123456-CHA^{II} ligand lying across a three-fold axis connects nine octahedral metal atoms in a *syn-anti* pattern (Fig. 34). If one neglects the cyclohexane rings from the viewpoint of a magnetic superexchange pathway, each metal atom is connected by four *syn-anti* μ_2-carboxylate bridges to form a 3-D tetrahedrally connected metal carboxylate inorganic network. The magnetic susceptibility indicated a weak antiferromagnetic coupling between the Mn(II) S = 5/2 spins [75], a relatively weak antiferromagnetic coupling between the Fe(II) S = 2 spins [75] and a significant

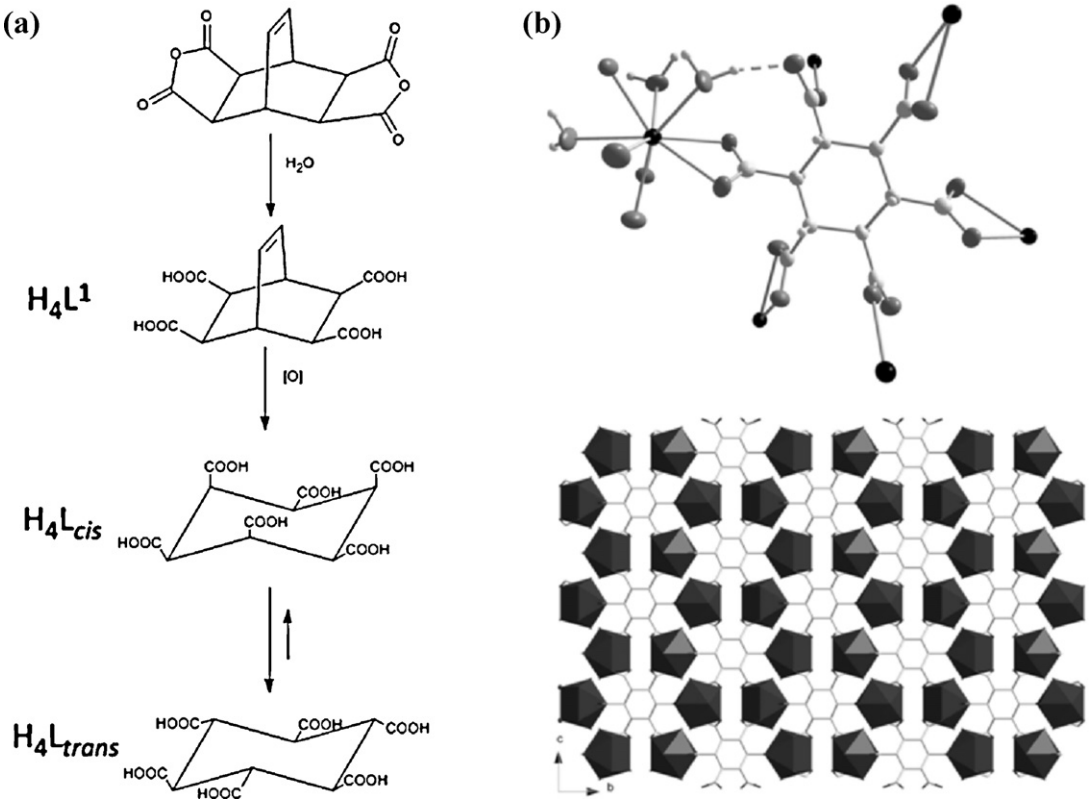

Fig. 33. (a) Formation of all-*trans*-123456-CHA from bicyclo[2.2.2]oct-7-ene-2,3,5,6-tetracarboxylic dianhydride and (b) structure of $[Eu_2(\mu_6\text{-}123456\text{-}CHA^{II})(H_2O)_8]\cdot 4H_2O$. The figures are adapted from [71].

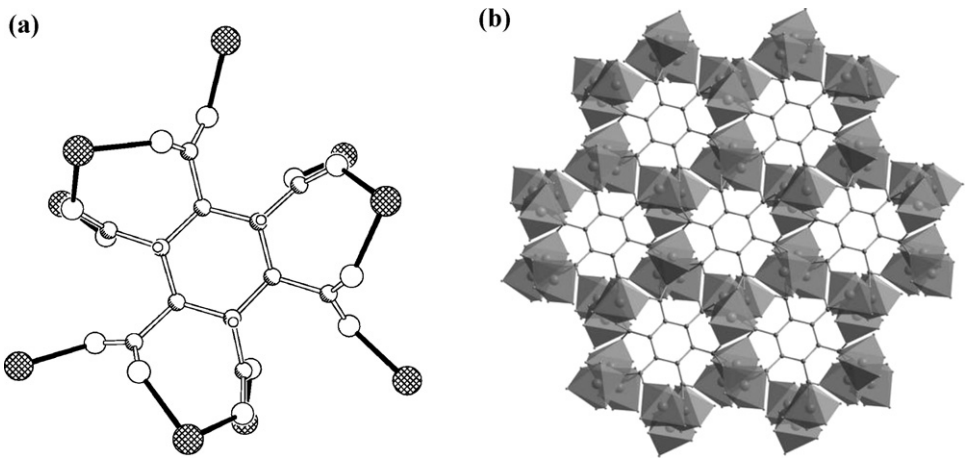

Fig. 34. Structures of $[M_3(\mu_9\text{-}123456\text{-}CHA^{II})(H_2O)_6]$ (M = Mn, Fe, Co and Ni). The figures are adapted from [75].

antiferromagnetic coupling between the Co(II) S = 3/2 spins [74], respectively through the *syn-anti* carboxylate bridges. The nickel analogue, however, exhibits ferromagnetic exchange through the only effective magnetic exchange pathway of *syn-anti* carboxylate groups present within the 3D net [75].

When the auxiliary ligands 2,2′-bipy or 4,4′-bipy were introduced into the above reaction systems with Mn^{2+}, Fe^{2+} or Co^{2+}, the same phases of $[M_3(\mu_9\text{-}123456\text{-}CHA^{II})(H_2O)_6]$ were always obtained. It was also the case when 2,2′-bipy was added into the Ni^{2+} reaction mixture and the same phase of $[Ni_3(\mu_9\text{-}123456\text{-}CHA^{II})(H_2O)_6]$ was formed [75]. The 2,2′-bipy seemed to have little influence on the construction of the frameworks in this specific reaction. However, when 4,4′-bipy was added to a mixture of nickel acetate and 123456-CHA, a new coordination structure, $[Ni_4(OH)_2(\mu_{10}\text{-}123456\text{-}CHA^{II})(4,4'\text{-bipy})(H_2O)_4]\cdot 6H_2O$, was formed. The ligand in conformation **II** connects ten Ni atoms through *syn-syn* (1*e*, 2*e*, 4*e* and 5*e*) and μ_2-η^2 (3*e* and 6*e*) carboxylate groups. Each chair-shaped tetranuclear $Ni_4(\mu_3\text{-}OH)_2$ SBU links four 123456-CHAs and each ligand connects to four SBUs, resulting in a (4,4)-layer (Fig. 35). The 4,4′-bipy ligands bridge the layers to form a 3D coordination framework with 2D channels extending along the *b*- and *c*-axes. Magnetic susceptibility versus temperature data (2–300 K) suggested a predominantly antiferromagnetic coupling between Ni^{2+} ions through the μ_3-OH and μ_2-carboxylate groups. In addition, when 1,10-phenanthroline was used as the auxiliary ligand, a 1D chained structure $[Ni_2(\mu_4\text{-}123456\text{-}CHA\text{-}H_2^{II})(1,10\text{-phen})_2]$ was obtained where the ligand in form **II** links four nickel atoms in a chelating mode like 1245-CTA [76].

Surprisingly, three conformations of 123456-CHA, **II**(*e*,*e*,*e*,*e*,*e*,*e*), **III**(*e*,*e*,*e*,*e*,*a*,*a*), and **VI**(*e*,*e*,*e*,*e*,*e*,*a*), derived from the conformational transformation of **I**(*a*,*e*,*a*,*e*,*a*,*e*) were trapped in cadmium complexes by careful control of the hydrothermal conditions. In the framework of $[Cd_{12}(\mu_6\text{-}123456\text{-}CHA^{II})(\mu_{10}\text{-}123456\text{-}CHA^{II})_3(\mu_2\text{-}H_2O)_6(H_2O)_6]\cdot 16.5H_2O$, six μ_{10}-123456-CHA^{II} in the *syn-syn* (3*e* and 6*e*) and μ_2-η^1:η^2 (1*e*, 2*e*, 4*e* and 5*e*) modes and two μ_6-123456-CHA^{II} in a monodentate style bridge thirty Cd^{2+} ions to generate a nanoscale Cd_{36}(123456-CHA)$_8$ cage of hexagonal prism shape in dimension of $23.0 \times 12.8 \times 12.8$ Å [77]. Each cage connects six neighboring ones to generate a novel 3D MOF (Fig. 36a). Slightly basic solution adjusted by NaOH resulted in a second cadmium compound $Na_{12}[Cd_6(\mu_6\text{-}123456\text{-}CHA^{II})(\mu_6\text{-}123456\text{-}CHA^{III})_3]\cdot 27H_2O$ [77]. Besides the **II** form, a new conformation **III** was also trapped in the complex. Notably, this phase with mixed conformations **II** and **III** could also be obtained at 150, 160, and 180 °C. However, the use of other bases including LiOH, KOH or Et_3N in the above reaction system cannot afford the same phase, suggesting that it is the Na^+ cation which has an appropriate radius, rather than the temperature factor, that controls the conformational conversion of the ligand and the construction of 3D framework. The introduction of Na^+ atoms, which are directly linked to the neighboring carboxylate groups within the cages, results in different coordination environments of the Cd^{2+} atoms from those found for the first cadmium compound. The ligands in both **II** and **III** adopt μ_6-bridging modes via the monodentate (2*e* and 3*e*)/chelating (1*e*, 4*e*, 5*a* and 6*a*) ways (considering Cd^{2+} only), respectively, connecting the metal ions to form a 3D MOF with hexagonal prism shaped cages in dimension of 13.0 Å × 13.0 Å × 10.5 Å (Fig. 36b). At a higher temperature of 180 °C, a structurally different 3D framework $[Cd_3(\mu_{13}\text{-}123456\text{-}CHA^{II})(\mu\text{-}H_2O)]$ was formed without the addition of NaOH. It is form **II** for 123456-CHA again in the compound (Fig. 36c). The ligand connects thirteen Cd atoms through the *syn-syn* (3*e* to 6*e*) and μ_3-η^1:η^2 (1*e* and 2*e*) carboxylate groups and along with the bridging water molecules, to generate a 3D condensed framework [75].

Auxiliary ligands have also been added into the reaction systems of cadmium and 123456-CHA to investigate whether they could induce conformational transformation of the ligand. In the presence of 2,2′-bipy, the fourth cadmium complex $[Cd_3(\mu_6\text{-}123456\text{-}CHA^{III})(2,2'\text{-bipy})_3(H_2O)_3]\cdot 2H_2O$ with a 2D layered structure was isolated [75]. The ligand in conformation **III** connects six Cd atoms through the monodentate (1*e* and 5*a*) and chelating (2*e*, 3*e*, 4*e* and 6*a*) carboxylate groups to form 2D rectangular layers (Fig. 37a).

When the auxiliary chelating 2,2′-bipy was replaced with the divergent bridging ligand 4,4′-bipy, three new complexes were obtained under similar hydrothermal conditions [75]. The reaction of Cd $(NO_3)_2\cdot 4H_2O$, 123456-CHA$^{I}\cdot H_2O$ and 4,4′-bipy in a 5:1:5 molar ratio at 160 °C resulted in a complicated coordination framework of $[Cd_4(\mu_4\text{-}123456\text{-}CHA^{VI})_2(4,4'\text{-Hbipy})_4(4,4'\text{-bipy})_2(H_2O)_4]\cdot 9.5H_2O$ (Fig. 37b). The two crystallographically unique 123456-CHA ligands in form **VI**(*e*,*e*,*e*,*e*,*e*,*a*) have slightly different μ_4-bridging modes. In the first ligand, four of the carboxylate groups (2*e*, 3*e*, 4*e* and 6*a*) adopt the chelating mode and the remaining COO^- keep uncoordinated (1*e* and 5*e*). In the second ligand, three of the five *e*-carboxylate groups (2*e*, 3*e* and 4*e*) adopt the chelating mode and the *a*-carboxylate group now adopts a monodentate mode. The μ_4-123456-CHA^{VI} ligands connect the Cd atoms to form a 2D porous layer on the *ac* plane, which is further extended through bridging 4,4′-bipy into a 3D framework with 1D rectangular channels extending along the *b*-axis. A different structure, $[Cd_2(\mu_6\text{-}123456\text{-}CHA^{II})(4,4'\text{-Hbipy})_2(H_2O)_{10}]\cdot 5H_2O$,

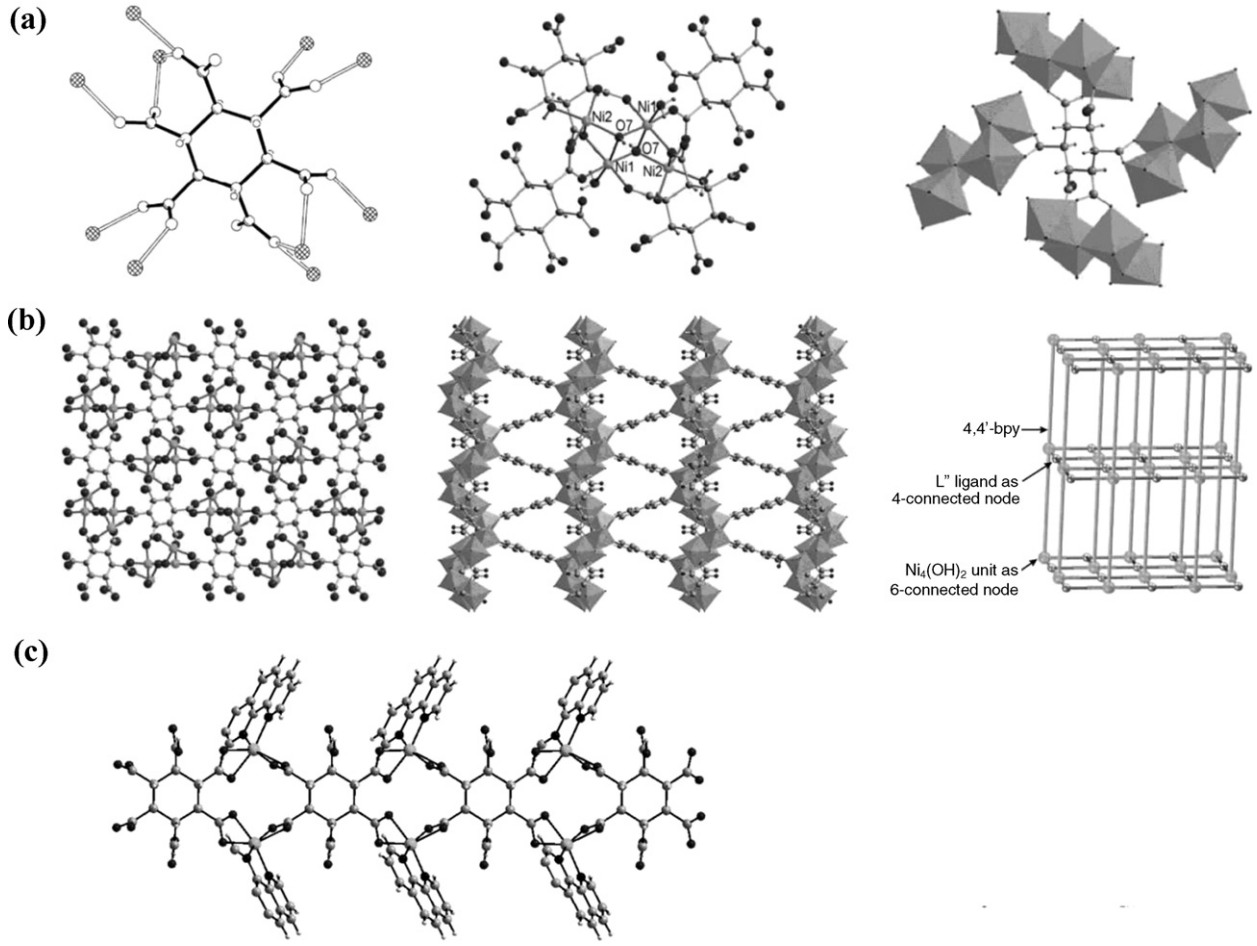

Fig. 35. (a) Coordination mode of 123456-CHA^{II} and tetranuclear $Ni_4(\mu_3\text{-}OH)_2$ SBU in $[Ni_4(OH)_2(\mu_{10}\text{-}123456\text{-}CHA^{II})(4,4'\text{-bipy})(H_2O)_4]\cdot 6H_2O$; (b) 3D coordination and topological structures of $[Ni_4(OH)_2\ (\mu_{10}\text{-}123456\text{-}CHA^{II})(4,4'\text{-bipy})(H_2O)_4]\cdot 6H_2O$ [75] and (c) structure of $[Ni_2(\mu_4\text{-}123456\text{-}CHA\text{-}H_2^{II})(1,10\text{-phen})_2]$ [76]. The figures are adapted from [75,76].

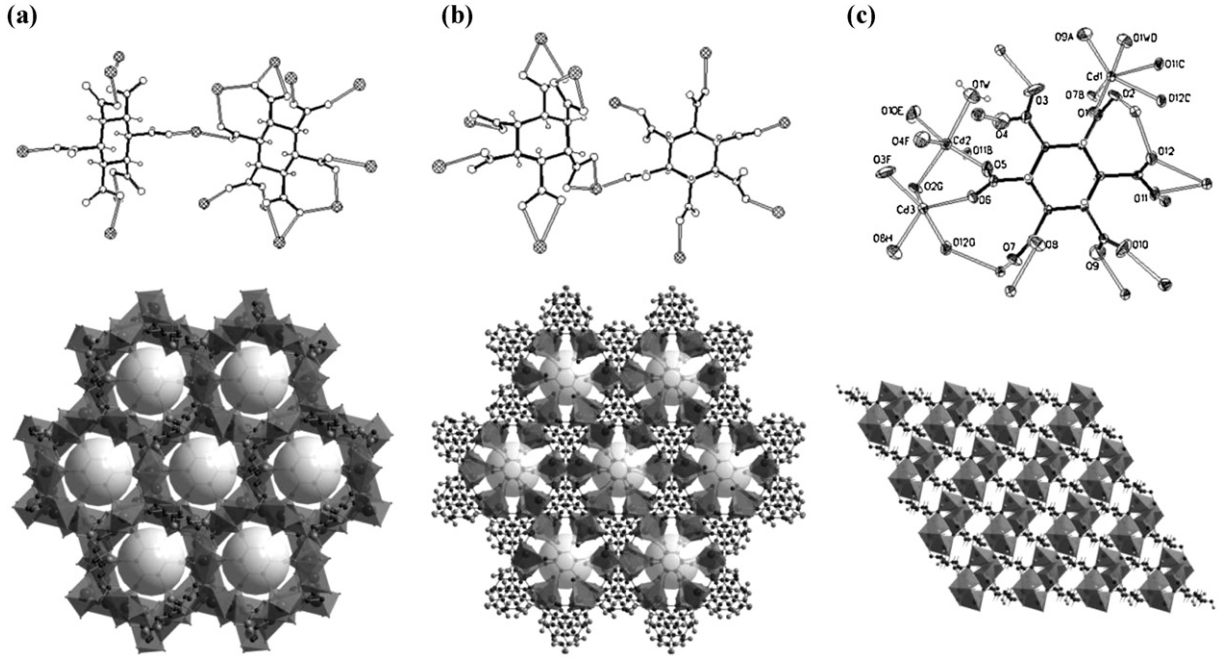

Fig. 36. Coordination modes of 123456-CHA and 3D coordination structures of $[Cd_{12}(\mu_6\text{-}123456\text{-}CHA^{II})(\mu_{10}\text{-}123456\text{-}CHA^{II})_3(\mu_2\text{-}H_2O)_6(H_2O)_6]\cdot 16.5H_2O$ (a), $Na_{12}[Cd_6(\mu_6\text{-}123456\text{-}CHA^{II})(\mu_6\text{-}123456\text{-}CHA^{III})_3]\cdot 27H_2O$ (b) [77] and $[Cd_3(\mu_{13}\text{-}123456\text{-}CHA^{II})(\mu\text{-}H_2O)]$ (c) [75]. The figures are adapted from [75,77].

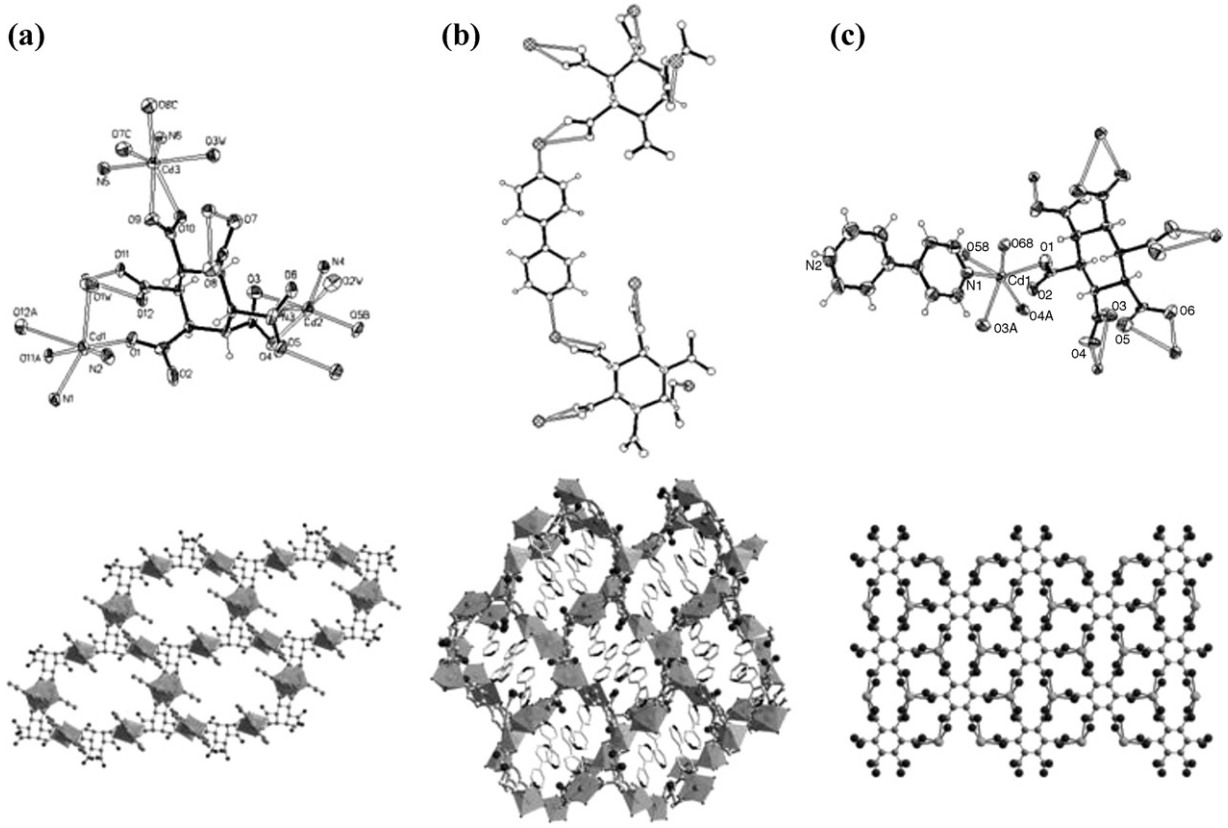

Fig. 37. Coordination mode of 123456-CHA and 3D coordination structures of $[Cd_3(\mu_6\text{-}123456\text{-}CHA^{III})(2,2'\text{-bipy})_3(H_2O)_3]\cdot 2H_2O$ (a), $[Cd_4(\mu_4\text{-}123456\text{-}CHA^{VI})_2(4,4'\text{-}Hbipy)_4(4,4'\text{-bipy})_2(H_2O)_4]\cdot 9.5H_2O$ (b) and $[Cd_2(\mu_6\text{-}123456\text{-}CHA^{II})(4,4'\text{-Hbipy})_2(H_2O)_{10}]\cdot 5H_2O$ (c). The figures are adapted from [75].

was obtained when the molar ratio of 4,4′-bipy was reduced from 5 to 2 equivalence under similar reaction conditions at 175 °C for 2 days. The 123456-CHA adopt the conformation **II** again to connect the Cd atoms via two monodentate (1*e* and 2*e*) and four chelating *e*-carboxylate groups into a 2D (6,3)-connected layer on the *ac* plane (Fig. 37c). The monoprotonated 4,4′-Hbipy ligands are arranged vertically above and below the layer and link the adjacent layers into a 3D supramolecular network.

On further decreasing the amount of 4,4′-bipy, a similar reaction at 180 °C for 3 days resulted in another new product complex $[Cd_3(\mu_{11}\text{-}123456\text{-}CHA^{VI})(H_2O)_3]$ [75]. Notably, no 4,4′-bipy was included in the final structure either as a ligand coordinated to the metal center or as a guest molecule within the channels. However, the presence of 4,4′-bipy in the reaction system was essential for the formation of this complex. Without 4,4′-bipy, only complex $[Cd_3(\mu_{13}\text{-}123456\text{-}CHA^{II})(\mu\text{-}H_2O)]$ was obtained, in which the ligand is in conformation **II**. The ligands in conformation **VI** connect eleven Cd atoms through five *syn-syn* (2*e*), μ_2-η^2 (5*e*) and μ_2-η^1:η^2 (1*e*, 3*e* and 4*e*) *e*-carboxylate groups and one distinct μ_3-η^1:η^2 *a*-carboxylate and thus form a 3D condensed coordination network (Fig. 38).

When the chemically active metal ion Cu^{2+} was employed in the reaction system, two different phases, the 1D chain-based mixed-valence complex $[Cu^{II}_2(\mu_4\text{-}123456\text{-}CHA^{II})(H_2O)_4][Cu^{I}_2(4,4'\text{-bipy})_2]$ and the 2D layer-based porous framework $[Cu^{II}(TMA\text{-}H)(4,4'\text{-bipy})(H_2O)]\cdot 3H_2O$ (TMA-H_3 = trimesic acid), were isolated from the same batch [75]. In the mixed-valence compound, 123456-CHA in the all-*trans* conformation **II** adopts a μ_4-bridging mode through their monodentate carboxylate groups (1*e*, 2*e*, 4*e* and 5*e*), linking the Cu^{2+} atoms into a 1D chain while 4,4′-bipy connects the Cu^{+} atoms to form a 1D double thread chain (Fig. 39). Two Cu^{+}-4,4′-bipy chains are arranged in parallel on either side of the Cu^{2+}-123456-CHA chain to form a sandwich-like band structure through weak coordinating

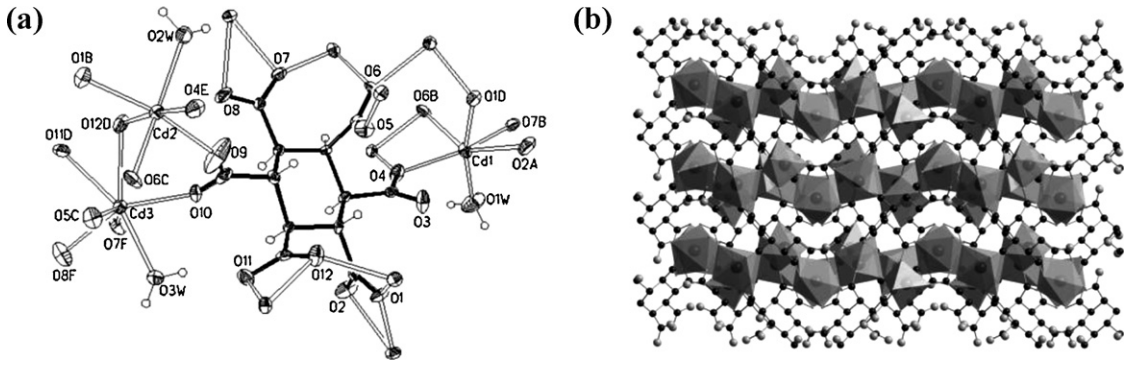

Fig. 38. Coordination mode of 123456-CHA (a) and 3D coordination structure (b) of $[Cd_3(\mu_{11}\text{-}123456\text{-}CHA^{VI})(H_2O)_3]$. The figures are adapted from [75].

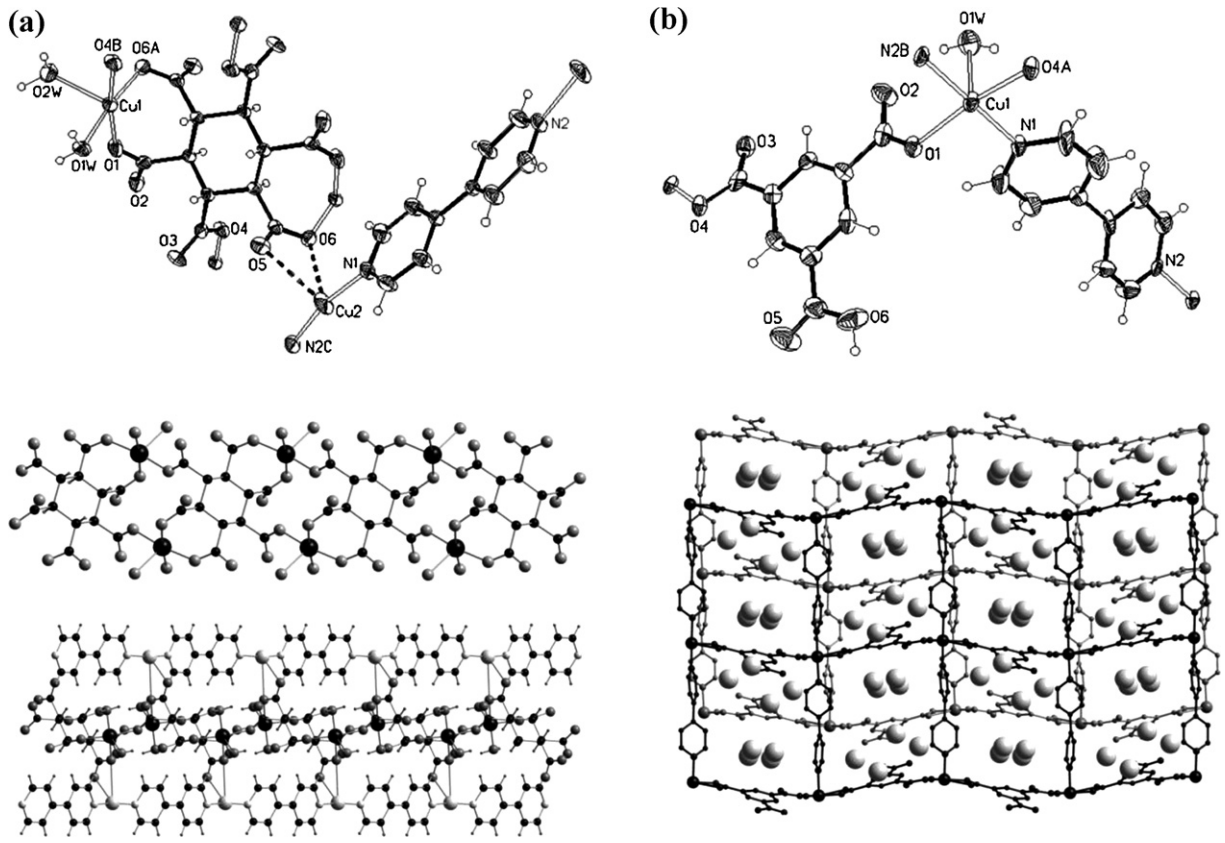

Fig. 39. Coordination modes of 123456-CHA and 3D coordination structures of $[Cu_2^{II}(\mu_4\text{-}123456\text{-}CHA^{II})(H_2O)_4][Cu_2^{I}(4,4'\text{-bipy})_2]$ (a) and $[Cu^{II}(TMA\text{-}H)(4,4'\text{-bipy})(H_2O)]\cdot 3H_2O$ (b). The figures are adapted from [75].

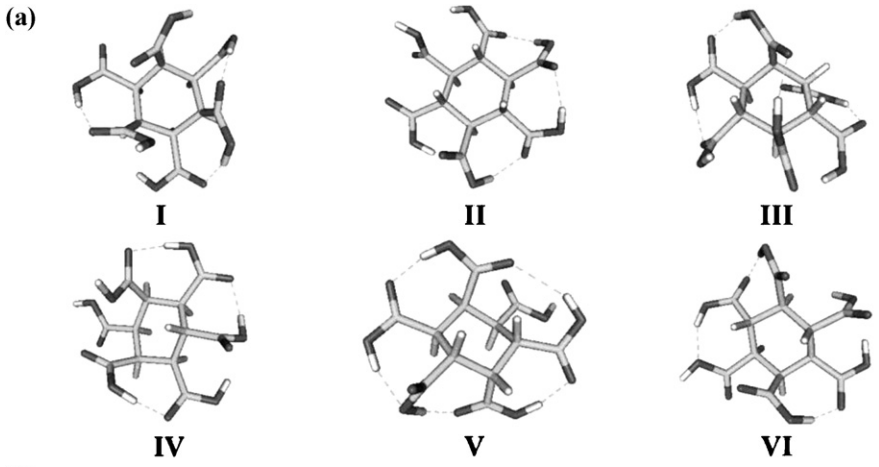

(b)

	a.u.	a.u. (ΔG)	kcal mol^{-1}(ΔG)	kJ mol^{-1}(ΔG)
I	-1367.056864	0.020566	12.91	54.00
II	-1367.069629	0.007801	4.90	20.48
III	-1367.066248	0.011182	7.02	29.36
IV	-1367.055235	0.022195	13.93	58.27
V	-1367.077430	0	0	0
VI	-1367.061843	0.015587	9.78	40.92

Fig. 40. (a) Structures of **I**(*a,e,a,e,a,e*), **II**(*e,e,e,e,e,e*), **III**(*e,e,e,e,a,a*), **IV**(*e,e,e,a,e,a*), **V**(*e,e,a,e,e,a*) and **VI**(*e,e,e,e,e,a*) for 123456-CHA optimized by the B3LYP method and 6-21G (d,p); (b) free energies of various conformations and ΔG values compared with conformation **V**. The figures are adapted from [75].

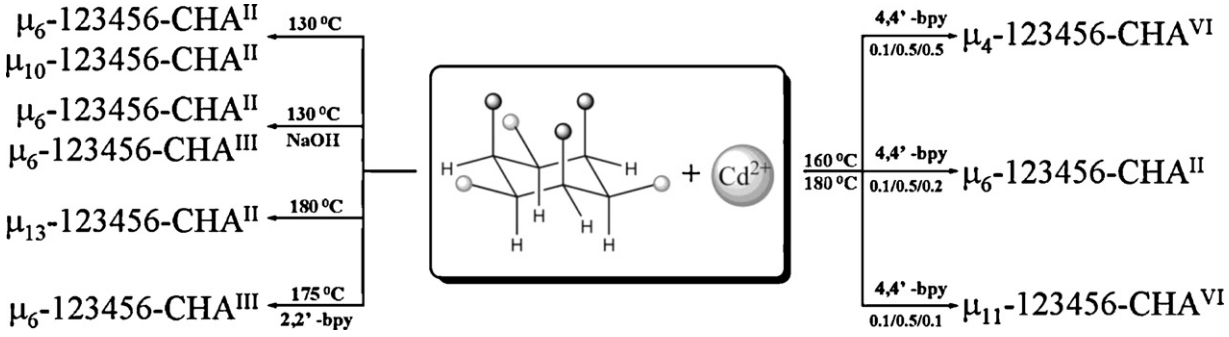

Scheme 11. Conformational transformation of 123456-CHA in the synthesis of cadmium 123456-CHA compounds.

interactions between Cu^+ and the 3*e*-/6*e*-carboxylate groups. Of particular interest is the copper(II) coordination polymer, in which TMA-H^{2-} was formed in situ from the 123456-CHA ligand. Such a product may provide some useful clues for the mechanism of conformational transformations of 123456-CHA.

6.2. Conformation studies on 1,2,3,4,5,6-cyclohexanehexacarboxylate

Theoretical calculations on the free 123456-CHA in different conformations reveal that the conformation **V**(*e*,*e*,*a*,*e*,*e*,*a*) is the most stable among the six conformations, which can be rationalized in terms of the formation of a large intramolecular ring of hydrogen bonds involving five carboxylic groups [75]. **II**(*e*,*e*,*e*,*e*,*e*,*e*) is the second most stable form and **III**(*e*,*e*,*e*,*e*,*a*,*a*) is only ~9 kJ mol^{-1} less stable than **II**. Conformation **I**(*a*,*e*,*a*,*e*,*a*,*e*) is 33.5 and 24.6 kJ mol^{-1} less stable than **II** and **III**, respectively (Fig. 40). Consequently the transformations from **I** to **II** or **III** should be thermodynamically allowed, which is in good agreement with the experimental results that complexes of **II** and **III** can be easily obtained at lower temperature (130 °C). Form **VI**(*e*,*e*,*e*,*e*,*e*,*a*) is 13 kJ mol^{-1} more stable than **I** but less stable than **II** and **III**. Therefore, some specific conditions such as higher temperature (160–180 °C) or adding 4,4′-bipy, are required to obtain complexes of **VI**. Conformation **IV** is 5 kJ mol^{-1} higher in energy than **I**, suggesting that the conversion from **I** to **IV** is thermodynamically inhibited. Indeed, complexes of **IV** have not been obtained from **I** experimentally. The reason why no complexes of **V** have been obtained from **I** may lie in the fact that the intramolecular hydrogen bonds are destroyed in aqueous solution. The conformation **V** becomes much less stable than in the gas state and can be easily transformed to other forms upon coordination.

In the previous discussion, several reaction factors have been shown to have a delicate influence in controlling the conformations of the flexible ligands, such as pH, reaction temperatures and time, reactant ratios, addition of auxiliary ligands and so on. Small changes in one or more of these parameters can give rise to profound changes in the conformation of the ligands and the structures of final products. The seven cadmium complexes with 123456-CHA in various conformations prepared under different hydrothermal conditions in the temperature range of 130–180 °C are summarized in Scheme 11. 123456-CHA in **I** underwent conformational conversion to **II** in slightly acidic solution at 130 and 180 °C, respectively and formed different cadmium coordination compounds while in a basic solution using NaOH to adjust the pH value, it converted to both **II** and **III**. Notably, the same metal complex with mixed conformations **II** and **III** could also be obtained at 150, 160, and 180 °C. Addition of other bases including LiOH, KOH or Et_3N in the above reaction system cannot afford the same phase, suggesting that the Na^+ cations play an important role in controlling the conformational conversion of 123456-CHA.

The addition of auxiliary N-donor ligands introduces competition upon coordination with carboxylate groups towards the metal ions. Therefore it has a subtle effect on both molecular arrangement and framework packing, and possibly the ligand conformations as well. In the Mn, Fe, Co and Ni 123456-CHA system, the ligand transformed from conformation **I** to **II** in the presence or absence of 2,2′-bipy or 4,4′-bipy. In the case of cadmium compounds, addition of 2,2′-bipy led to the yield of conformation **III**. The divergent bridging ligand 4,4′-bipy apparently has a more profound influence on the conformational conversion. The reactions of $Cd(NO_3)_2{\cdot}4H_2O$, 123456-CHA$^{\mathbf{I}}$ and 4,4′-bipy in molar ratios of 5:1:5, 5:1:2 and 5:1:1 at 160–180 °C resulted in different cadmium coordination frameworks in forms **II** or **VI**. Complexes with the ligand in conformations

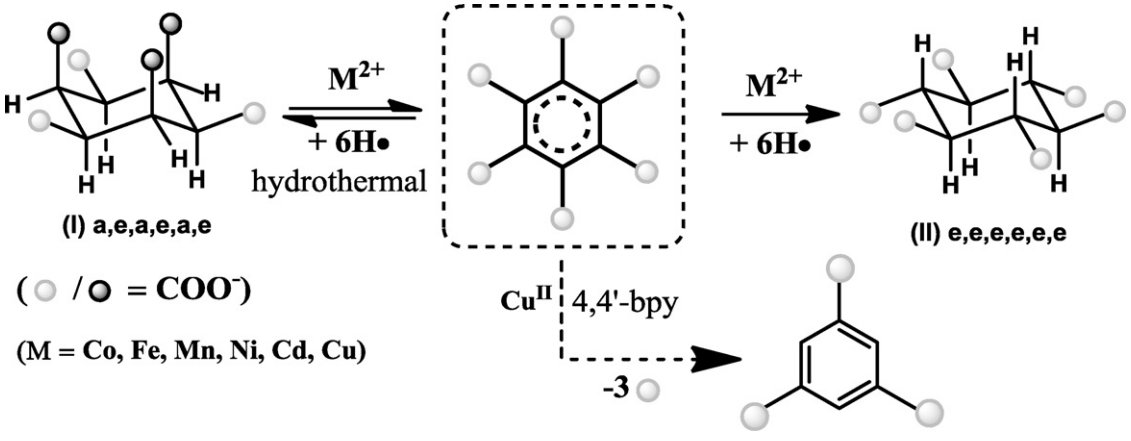

Scheme 12. Possible reaction mechanism of the conformational transformation for 123456-CHA under hydrothermal conditions.

III or **VI** were produced in very low yields, which may be due to the low conformational conversion efficiency from **I** to the **III** or **VI** forms. The large atomic radius and moderate coordination habits for Cd^{2+} ion may be helpful for the stabilization and separation of various conformations of 123456-CHA.

Since four of the six stable conformations for 123456-CHA have been trapped in metal-organic framework structures under different hydrothermal conditions, the question arose how the conformational transformation occurred and what reaction mechanism could be. Inspired by our previous work, we chose the relatively reactive and catalytically active metal ion Cu^{2+} to trap the intermediates of the conformational transformation through its coordination. As expected, the reaction of $Cu(OAc)_2{\cdot}H_2O$, 123456-CHA$\cdot H_2O$ and 4,4′-bipy in a molar ratio of 5:1:5 resulted in two different crystalline phases, $[Cu^{II}_2(\mu_4$-123456-CHA$^{\mathbf{II}})(H_2O)_4][Cu^{I}_2(4,4'\text{-bipy})_2]$ and $[Cu^{II}(TMA\text{-}H)(4,4'\text{-bipy})(H_2O)]{\cdot}3H_2O$. In the former mixed-valence compound, the conformation of the ligand was transformed from **I** to **II**, while in the latter compound 123456-CHA was oxidized and decarboxylated into 1,3,5-benzenetricarboxylate. Similar decarboxylation has also been observed in 1245-CHA as discussed before.

As far as the conformations of the cyclohexanehexacarboxylate ligand are concerned, we proposed that the approach of a metal ion to the ligand can activate the *a*-protons on the ligand, leading to their removal with the formation a metastable state L*, similar to benzenehexacarboxylate, under the hydrothermal conditions (Scheme 12). The carboxylate groups rapidly adopt their optimal positions and coordinate to the metal ions. The *a*-protons return to their corresponding positions to form the final conformation of the ligand in the frameworks. In the case where copper ions existed in the reaction, rapid decarboxylation occurred at the 1,3,5-positions of L* probably due to steric hindrance as soon as the *a*-protons were removed, leading to the formation of benzenetricarboxylate. Under such circumstances, Cu^{2+} acts as an essential oxidant, as illustrated in the conformational transformation of 1245-CHA.

7. Conclusion and outlook

The metal cyclohexanepolycarboxylate frameworks are often similar to benzene polycarboxylate systems and the less investigated cyclohexene polycarboxylate coordination compounds [26]. In this review we show that cyclohexanepolycarboxylate ligands provide a wide range of different geometric isomers, multiple protonated carboxylate groups, a large variety of bonding behavior for the carboxylate groups and specifically, various conformations and geometries of the acid groups in relation to the central cyclohexane ring. Such structural and coordination characteristics make them elegant building components for the construction of metal coordination frameworks and organo-inorganic hybrid solids. In particular, interesting materials with diverse magnetic properties ranging from antiferromagnetic to single-chain magnet, and to magnetic ordering behavior have been assembled from the types of flexible ligands. Conformational transformation of cyclohexane carboxylate groups occurs extensively under hydrothermal conditions in the presence of different metal ions or auxiliary ligands. The α-proton removal mechanism of conformational transformation is discussed and supported by successfully trapping the reaction intermediates via the formation of metal complexes with corresponding benzene polycarboxylate groups.

We may expect that cyclohexanepolycarboxylic acids have a more significant and tremendous contribution to supramolecular chemistry and materials science as long as better understandings, and consequently better controls on their flexibility and versatility.

Acknowledgements

This work was supported by the National Natural Science Foundation of China (Grant nos. 20525102, 20821001, 90922009, 50872157 and 20901084) and the "973 Project" (2007CB815305).

References

[1] (a) D.E.W. Vaughan, in: K.R. Seddon, M. Zaworotko (Eds.), Crystal Engineering: the Design and Application of Functional Solids, Kluwer Academic, 1999, p. 451; (b) J.W. Steed, J.L. Atwood, Supramolecular Chemistry, Wiley, 2000, p. 261.
[2] (a) S. Kitagawa, R. Kitaura, S.-I. Noro, Angew. Chem. Int. Ed. 43 (2004) 2334; (b) M.W. Hossein, in: D. Braga, F. Grepioni, A.G. Orpen (Eds.), Crystal Engineering: from Molecules and Crystals to Materials, Springer, 1999, p. 181.
[3] (a) D. Bradshaw, J.B. Claridge, E.J. Cussen, T.J. Prior, M.J. Rosseinsky, Acc. Chem. Res. 38 (2005) 273; (b) H.W. Roesky, M. Andruh, Coord. Chem. Rev. 236 (2003) 91; (c) S.R. Batten, K.S. Murray, Coord. Chem. Rev. 246 (2003) 103; (d) K. Biradha, M. Sarkar, L. Rajput, Chem. Commun. (2006) 4169.
[4] (a) R.J. Hill, D.-L. Long, N.R. Champness, P. Hubberstey, M. Schröder, Acc. Chem. Res. 38 (2005) 335; (b) O.M. Yaghi, M. O'Keeffe, N.W. Ockwig, H.K. Chae, M. Eddaoudi, J. Kim, Nature 423 (2003) 705; (c) D.J. Tranchemotagne, J.L. Mendoza-Cortés, M. O'Keeffe, O.M. Yaghi, Chem. Soc. Rev. 38 (2009) 1257.
[5] (a) W. Zhang, H.Y. Ye, R.G. Xiong, Coord. Chem. Rev. 253 (2009) 2980; (b) S.L. Qiu, G.S. Zhu, Coord. Chem. Rev. 253 (2009) 2891; (c) R.J. Kuppler, D.J. Timmons, Q.-R. Fang, J.-R. Li, T.A. Makal, M.D. Young, D.Q. Yuan, D. Zhao, W.J. Zhuang, H.-C. Zhou, Coord. Chem. Rev. 253 (2009) 3042; (d) G.E. Kostakis, A.M. Ako, A.K. Powell, Chem. Soc. Rev. 38 (2010) 2238; (e) D. Farrusseng, S. Aguado, C. Pinel, Angew. Chem. Int. Ed. 48 (2009) 7502.
[6] S.S.-Y. Chui, S.M.-F. Lo, J.P.H. Charmant, A.G. Orpen, I.D. Williams, Science 283 (1999) 1148.
[7] M. Eddaoudi, J. Kim, N. Rosi, D. Vodak, J. Wachter, M. O'Keeffe, O.M. Yaghi, Science 295 (2002) 469.
[8] G. Ferey, C. Mellot-Draznieks, C. Serre, F. Millange, J. Dutour, S. Surble, I. Margiolaki, Science 309 (2005) 2040.
[9] (a) M. Eddaoudi, D.B. Moler, H.L. Li, B.L. Chen, T.M. Reineke, M. O'Keefe, O.M. Yaghi, Acc. Chem. Res. 34 (2001) 319; (b) N.W. Ockwig, O. Delgado-Friedrichs, M. O'Keefe, O.M. Yaghi, Acc. Chem. Res. 38 (2005) 176; (c) C.N.R. Rao, S. Natatajan, R. Vaidhyanathan, Angew. Chem. Int. Ed. 43 (2004) 1466; (d) B.-H. Ye, M.-L. Tong, X.-M. Chen, Coord. Chem. Rev. 249 (2005) 545.
[10] (a) L. Carlucci, G. Ciani, D.M. Prosepio, Coord. Chem. Rev. 246 (2003) 247; (b) R.L. LaDuca, Coord. Chem. Rev. 253 (2009) 1759.
[11] T.-F. Liu, J. Lü, R. Cao, CrystEngComm 12 (2010) 660.
[12] (a) S. Kitagawa, R. Matsuda, Coord. Chem. Rev. 251 (2007) 2490; (b) J.P. Zhang, S. Horike, S. Kitagawa, Angew. Chem. Int. Ed. 46 (2007) 889.
[13] J. McMurry, Organic Chemistry, 7th ed., Thomson Brooks, 2008.
[14] G. Gill, D.M. Pawar, E.A. Noe, J. Org. Chem. 70 (2005) 10726.
[15] For example: (a) C.H. Huang, H.P. Liu, B.G. Li, G.X. Xu, Y.Z. Han, Z.S. Ma, Prog. Nat. Sci. 2 (1992) 25; (b) A. Thirumurugan, M.B. Avinash, C.N.R. Rao, Dalton Trans. (2006) 221; (c) S. Surblé, C. Serre, F. Millange, F. Pellé, G. Férey, Solid State Sci. 9 (2007) 131; (d) D.T. de Lilla, C.L. Cahill, Chem. Commun. (2006) 4946.
[16] N.V. Gerbeleu, Yu.T. Struchkov, O.S. Manole, G.A. Timko, Dokl. Akad. Nauk SSSR (Proc. Natl. Acad. Sci. USSR) 332 (1993) 183.
[17] S. Bruckner, L.M. Giunchi, G. DiSilvestro, M. Grassi, Acta Crystallogr. B37 (1981) 586.
[18] (a) V. Chandrasekhar, R.O. Day, R.R. Holmes, Inorg. Chem. 24 (1985) 1970; (b) R.R. Holmes, C.G. Schmid, V. Chandrasekhar, R.O. Day, J.M. Holmes, J. Am. Chem. Soc. 109 (1987) 1408; (c) V. Chandrasekhar, C.G. Schmid, S.D. Burton, J.M. Holmes, R.O. Day, R.R. Holmes, Inorg. Chem. 26 (1987) 1050.
[19] (a) F. Gao, Q.G. Meng, Y.L. Chi, W.M. Bu, Y.G. Fan, L. Ye, G.D. Yang, Wuji Huaxue Xuebao (Chin. J. Inorg. Chem.) 13 (1997) 427; (b) D.L. Zhang, C.H. Huang, G.X. Xu, J. Yang, X.Y. Lin, Z.J. Lin, Zhongguo Xitu Xuebao (J. Chin. Rare Earth Soc.) 8 (1990) 161.
[20] Y.-Z. Zheng, W. Xue, W.-X. Zhang, M.-L. Tong, X.-M. Chen, Inorg. Chem. 46 (2007) 6437.
[21] I.F. Hernandez-Ahuactzi, H. Hopfl, V. Barba, P. Roman-Bravo, L.S. Zamudio-Rivera, H.I. Beltran, Eur. J. Inorg. Chem. (2008) 2746.
[22] A.J. Bailey, C. Lee, R.K. Feller, J.B. Orton, C. Mellot-Draznieks, B. Slatter, W.T.A. Harrison, P. Simoncic, A. Navrotsky, M.C. Grossel, A.K. Cheetham, Angew. Chem. Int. Ed. 47 (2008) 8634.
[23] Y.-Z. Zheng, M.-L. Tong, W.-X. Zhang, X.-M. Chen, Chem. Commun. (2006) 165.
[24] Y.-Z. Zheng, M.-L. Tong, W.-X. Zhang, X.-M. Chen, Angew. Chem. Int. Ed. 45 (2006) 6310.
[25] Y.-Z. Zheng, W. Xue, M.-L. Tong, X.-M. Chen, S.-L. Zheng, Inorg. Chem. 47 (2008) 11202.
[26] Y.-Z. Zheng, W. Xue, S.-L. Zheng, M.-L. Tong, X.-M. Chen, Adv. Mater. 20 (2008) 1534.

[27] H. Van Koningsveld, Acta Crystallogr. C40 (1984) 1857.
[28] (a) R.-F. Zhang, Q.-F. Wang, M.-Q. Yang, Y.-R. Wang, C.-L. Ma, Polyhedron 27 (2008) 3123;
(b) M.R. Rizal, S.W. Ng, Acta Crystallogr. E65 (2009) m1178.
[29] (a) P. Thuery, CrystEngComm 11 (2009) 232;
(b) M.R. Rizal, S.W. Ng, Acta Crystallogr. E65 (2009) m1179.
[30] (a) K. Prabhakara Rao, A. Thirumurugan, C.N.R. Rao, Chem. Eur. J. 13 (2007) 3193;
(b) A. Thirumurugan, R.A. Sanguramath, C.N.R. Rao, Inorg. Chem. 47 (2008) 823.
[31] E.L. Eliel, N.L. Allinger, S.J. Angyal, G.A. Morrison, Conformational Analysis, John Wiley, New York, 1996.
[32] (a) Y.J. Kim, D.Y. Jung, Chem. Commun. (2002) 908;
(b) J. Lu, W.-H. Bi, F.-X. Xiao, S.R. Batten, R. Cao, Chem. Asian J. 3 (2008) 542;
(c) G.-B. Che, C.-B. Liu, H. Liu, B. Liu, Acta Crystallogr. E62 (2006) m480.
[33] W.H. Bi, R. Cao, D.F. Sun, D.Q. Yuan, X. Li, Y.Q. Wang, X.J. Li, M.C. Hong, Chem. Commun. (2004) 2104.
[34] (a) M. Yu, L.H. Xie, S.X. Liu, C.L. Wang, H.Y. Cheng, Y.H. Ren, Z.M. Su, Inorg. Chim. Acta 360 (2007) 3108;
(b) M. Du, H. Cai, X.-J. Zhao, Inorg. Chim. Acta 358 (2005) 4034;
(c) Y.J. Qi, Y.H. Wang, C.W. Hu, M.H. Cao, L. Mao, E.B. Wang, Inorg. Chem. 42 (2003) 8519;
(d) Y. Gong, C.W. Hu, H. Li, K.L. Huang, W. Tang, J. Solid State Chem. 178 (2005) 3152;
(e) J. Yang, G.-D. Li, J.-J. Cao, Q. Yue, G.-H. Li, J.-S. Chen, Chem. Eur. J. 13 (2007) 3248.
[35] F.A. Cotton, J.P. Donahue, C. Lin, C.A. Murillo, Inorg. Chem. 40 (2001) 1234.
[36] M. Kurmoo, H. Kumagai, S.M. Hughes, C.J. Kepert, Inorg. Chem. 42 (2003) 6709.
[37] M. Kurmoo, H. Kumagai, M. Akita-Tanaka, K. Inoue, S. Takagi, Inorg. Chem. 45 (2006) 1627.
[38] H. Kumagai, M. Akita-Tanaka, K. Inoue, K. Takahashi, H. Kobayashi, S. Vilminot, M. Kurmoo, Inorg. Chem. 46 (2007) 5949.
[39] Y.-Z. Zheng, W. Xue, W.-X. Zhang, M.-L. Tong, X.-M. Chen, F. Grandjean, G.J. Long, S.-W. Ng, P. Panissod, M. Drillon, Inorg. Chem. 48 (2009) 2028.
[40] P. Ballester, M. Capo, A. Costa, P.M. Deya, R. Gomila, A. Decken, G. Deslongchamps, Org. Lett. 3 (2001) 267.
[41] (a) B.R. Bhogala, P. Vishweshwar, A. Nangia, Cryst. Growth Des. 2 (2002) 325;
(b) B.R. Bhogala, A. Nangia, Cryst. Growth Des. 3 (2003) 547;
(c) B.R. Bhogala, P. Vishweshwar, A. Nangia, Cryst. Growth Des. 5 (2005) 1271;
(d) B.R. Bhogala, S. Basavoju, A. Nangia, Cryst. Growth Des. 5 (2005) 1683;
(e) B.R. Bhogala, S. Basavoju, A. Nangia, CrystEngComm 7 (2005) 551;
(f) B.R. Bhogala, A. Nangia, Cryst. Growth Des. 6 (2006) 32;
(g) B.R. Bhogala, A. Nangia, New J. Chem. 32 (2008) 800;
(h) B.R. Bhogala, S.K. Chandran, L.S. Reddy, R. Thakuria, A. Nangia, CrystEngComm 10 (2008) 1735.
[42] (a) P. Ballester, A. Costa, P.M. Deya, G. Deslongchamps, D. Mink, A. Decken, R. Prohens, S. Tomas, M. Vega, Chem. Commun. (1997) 357;
(b) O. Ermer, J. Neudorfl, Chem. Eur. J. 7 (2001) 4961;
(c) P. Gangopadhyay, T.P. Radhakrishnan, Mol. Cryst. Liq. Cryst. Sci. Technol. Sect. A 369 (2001) 167;
(d) N. Shan, E. Batchelor, W. Jones, Tetrahedron Lett. 43 (2002) 8721;
(e) N. Shan, A.D. Bond, W. Jones, Cryst. Eng. 5 (2002) 9;
(f) N. Shan, A.D. Bond, W. Jones, New J. Chem. 27 (2003) 365.
[43] D. Braga, F. Grepioni, Acc. Chem. Res. 33 (2000) 601.
[44] (a) K.-Y. Choi, Y.-Y. Kim, J.-W. Ryu, N.-D. Sung, J. Chem. Crystallogr. 33 (2003) 951;
(b) S.-L. Zheng, M. Gembicky, M. Messerschmidt, P.M. Dominiak, P. Coppens, Inorg. Chem. 45 (2006) 9281.
[45] K.S. Min, M.P. Suh, Chem. Eur. J. 7 (2001) 303.
[46] K.-Y. Choi, K.-J. Kim, Polyhedron 27 (2008) 1311.
[47] Q.R. Fang, G.S. Zhu, M. Xue, J.Y. Sun, G. Tian, G. Wu, S.L. Qiu, Dalton Trans. (2004) 2202.
[48] M. Xue, G.S. Zhu, Y.J. Zhang, Q.R. Fang, I.J. Hewitt, S.L. Qiu, Cryst. Growth Des. 8 (2008) 427.
[49] C.-K. Tan, J. Wang, J.-D. Leng, L.-L. Zheng, M.-L. Tong, Eur. J. Inorg. Chem. (2008) 771.
[50] (a) X.-J. Liu, Q.-R. Fang, G.-S. Zhu, M. Xue, X. Shi, G. Wu, G. Tian, S.-L. Qiu, L. Fang, Inorg. Chem. Commun. 7 (2004) 31;
(b) M. Xue, G.-S. Zhu, Q.-R. Fang, X.-D. Guo, S.-L. Qiu, Inorg. Chem. Commun. 9 (2006) 603.
[51] O.M. Yaghi, R. Jernigan, H.-L. Li, C.E. Davis, T.L. Groy, J. Chem. Soc., Dalton Trans. (1997) 2383.
[52] H. Kumagai, M. Akita-Tanaka, K. Inoue, M. Kurmoo, J. Mater. Chem. 11 (2001) 2146.
[53] L. Pan, E.B. Woodlock, X.T. Wang, C. Zheng, Inorg. Chem. 39 (2000) 4174.
[54] C. Daiguebonne, O. Guillou, Y. Gerault, K. Boubekeur, J. Alloys Compd. 323 (2001) 199.
[55] X.J. Zhao, G.S. Zhu, Q.R. Fang, Y. Wang, F.X. Sun, S.L. Qiu, Cryst. Growth Des. 9 (2009) 737.
[56] D.T. de Lill, C.L. Cahill, Chem. Commun. (2006) 4946.
[57] Y.-C. Ou, M.-L. Tong, unpublished results.
[58] A. Uchida, M. Hasegawa, H. Manami, Acta Crystallogr. C59 (2003) o435.
[59] J. Wang, Y.-C. Ou, Y. Shen, L. Yun, J.-D. Leng, Z.-J. Lin, M.-L. Tong, Cryst. Growth Des. 9 (2009) 2442.
[60] Y.-C. Ou, W.-T. Liu, J.-D. Leng, Z.-J. Lin, M.-L. Tong, CrystEngComm (2010), doi:10.1039/c003764h.
[61] Y.-C. Ou, Z.-J. Lin, M.-L. Tong, CrystEngComm (2010), doi:10.1039/c004258g.
[62] Y.-C. Ou, J.-D. Leng, Z.-J. Lin, M.-L. Tong, unpublished results.
[63] (a) R. Kuhn, A. Wassermann, Helv. Chim. Acta 11 (1928) 50;
(b) Z. Welvart, Soc. Chim. 5 serie (1964) 2203.
[64] Y.-H. Wen, Y.-Y. Qin, J. Zhang, Z.-J. Li, J.-K. Cheng, Y. Kang, Y.-G. Yao, Acta Crystallogr. C60 (2004) m371.
[65] R.M. Wang, J. Zhang, L.J. Li, Inorg. Chem. 48 (2009) 7194.
[66] Y.-C. Ou, J. Wang, J.-D. Leng, Z.-J. Lin, M.-L. Tong, unpublished results.
[67] M. Farina, M. Grassi, G. Di Silvestro, J. Am. Chem. Soc. 107 (1985) 5100.
[68] S. Bruckner, L.M. Giunchi, G. Di Silvestro, M. Grassi, Acta Crystallogr. B37 (1981) 586.
[69] S. Bruckner, L. Malpezzi, M. Grassi, Cryst. Struct. Commun. 11 (1982) 1043.
[70] J. Wang, S. Hu, M.-L. Tong, Eur. J. Inorg. Chem. (2006) 2069.
[71] P. Thuéry, B. Masci, Cryst. Growth Des., doi:10.1021/cg100500p.
[72] P. Thuéry, Cryst. Growth Des. 10 (2010) 2061.
[73] L. Cañadillas-Delgado, O. Fabelo, J. Pasán, M. Julve, F. Lloret, C. Ruiz-Pérez, Polyhedron 29 (2010) 188.
[74] J. Wang, L.-L. Zheng, C.-J. Li, Y.-Z. Zheng, M.-L. Tong, Cryst. Growth Des. 6 (2006) 357.
[75] J. Wang, Z.-J. Lin, Y.-C. Ou, Y. Shen, R. Herchel, M.-L. Tong, Chem. Eur. J. 14 (2008) 7218.
[76] Z.-F. Li, H.-Z. Xie, Y.-Q. Zheng, Acta Crystallogr. C62 (2006) m455.
[77] J. Wang, Y.-H. Zhang, M.-L. Tong, Chem. Commun. (2006) 3166.